Investigating the role of Cry2Aa's N terminus in its activity towards dipteran species *Aedes aegypti*

Faisal Alzahrani

Submitted for the award of the Degree of Doctor of Philosophy

Department of Biochemistry

School of Life Science

University of Sussex

April, 2022

Work not submitted elsewhere for examination

I hereby declare that this thesis has not been submitted in whole or in part to this or any other university for the award of a degree.

Faisal Alzahrani

Acknowledgement

To those who are courage, patient, and steadfast.

First and foremost I am extremely grateful to my supervisor Professor Neil Crickmore for his invaluable advice, continuous support, and patience during my PhD study. His immense knowledge and plentiful experience have encouraged me in all the time of my academic research.

Special thanks to my parents who were continuously willing to feel this moment and read these words! All my success in the past, present and future is dedicated to them.

My PhD journey would not be as happy as it was without the two special individuals in my life, my wife Jasmine Alzahrani and our little daughter Farah! Their love and encouragement have definitely helped me overcome many difficulties.

Many thanks to all my older sisters and brothers for their warm and unconditional support and advice.

I would like also to thank every member in Professor Crickmore`s lab: Widad Souissi, Mojtaba Nasiri, Nelly Igwe, Nicole Bryce- Sharron and others for their support; it could not have been enjoyable without you guys!

Special thanks to King AbdulAziz University in Jeddah- Saudi Arabia, for funding my PhD. I am very proud being one of their faculty members.

Abstract

Bacillus thuringiensis is known to produce pesticidal proteins that have been used to control a variety of insect species. Cry2Aa, a three-domain pore-forming toxin, has been shown to have activity against both lepidopteran and dipteran insects. In particular it has been shown to have activity against the yellow fever mosquito (*Aedes aegypti*) whereas the closely related protein, Cry2Ab, does not possess such activity. The specificity of these proteins to a particular insect has generally been associated with the binding of domains II and III to a particular receptor on the surface of midgut epithelial cells. Recent work however has shown that domain I of Cry2Aa heavily influences the activity of the protein to this mosquito, and that changing just four amino acids within the N-terminal region was enough to introduce this activity to Cry2Ab.This project sought to understand the role of domain I, and these four amino acids in particular, in the activity of Cry2A proteins against *A. aegypti*. Initially we discounted the hypothesis that this region was directly involved in receptor binding by demonstrating that it was removed during the proteolytic activation step. We then went on to show that it was whether or not the protein was cleaved around these four amino acids by the mosquito digestive enzymes that determined whether or not it would have activity against the insect. This led to a new hypothesis that cleavage of the protein in this region revealed

a new epitope involved in receptor binding. This was tested by performing binding assays with different truncated forms of Cry2Aa which showed that the region of domain I between amino acids 49 and 144 was required for the binding of the protein to the midgut of *A. aegypti*.

List of abbreviations

A.aegypti: Aedes aegypti

ABC: ATP-binding cassette

AMJ: *Aedes aegypti* mid gut juice

BBMV: brush border membrane vesicle

bp: base pairs

BSA: Bovine serum albumin

Bt: *Bacillus thuringiensis*

^{0}C: degree Celsius

Cry: Bt Crystal toxin

Cyt: Bt cytolytic toxin

DNA: Deoxyribonucleic acid

E.coli: *Escherichia coli*

g- Gram

GABA: Gamma amino butyric acid

IPTG: Isopropyl-β-D-1-thiogalactopyranoside

kDa: Kilo Dalton

kV: Kilo Volt

LB: Luria Bertani

LC50: Concentration that kills 50% of a population

M: Molar

mM: millemolar

ml: Millilitre

mg/ml: Milligram per millilitre

PBS: Phosphate buffered saline

PCR: Polymerase chain reaction

OD: Optical density

ORF: Open reading frame

SDS-PAGE: Sodium dodecyl sulphate Polyacrylamide gel electrophoresis.

RGB- Resolving gel buffer.

SGB- Stacking gel buffer.

TBE: Tris-Borate-EDTA

TEMED: Tetramethylethylenediamine

WHO: World Health Organisation

Table of Contents

1. General introduction

1.1 Bacillus thuringiensis

Bacillus thuringiensis is a gram positive and spore-forming bacterium that is derived from *Bacillus cereus sensu lato* group including *B. anthracis* and *B. cereus* (Rasko et al., 2005). Bt produces insecticidal proteins in crystalline form which is a special characteristic of this species (Tay et al., 2015) (Asano et al., 1997). Bt was first isolated in 1902 by Japanese scientist Ishiwata from *silkworm* larvae. In 1915, Bt was formally characterized by German scientist Ernst Berliner (Milner, 1994). Bt proliferates when conditions such as nutrients and heat are available. However, when there is a lack of these conditions, the formation of spores occurs to maintain the existence of the bacterium. In addition, other factors may increase the level of spore formation; such as cell density (Hilbert and Piggot, 2004). Bt toxin classification was previously based solely on the sequences similarity (Crickmore et al., 1998). However, it has been recently revised, classifying them on both their sequence and structure (Crickmore et al., 2021).

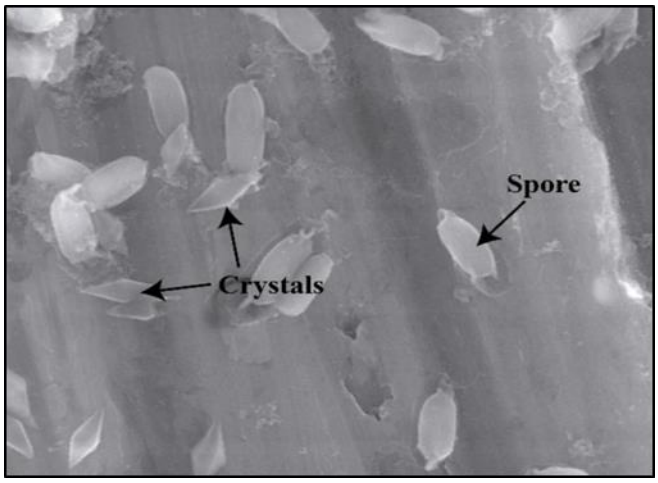

Figure: 1.1.1: Protein crystals (bipyramidal) mixed with spores from Bt strain H29.3 *(figure taken from Palma et al., 2014).*

1.2 Bt toxin nomenclature

The old nomenclature classified Bt toxins based solely on their sequence similarity (Crickmore et al., 1998). However, in the new structure-based nomenclature, there are 16 newly defined classes of Bt toxins. Three classes have not changed from the previous nomenclature: Cry, Cyt, and Vip3. For Cry class, it comprises insecticidal proteins with a 3-domain structure, either containing/or not containing an extended C-terminus, and others containing additional regions such as beta-trefoil domains. Toxins classified previously as Cry toxin which do not possess the 3-domain feature have now been reclassified. The three letter in the new mnemonics reflects either the pesticidal protein they possess; for instance, Mpp-Mtx2-like, Tpp-Toxin10-like; or historical names, for instance, Mcf, Mtx. Additionally, one new class was temporarily added, Xpp, which contains a group of toxins that have insufficient available information to assign to a structural class (figure 1.2.1) (Crickmore et al., 2021).

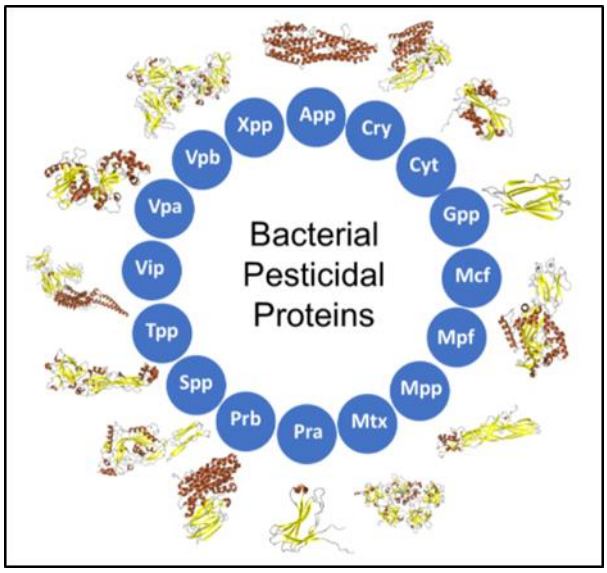

Figure 1.2.1: The newly released 16 classes of Bt toxins *(figure taken from Crickmore et al., 2021).*

The three domain Cry insecticidal proteins are made up of three structural domains (figure 1.2.2). The N-terminal of domain I is made up of a seven-helix bundle including helices long enough to traverse a hydrophobic cell membrane. Six amphipathic helices surround the core hydrophobic α-helix 5 (Pigott and Ellar, 2007, De Maagd et al., 2001). In addition, domain I function is comparable to that of other pore-forming bacterial toxins, showing implication of toxin insertion into the cell membrane (Li et al., 1991). Domain II is made up of three antiparallel β-sheets that are believed to be involved in receptor binding (Schnepf et al., 1998). Domain III is made up of two anti-parallel sandwich sheets forming jellyroll topology and is also implicated in receptor binding (Li et al., 1991). These two β-sheets contain five β-strands; the inner sheet is connected to the second domain while the outer sheet is accessible to the solvent (Li et al., 1991).

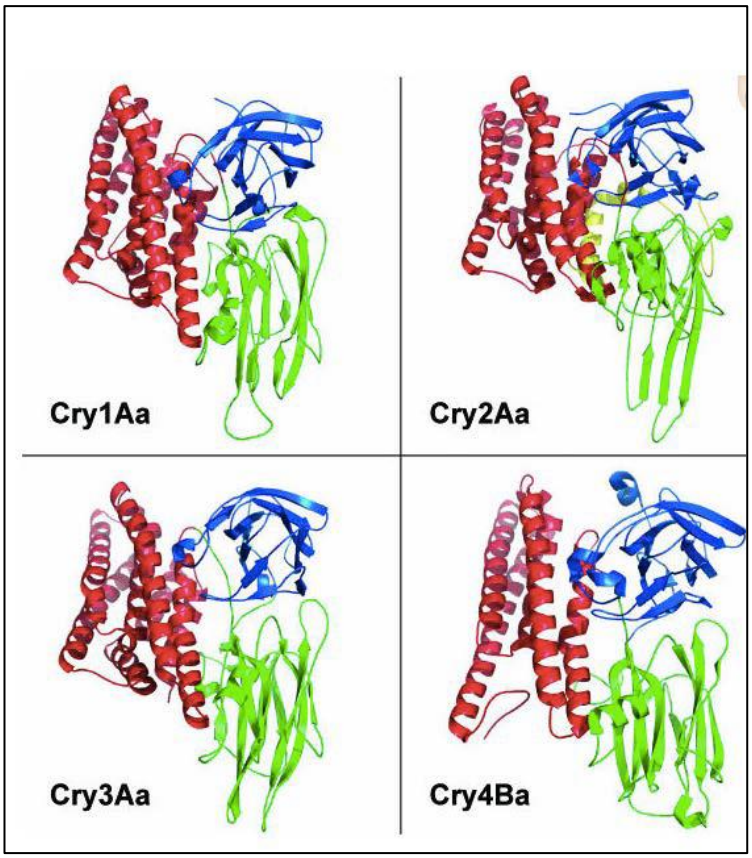

Figure 1.2.2: Illustration of the 3-domain Cry toxins. Domain I is shown in red; domain II in green, and domain III in blue *(figure taken from Pigott and Ellar, 2007).*

1.3 Cry2A toxin family

The Cry2A toxin family shows dual activity toward some dipteran and lepidopteran orders (Yamamoto and Mclaughlin, 1981, Donovan et al., 1988). It consists of 11 insecticidal proteins with molecular sizes ranging between 60- 72kDa (Dankocsik et al., 1990). Among the Cry2A proteins, only Cry2Aa has had its structure solved. Cry2Aa is a three-domain protein made of 633 amino acids. An N-terminal region of 49 amino acids needs to be cleaved for toxin activation (Morse et al., 2001). It is hypothesized that the cleavage of the N-terminal of Cry2Aa toxin by gut proteases is a required step to

expose a binding epitope to its receptor on the target cell; therefore showing activity (Morse et al., 2001).

1.4 Cry toxins bind to putative receptor

The major factor to determine the toxicity of a Cry toxin to any insect is the ability of the toxin to bind to a specific receptor on the cell linning. Many studies have shown the importance of toxin-receptor binding for activity; for instance, Cry1Ab and Cry1Ba were both active and able to bind to the BBMV of *Pieris brassicae*. However, only Cry1Ab bound to the BBMV of tobacco hornworm *Manduca sexta* and showed toxicity; whereas Cry1Ba did not bind or show toxicity (Hofmann et al., 1988).

Nevertheless, binding affinity is not an absolute indication of high toxicity. That was found when Cry1Ac which has a high binding affinity for the BBMV of *L. dispar* insect showed low toxicity while Cry1Ab has higher toxicity but lower binding affinity to *L. dispar* BBMV (Wolfersberger, 1990). Another study tested the binding affinity of the same toxin (Cry1Ac) to susceptible and resistant populations of *P. gossypiella*. It showed similar binding affinity within the two populations but with very different toxicities, concluding that toxin-receptor binding is important for toxicity, but that binding affinity does not associate with the level of toxicity (Ocelotl et al., 2015). Cry toxin interactions with putative receptors have been studied extensively. Many receptors within lepidopteran insects were identified to bind different Cry proteins. It was found that four

receptors within lepidopteran species were particularly involved in binding of Cry1A toxin family. These binding receptors are: cadherin-like protein (CADR) (Gahan et al., 2001), aminopeptidase N (APN) (Wei et al., 2016), alkaline phosphatase (ALP) (Mcnall and Adang, 2003), and ATP-Binding Cassette (ABC) (Heckel, 2012) (figure 1.4.41).

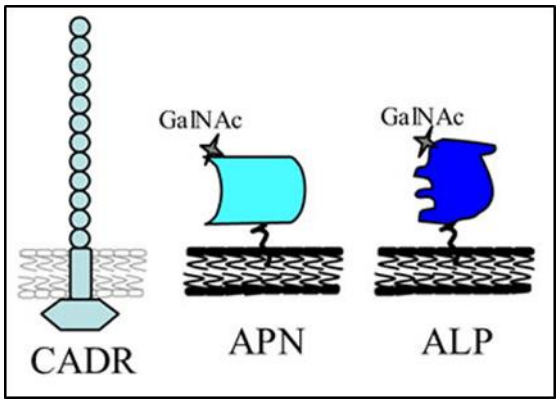

Figure 1.4.1: Representation of different molecules of Cry1A toxins *(figure taken from Bravo et al., 2007).*

1.4.1 Cadherin

Cadherin is a member of the calcium-dependent glycoprotein transmembrane family that has different functions such as, cell adhesion and movement (Angst et al., 2001). This transmembrane protein is believed to be a putative receptor for many Cry proteins. It is expressed in different insect species within different orders including; lepidopteran, coleopteran, and dipteran insects (Wu, 2014).

Different larval phases express different levels of cadherin receptor, and its role within these phases is related to the development of the larval epithelial midgut. In lepidopteran species, different Cry1A proteins bind to cadherin receptors of insect species; for example, Cry1Ac, Cry1Ab, and

Cry1Aa bind cadherin in *M. sexta* (Hua et al., 2004). Moreover, mutations in the cadherin gene results in toxin resistance to Cry1A family (Gahan et al., 2001). Other Cry insecticidal proteins bind cadherin, such as Cry11Aa, in *A. aegypti* (Chen et al., 2009), Cry3Ba in *Tribolium castaneum* (Contreras et al., 2013), and Cry4Ba in *Anopheles gambiae* (Hua et al., 2008).

1.4.2 Aminopeptidase N (APN)

Aminopeptidase N (APN) is a glycoprotein GPI-anchored protein member of metalloprotease family which proteolyses the N-terminal regions of diet proteins after being ingested in their midgut. In lepidoptera, APN proteins are classified into 8 subfamily proteins (APN1-8); for instance, APN1 is believed to be implicated in binding of Cry1Ac but not Cry2Ab in *Helicoverpa zea* (Wei, 2016); additionally, APN1, but not APN5, in *P. xylostella* was shown to be receptor for Cry1Ac (Guo et al., 2020). It is believed that APN receptor is bound to the microvilli membrane in the midgut by the glycosylphosphatidylinositol anchor (GPI).

GalNAc, a carbohydrate, has been shown to be an important in the binding of different Cry proteins to APN receptor; for instance, Cry1Aa, Cry1Ab, and Cry1Ac bound to *M. sexta* and *H. virescens* APNs (Masson et al., 1995, Luo K, 1997); Cry11Ba was found to bind *Anopheles gambiae* APN (Zhang et al., 2008); Cry1Ba was found to bind *Epiphysa postvittana* APN (Simpson Rm, 2000). In addition, a study showed that knocking down APN

expression by RNAi in the epithelial cells of *H. zea* population abolished the toxicity of Cry1Ac (Wei, 2016).

1.4.3 ATP-Binding Cassette (ABC)

ABC proteins form a big family of intracellular proteins that hydrolyse ATP molecules to transport molecules through lipid bilayer membranes. These proteins consists of two nucleotide-binding domain (NBD) and two transmembrane domains (TMD) (figure 1.4.2).

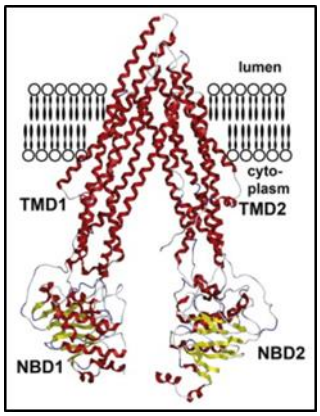

Figure 1.4.2: Structure of P-glycoprotein (ABCB1) from mouse. NBD, nucleotide binding domain; TMD, transmembrane domain. Structure from Protein Data Bank Accession 3G5U, rendered in the Molecular Operating Environment program *(figure taken from Heckel D., 2012).*

In general, there are eight sub families of ABC protein (ABCA-H) (Heckel, 2012). It was found that Cry1A family interacts with ABCC2 in (Bretschneider et al., 2016); and creating mutations within ABCC2 receptor causes resistance to Cry1 and Cry2Ab in *Heliothis virescens* (Heckel, 2012, Tay et al., 2015). Additionally, the resistance of Cry1A in *P. xylostella* (NO-QA strain) is believed due to alteration of ABBC2 receptor (Hernandez-Martinez et al., 2012).

1.4.4 Alkaline phosphatase

ALP is a glycoprotein GPI-anchored membrane which is engaged in dephosphorylation reactions. Low levels of ALP was associated with resistance of Cry1Ac, Cry2Ab, and Cry1F in *Spodoptera frugiperda* (Jurat-Fuentes et al., 2011). It was found that ALP is a binding receptor for some Cry insecticidal proteins, such as Cry11Aa and Cry4Ba, in *A. aegypti* (Fernandez et al., 2006, Buzdin et al., 2002).

1.5 Mode of action of Cry toxins

There are several proposed hypotheses concerning how Cry proteins cause toxicity to Lepidoptera. The colloid-osmotic lysis model is widely accepted (Knowles and Ellar, 1987); this was established by testing a three domain Cry toxin with different insects specificity. Insect larvae uptake the Bt crystals in the midgut, which are then solubilized in the alkaline condition of the insect's gut. An alkaline condition is necessary for proper solubilisation of Bt crystals (Du et al., 1994). Upon solubilisation, protoxin is released, cleaved by midgut protease, and interacts with its receptor in the cell membrane.

Previous experiments indicated that interaction with the cell membrane triggers the formation of oligomers from monomeric Cry proteins (Guereca and Bravo, 1999). After that, insecticidal proteins undergo an insertion process; forming pores in the cell membrane. Pore-formation results in cell swelling, osmotic imbalance; and eventually, larval death

(Knowles and Dow, 1993). More recent studies proposed variations to this simple model.

1.5.1 Sequential binding model

This was proposed based on the interaction between Cry1Ab toxin and *M. sexta* BBMV (Bravo et al., 2004) (Figure 1.5.1.1). Immunoprecipitation analysis revealed that Cry1Ab binds two receptors; cadherin-like protein (Bt-R1), and aminopeptidase N. After toxin solubilisation, midgut juice initially cleaves the protoxin. That is followed by binding to cadherin-like protein (Bt-R1) which facilitates a second cleavage by a membrane-bound protease triggering the formation of oligomeric toxins, which subsequently bind to APN. After that, toxin oligomer is inserted into the cell membrane, causing pore formation and cell death. The immunoprecipitation analysis of APN showed mostly a detection of oligomeric form of the toxin, while cadherin-like protein (Bt-R1) immunoprecipitation analyses showed detection of the monomeric form of the toxin. It was found that oligomers of Cry1Ab were more preferably inserted into the membrane than the monomeric form (Rausell et al., 2004).

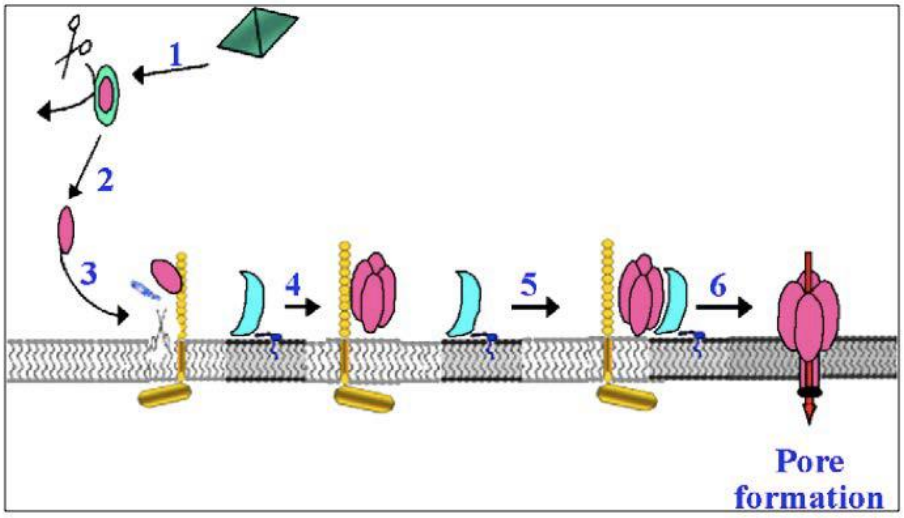

Figure 1.5.1.1: Diagram illustration of Cry toxin sequential mode of action. 1: Cry toxin solubilization; 2: cleavage by midgut protease; 3: toxin monomer binding to its receptor and second cleavage by membrane proteases; 4: toxins oligomer formation; 5: receptor-oligomer binding; and 6: pore formation process *(figure taken from Bravo et al. 2004).*

1.5.2 Signal transduction model

An alternative mode of action of Cry toxins was proposed by Zhang et al which hypothesized that cell death is linked to the binding of the monomeric form of the toxin, Cry1Ab, to a specific cadherin-like protein receptor (BT-R1) (Zhang et al., 2005). Moreover, this interaction does not result in pore-formation but instead is linked to a Mg^{2+} dependent signal cascade pathway (Figure 1.5.2.1).

Cry1Ab toxin and undifferentiated ovarian cells from *Trichoplusia ni* were used in this study. This cell line, named (S5), was designed to express the cadherin BT-R1 receptor on its cell surface. The monomeric form of the toxin was incorporated into the membrane of cells expressing BT-R1 receptors, revealed by Western blot assay; however, the oligomeric form of Cry1Ab was discovered in the membrane of both susceptible and non-

susceptible cells. In addition, inhibiting the cadherin binding site abolished activity but did not affect oligomer formation on the cell membrane. Therefore, it was hypothesized that oligomer formation happens but without causing any activity (Zhang et al., 2005).

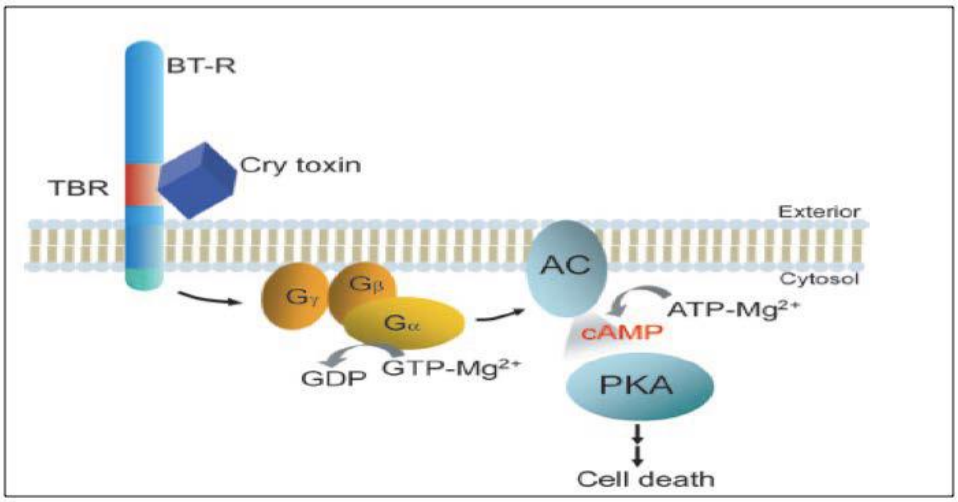

Figure 1.5.2.1: Illustration of Cry toxin mode of action proposed by Zhang. *(figure taken from (Ibrahim et al., 2010).*

1.6 Cry toxin oligomerization during mode of action

Toxin oligomerization is the aggregation of toxin monomers forming a protein complex either on a cell receptor or on the surface of the cellular membrane.

In the sequential binding model, toxin oligomerization is a critical step for toxin activity. Many studies have shown evidence of Cry toxin`s ability to form oligomers; either in the presence of cell receptors from insect BBMV or in the absence of cell receptors. A study tested the formation of oligomers in the absence of insect BBMV using size exclusion chromatography and non-denaturing PAGE (Guereca and Bravo, 1999).

After toxin activation, it was found that Cry1C and Cry1D had high molecular weight bands on the non-denaturing PAGE when the samples were heated at 60C^{O} instead of boiling, suggesting formation of toxin oligomers. It is important to note that the formation of the oligomers are not believed due to the presence of disulfide bonds as all toxins were treated with reducing agents. Another evidence of forming toxin oligomers in the absence of insect`s BBMV is the ability of Cry1Ia to oligomerize not only in the absence of the BBMV, but also prior Cry1Ia activation by midgut juice (protoxin) (Khorramnejad et al., 2022)

However, many studies showed the implication of toxin oligomerization in the presence of insect BBMV. A study found an association between an ABCC2 receptor and oligomerization; Cry1Ac oligomerization was more efficient in a susceptible strain of *P. xylostella* than the resistant strain which contained mutant a form of ABCC2 (Ocelotl et al., 2017).

In the case of Cry2A proteins, Xu et al., 2018 found that after toxin activation by *P. xylostella* midgut juice, helices α4 and α5 within domain I of Cry2Ab were associated with toxin oligomerization; however, the exposure of these helices only induced toxin oligomerization but did not increase the efficiency of toxin binding to the insect`s BBMV. Moreover, Pan et al., 2021 found key residues in Cry2Ab that contributed to Cry2Ab oligomerization. Residues N151, T152, F157, L183, L185, and I188 were

all substituted to alanine; and caused a reduction in toxin oligomerization and activity to *P. xylostella* (Pan et al., 2021).

1.7 *Aedes aegypti*

Aedes aegypti Mosquitoes cause major health issues because they transmit pathogens such as viruses and parasites through blood feeding, resulting in serious human diseases such as malaria, dengue fever, west Nile fever, and zika fever. These diseases are highly common in tropical regions environments which are optimal for mosquito reproduction. Therefore, they result in billions of disease cases and millions of fatalities globally (Who, 2006).

Chemical, biological, and physical approaches have been employed to control *Aedes* mosquitos for a long time. From the 1940s, chemical pesticides such as DDT, Malathion, and pyrethroids were employed all over the world.

However, there are some limitations of using those methods; resistant populations of *Aedes* mosquitoes have emerged in different parts of the world as a result of widespread insecticide use (Rodriguez et al., 2007, Harris et al., 2010). Pesticides kill non-target creatures and contribute to pollution, whereas physical approaches, such as destroying breading sites, have some practical constraints. As a result, biological measures, such as the introduction of parasites and predators, or the use of pathogens to target

mosquitoes, are considered a better alternative approach. Various bacterial strains, such as *Bacillus thuringiensis*, are among the pathogens employed to inhibit mosquito larvae spreading. *B. thuringiensis* possesses high insecticidal activity and is non-toxic to non-target organisms. As a result, it has been employed to control *A. aegypti* and other mosquito species globally (Alphey et al., 2013).

1.8 Life cycle of *A. aegypti*

Aedes aegypti frequently breeds in unclean containers such as flowerpots, swimming pools, and drainage ditches. They become more dangerous when they get in close contact with humans as a source of blood and thereby transmit diseases. Additionally, regions that lack proper water systems, such as stored water rather than running water, become extremely good places for *A. aegypti* to bread. Female and male adult mosquitoes feed on plant nectar; however, female adult mosquitoes require blood feeding in order to produce eggs. These eggs can survive for months in wet conditions enabling them to spread into different locations. Female adult *A. aegypti* produce 100 to 200 eggs in each batch. The number of eggs depends on the blood amount taken in every meal. During their lifetime, females usually lay up to five batches (Nelson, 1986). They prefer to lay eggs near water surfaces such as tree holes and containers. Eggs are usually laid singly or grouped, and females lay eggs more than one time rather than laying them at once in multiple sites (Clements, 1999) (Foster, 2002a).

The morphology of *A. aegypti* eggs is around one millimetre long and ovoid shaped. They are usually white but they turn black later. Once eggs are submerged in water, they start to hatch (Nelson, 1986). The development of eggs depend on climate; in tropical climate, they usually hatch within two days while in higher temperature environments they hatch within one week (Foster, 2002b) After hatching, eggs develop into larvae. Larval development depends on temperature changes. During its development, larvae pass through four stages; they spend a short time in the first three stages; however, the last stage (fourth instar stage) takes around three days. It was noticed that male *Aedes* pupate faster than females. Larvae are around 8 millimetres long. In cool climates, *A. aegypti* can remain in larval stages for longer time (Foster, 2002b).

A. aegypti enters the pupal stage after the fourth instar stage. The pupae are mobile and can respond to stimuli. Usually, pupae take two to four days to develop to adults. Depending on environment conditions, the adult *A. aegypti* life spans from two weeks to months. There are three groups (polytypic) of *A. aegypti*: domestic, sylvan and peri domestic. Domestic populations usually breed in urban areas, while sylvan populations breed mainly in forests. Peri domestic breed in coconut groves and modified environments (Tabachnick et al., 1979).

1.9 Approaches to control *A. aegypti* populations

It has been globally concerning as to how to control the threat of mosquito-borne diseases. Although the use of some chemical insecticides showed positive outcomes in controlling mosquitoes, populations showing resistance to those chemical pesticides arose around the world (Gomez-Dantes and Willoquet, 2009). Additionally, these chemical insecticides showed toxicity toward other organisms that are necessary for the environment. Physical approaches also showed some limitations on controlling the breeding sites of these mosquitoes. A first limitation is that the multiple breeding areas for mosquitoes are hard to be covered or discarded. A second limitation is destroying other organisms that share same habitat; leading to an unbalanced ecosystem. Given these limitations, the usage of biological approaches has become more important. These approaches include parasites or predators being introduced into the breeding sites of mosquitoes. One controlling approach is “Self-limiting insects” (Alphey et al., 2013). This program showed high effectiveness in controlling mosquito breeding by reducing up to 90% of population (Carvalho et al., 2015). However, the high costs of this program is a disadvantage especially in countries where there is a major threat of *A. aegypti*. As a result, using Bt protein products became a perfect alternative to control the spread of *A. aegypti*. Bt proteins are environmentally friendly and more specific to *A. aegypti* with no reported resistant populations.

1.10 Specificity determination of Cry insecticidal proteins to pest species

The importance of studying the specificity determination of Cry insecticidal proteins enabled scientist to specify the effective factors that influence the effectiveness of the toxin; these factors may include; identifying domains (or residues) that affect activity toward insects; it also includes understanding the mechanism of action of a certain toxin toward a given insects.

1.10.1 Specificity determination of Cry insecticidal proteins in their mode of action

Seven main factors affecting Cry toxins specificity toward pests have been described. First, the ability of Cry toxin to encounter its target insect. One of the limitations is the inability of Bt to colonize from one site to another site (Maduell et al., 2008). However, this can be overcome by transmission through insect-insect interaction (Milutinovic et al., 2015).

The second factor is crystal solubilisation. The presentation of Cry proteins in crystals form has an importance as it provides proteins stability against the environmental conditions. Nevertheless, these crystals must be solubilized in the host digestive juice in order to undergo intoxication process (Angus, 1954). For example, the activity of Cry1B crystal toward coleopteran larvae was only observed after *in vitro* solubilisation (Bradley et al., 1995). The third factor comes after toxin solubilisation; toxins stability and processing. Cry toxins become susceptible to proteolytic cleavage by host midgut juice upon solubilisation. This proteolytic processing varies for each toxin family. Cry1 proteins, for example, are

mostly 120 kDa while Cry3 or Cry2 toxins lack an extensive C terminus protoxin domain and are lower size (70–73 kDa). In several cases, the production of a stable toxin has been established to determine, or influence specificity. Cry1A susceptible populations, *Pieris brassicae, Bombyx mori,* and the Cry1A resistant populations, *Mamestra brassicae, Spdoptera litura*, hosts were compared and it was revealed that the resistant larvae were less effective at activating toxin, suggesting an association between susceptibility and the production of stable toxin. It was also noticed that degradation or slow activation of toxins is associated with low activity (Elleuch et al., 2015). For instance; slow activation of the Cry3Aa protein to an active 55 kDa fragment in the midgut of *Diabrotica virgifera* suggested that slow activation is associated with Cry3Aa is low activity against these rootworms; moreover, addition of a chymotrypsin G site to Cry3Aa protein, mCry3Aa, caused faster activation to the 55 kDa active fragment, and subsequently increased the activity against rootworms (Walters et al., 2008).

The fourth factor is the ability of the toxin to remain resistant to other digestive enzymes. For instance, *Choristoneura fumiferana* contains elastase enzyme which is able to bind Cry1A and lower its activity to *C. fumiferana* (Milne et al., 1998). In addition, an obstruction of intoxication

process by esterase in Cry1Ac resistant *Helicoverpa armigera midgut* was associated with low activity (Gunning et al., 2005).

The fifth factor is the ability of Cry toxin to pass through the mucus like layer known as peritrophic matrix. The function of the peritophic matrix is to provide protection to the insect`s midgut from pathogens, however, Cry toxin are capable to pass through the pores within this matrix (Brandt et al., 1978). Some three domain Cry toxins contains Lectin-like folds which can interact with the glycosylic residues within the peritrophic matrix; sebsequently, causing obstruction to the intoxication process. In *Orgyia pseudotsugata*, a Cry1A binding protein in the peritrophic membrane is known to have GalNAc rsidues which prevent binding to its receptor in the brush border (Valaitis and Podgwaite, 2013, Burton et al., 1999). Additional evidence showed the implication of the GalNAc residues in reducing toxin susceptibility, when Cry1Ac, a non-active toxin toward *B. mori*, gained activity after adding GalNAc molecules along with the toxin. That, as a result, enabled the toxin to pass through the peritophic matrix and bind its receptor (Hayakawa et al., 2004). The sixth factor is the ability of the toxin to bind its receptor. Many different potential Cry toxin receptors were identified including protein and glycolipid (Pigott and Ellar, 2007). Many studies, for instance, showed the implication of ABC proteins family, particularly ABCC2 and ABCA subfamilies; however, mutations

within these receptors are associated with Cry1 and Cry2Ab resistance (Park et al., 2014, Heckel, 2012, Tay et al., 2015).

The seventh factor is the post-binding effects; for instance toxin oligomerization. An evidence of toxin oligomerization importance is the inability of mutant Cry1Ab to form oligomerization, and subsequently, lost activity to *M. sexta* (Jimenez-Juarez et al., 2007).

1.10.2 Specificity determination of Cry toxins

The role of individual domains is specificity determination has been extensively studied. Experiments using single cross hybrid toxins and homologue-scanning mutagenesis have enabled scientists to identify the amino acids (or domains) implicated in determining the specificity in toward a particular group of insects (Widner and Whiteley, 1990, Liang and Dean, 1994, Shu et al., 2016).

One study tested 37 different hybrid insecticidal proteins created by single crossover mutagenesis from two members of the Cry2A family; Cry2Aa, Diptera and Lepidoptera active, and Cry2Ad, diptera and lepidoptera non-active, on different lepidopteran species: *O. furnacalis, C. suppressalis, H. armigera,* and *P. xylostella*. It was found that a group of hybrid proteins containing 402 amino acids from Cry2Aa N-terminal region (64%), and a minimum of 224 amino acids from Cry2Ad C-terminus (36%) showed the activity of Cry2Ad (figure 1.10.2.1- R0-R23). On the other hand, a group of toxin containing around 170 amino acids or less from Cry2Ad at the C-

terminus showed activity related to Cry2Aa (figure 1.10.2.1- R27-R37). Additionally, it was noticed that since the boundary between domain I and II is at amino acid 267, while that between domain II and III is at amino acid 474; therefore, substitution of domain I from Cry2Aa has no significant effect on Cry2Ad specificity and substitution of domain III of Cry2Ad did not affect Cry2Ad specificity. Nevertheless, hybrid toxins in which the crossover occurred within domain II, showed specificity exchanged either from Cry2Aa to Cry2Ad or from Cry2Ad to Cry2Aa, indicating that insect`s specificity is within domain II that includes hybrid R23 and R24 for *O. furnacalis*, R25 and R26 for *P. xylostella*, and R26 and R27 for *H. armigera*. The change in specificity in these hybrids could be explained by two proposed reasons; first, the potential binding between the toxin and its receptor in insect`s gut is mediated by different regions of the toxin in different species; second, the insect`s defence pathway affects toxin virulence; that includes toxin cleavage at specific site by midgut protease or toxins being sequestered (Shu et al., 2016).

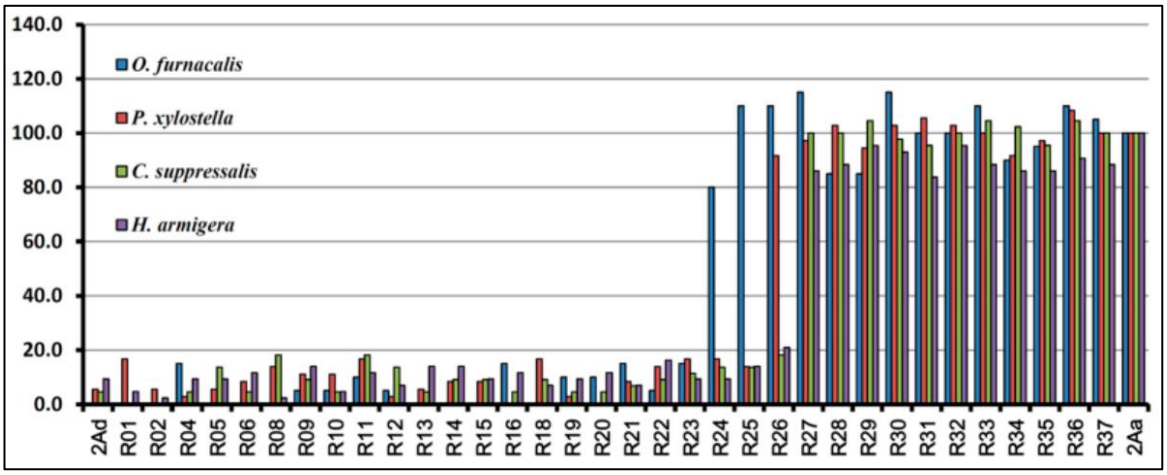

Figure 1.10.2.1: Biological activity of Cry2Aa/ Cry2Ad chimeras.2Aa and 2Ad refer to the Cry2Aa and Cry2Ad toxins respectively, and R01 through R37 represent the individual chimeras. The y-axis indicates the toxin's relative toxicity following exposure of the test insect to 50 ppm toxin. The relative activity of each toxin was normalized to the activity of Cry2Aa *(figure taken from Shu et al., 2016).*

In addition, a1990 study created hybrids via domain swapping and homologue scanning mutagenesis of Cry2Aa and Cry2Ab; hybrid proteins were assayed against *Manduca sexta* and *A. aegypti* to measure the potential toxicity changes compared to both wildtype toxins (Widner and Whiteley, 1990) (figure 1.10.2.2).

It was found that hybrids mostly comprised of Cry2Ab N-terminal showed low activity to *Aedes* compared to Cry2Aa-wildtype. Hybrid 7, which contains regions between 307-382 from Cry2Ab also showed no activity to *Aedes*. Hybrids 8-15 showed differential activity to *A. aegypti*; in fact, hybrids 8-10 showed low activity to *Aedes* compared to Cry2Aa wildtype; while hybrids 12 and 13 showed activity as similar as Cry2Aa wildtype. Hybridrs 14 and 15, containing partial region of 307-382, showed no activity. It was concluded that the non-active hybrids (6,7,14, and 15) lacked the mosquitocidal active region (307-382). In addition, it was also suggested that the boundaries between hybrids 5-13 possess the minimal active site to *Aedes*; therefore, hybrid 513 were created, and its activity was 20 fold lower than the activity of Cry2Aa. This s suggested that there are other residues outside the 307-382 region that are important to cause activity to *Aedes*.

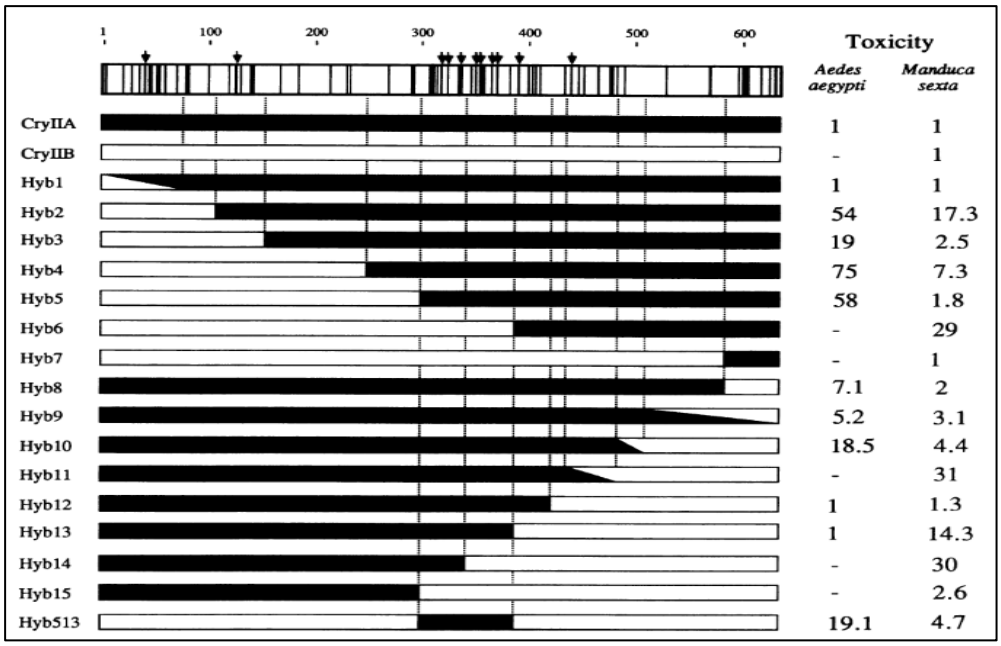

Figure 1.10.2.2: Cry2Aa (shaded bar), Cry2Ab (non-shaded bar), and hybrid gene products (combination of the two patterns) and their toxicities to *A. aegypti* and *M. sexta*. All of the toxicities are relative to that of Cry2Aa (value of 1); a fivefold difference in toxicity is considered significant. The bar at the top of the figure is a diagram depicting a FASTP alignment of the Cry2Aa and Cry2Ab polypeptides; vertical lines represent differences between the two, and arrows above the bar denote the locations of non-conservative changes. Vertical broken lines show locations of the hybrid junctions determined by restriction mapping (hybrids 1, 9, 10, and 11) and DNA sequence analysis (hybrids 2 to 4, 6, 8, 12 to 14, and 513). The dotted lines extend upwards to the alignment diagram to show where the junctions are located with regard to the amino acid differences that exist between the two polypeptides *(figure taken from Widner and Whiteley, 1990).*

Liang and Dean study also determined the regions within Cry2A toxins important for specificity toward dipteran and lepidoptera insects by creating hybrids between Cry2Aa and Cry2Ab (Liang and Dean, 1994).

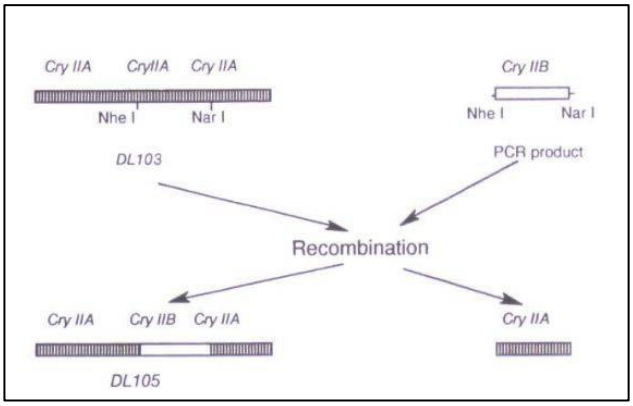

Figure 1.10.2.3: Total replacement of domain II of Cry2Aa with domain II of Cry2Ab. The filled bar indicates DNA from Cry2Aa, the open bar from Cry2Ab. Gene DL103 is a wild-type Cry2Aa gene. Gene DL105 is a recombinant gene which had domain I and domain III of Cy2Aa origin and domain II of Cry2Ab origin *(figure taken from Liang and Dean, 1994).*

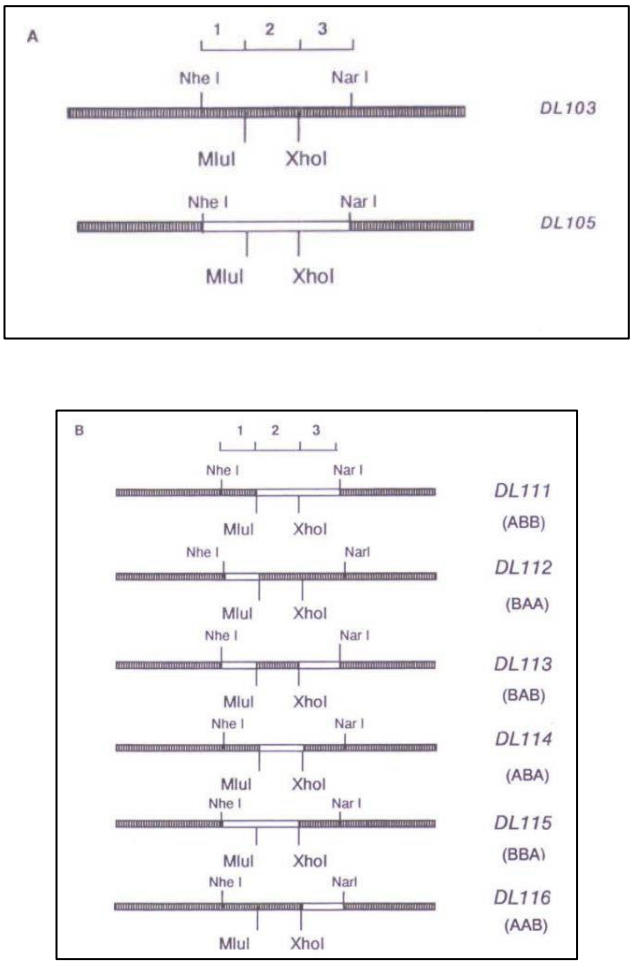

Figure 1.10.2.4: Homologous-scanning mutagenesis. The filled bar indicates DNA from Cry2Aa; the open bar indicates DNA from Cry2Ab. **A** *MIuI* and *Xhol* sites introduced into DL103 and DL105. *MIuI* and *Xhol* almost equally divide domain M into three regions, which have been named (from N-terminal to C-terminal) regions 1, 2, and 3, *Nhel* and *Narl* are naturally occurring sites bordering domain II of Cry2Aa. **B** Homologue-scanning mutagenesis of domain II of Cry2Aa. Letters in parentheses indicate the origin of each of the three regions. A= Amino acid section taken from Cry2Aa, B= Amino acid section taken from Cry2Ab. Protein marked Cry2Ab is made wholly of Cry2Ab residues, protein marked DL105 is a Cry2Aa with the three regions of domain II substituted by Cry2Ab residues (table *taken from Liang and Dean, 1994*).

Table 1.14.1: The LC50 values of Cry2A domain II swap mutants against *A. aegypti* and ID50 against *Lymantria dispar* (figure taken from *Liang and Dean, 1994*).

Toxins	**Domain II origin**	**LC50 of *A. aegypti* (95%confidence interval)(ng/ml)**	**ID 50 of *Lymantria dispar* (95% confidence interval) (ng)**
DL103	aaa	65.5 (41.1-100)	102 (77-181)
DL105	bbb	$>105^5$	304 (226 - 418)
DL111	abb	ND	ND
DL112	baa	1.23×10^5 (2.82×10^4-8.33×10^5)	126 (85.7 - 187)
DL113	bab	1.50×10^5 (1.05×10^5-1.02×10^6)	88.7 (58.0 - 129)
DL114	aba	ND	ND
DL115	bba	$>10^5$	3200 (1340 - 51900)
DL116	aab	52.2 (25.7-107)	90.6 (57.7 - 136)

1.11 The role of Cry2A domain I in specificity determination to *A. aegypti*

Naturally existing hybrid of Cry2A (Cry2Aa17) consists of domain I from Cry2Ab while domain II and III are from Cry2Aa (Shu et al., 2017). Additionally, domain I swapped hybrid toxin between Cry2Aa and Cry2Ab (domain I of Cry2Aa while domain II and III from Cry2Ab) were created for further investigation on domain I specificity to *A. aegypti* (Joseph, 2019). The activity assay of both proteins showed that they followed the toxicity profile of Cry2Ab (not active to *A. aegypti*) but still retaining activity to lepidopteran species (Shu et al., 2017, Joseph, 2019). Additionally, Cry2Aa N-terminal (first 49 amino acids), in particular, influenced specificity to *A. aegypti*. That was established after exchanging the non-active Cry2Ab 49 N-terminal amino acids with the equivalent amino acids from *Aedes* active Cry2Aa, which, subsequently, conferred *Aedes* activity to Cry2Ab. Further investigations on the N-terminal region of Cry2Aa (and other *Aedes* active and non-active Cry2A roteins) found that there are four residues E27, R43, T44, and D45 (figure 1.11.1); that are conserved in the active toxins.

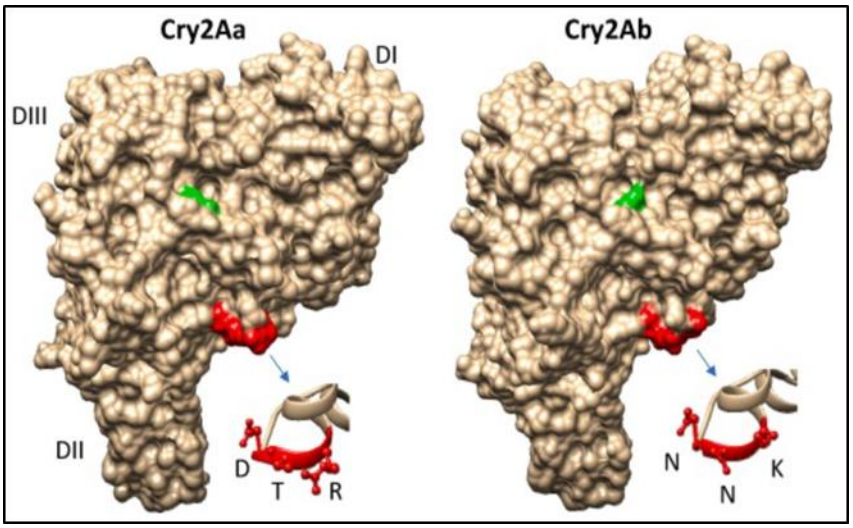

Figure 1.11.1: Comparison of *A. aegypti* specificity motifs in Cry2Aa and Cry2Ab. The Cry2Aa structure was determined experimentally (Morse et al., 2001) and that of Cry2Ab using Phyre2 modelling (Kelley et al., 2015). The amino acids associated with *A. aegypti* specificity are highlighted by colour and the inserts show ball and stick representations of the 43–45 triads *(figure taken from Goje et al., 2020).*

It was also found that all of these four residues must be included in the N-terminal in order to confer activity in Cry2Ab; while changing or substituting any one of them was found to cause loss of activity in Cry2Aa. Since they were all solvent exposed, the ERTD residues were hypothesized to be involved in toxin binding (figure 1.11.2) (Joseph, 2019).

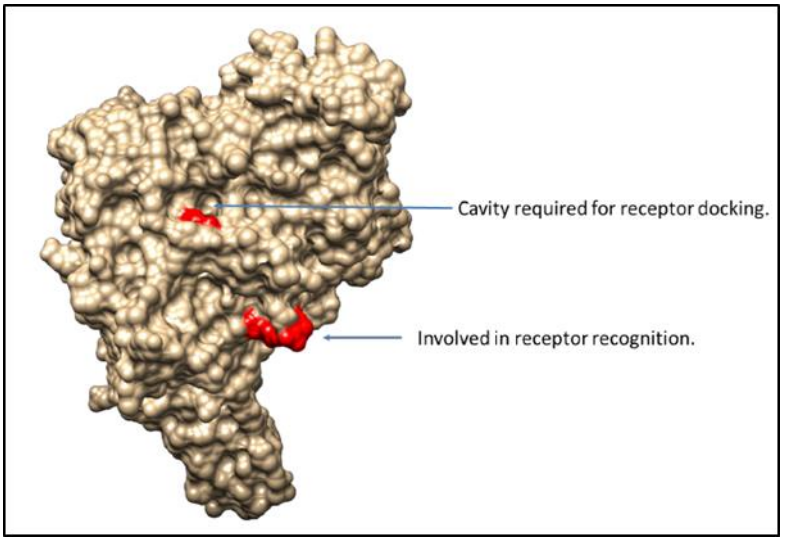

Figure 1.11.2: Structure showing the positions of the tetrad 'ERTD' in Cry2A toxins and their proposed roles. The arrows point at their locations on Cry2Aa toxin structure. The areas shaded indicate the positions of the amino acids 'E' and 'RTD' respectively in Cry2Aa structure *(figure taken from Joseph 2019).*

However, Cry2Aa`s N-terminus is removed during activation; and that removal has been hypothesized to be crucial for activity (Morse et al., 2001). For instance, Cry2Aa activation by *Aedes* midgut juice includes removal of the 49 N-terminal amino acids (Goje et al., 2020). Audtho et al study found that *L. dispar* midgut juice partially activates Cry2Aa to a 58 kDa fragment followed by a final activation producing 50 kDa fragment. N-terminal sequencing revealed that the production of the 58 kDa fragment is due to cleavage after amino acid Y49 while the 50 kDa fragment was after L144 (Audtho et al., 1999).

The activity assay showed that the 58 kDa fragment is active toward *L. dispar* (Audtho et al., 1999) and *A. aegypti* (Goje et al., 2020) while the 50 kDa is not for both insects; although the 50 kDa fragment showed activity to some lepidopteran species.

It was proposed that Aedes gut protease activates Cry2Aa at amino acid Y49, producing a 58 kDa fragment.

The dilemma of understanding the specificity of Cry2Aa N-terminal and the involvement of ERTD residues in *Aedes* activity led to propose the “intact N-terminal model” hypothesis, which states that Cry2Aa N-terminus is cleaved in *Aedes* gut but remains attached to the whole protein in which the ERTD can still participate in receptor binding (figure 1.11.3) (Joseph, 2019).

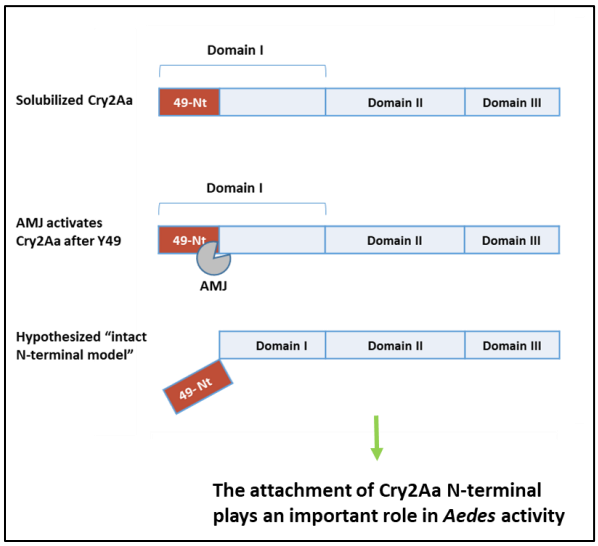

Figure 1.11.3: diagram illustration of the "intact N-terminal model" suggested by Joseph, 2019.

❖ Project aims and objectives

The primary aim of this research project was to understand how the N-terminus of Cry2A insecticidal proteins is important for *A. aegypti* activity. Four specific objectives were identified:

- To test the hypothesis that the N-terminal region of Cry2Aa remains attached following cleavage by *Aedes* gut protease.
- If it remains attached, we then aim to identify the binding force between the N-terminus and the rest of the protein.
- Understanding the role of the four identified residues within the Cry2A N-terminus that were shown to be crucial for activity to *A. aegypti*.
- To understand the role that the N-terminus plays in Cry2Aa`s activity against *A. aegypti*.

2. Materials and methods

2.1 Materials

2.1.1 Plasmids

Plasmid	Toxin	Source
pHT315	Cry2Aa	Crickmore lab
pHT315	His-Cry2Aa	In this study
pHT315	His-Cry2Aa-L144A	In this study
pHT315	His-Cry2Aa-L48A/Y49A	In this study
pHT315	His-Cry2Aa-L144A/KNN	In this study
pHT315	His-Cry2Aa-E27Q	In this study
pHT315	His-Cry2Aa-KNN	In this study
pHT315	Cry2Ab	Crickmore lab
pHT315	Cry2Ab-RTD	In this study
pHT315	Cry2Aa-His (C-terminus His tag)	In this study
pHT315	His-Cry2Aa-T56A	In this study
pHT315	His-Cry2Aa-T56A/L63A	In this study
pEB	Cry2Aa17	(Joseph, 2019)
pEB	Cry2Ah	(Joseph, 2019)
pEB	Cry2Am	(Joseph, 2019)
pHT315	Cry2Ac	Crickmore lab

2.1.2 Bacterial strains

Strain	Procedure
Bt (78/11)	Bt subspecies *israelensis* lacking crystals used as host for protein expression.
***E. coli* (DH5α)**	Host for transformation.
***E. coli* (BL21)**	Protein expression system.

2.1.3 Buffers

10 x TBE buffer: 108 g of Tris base, 55 g of boric acid, 40 ml of0.5 M EDTA, 2 l of dH_2O, pH 8.0.

Resolving Gel Buffer (RGB): 18.18 g Tris-(Hydroxymethyl) amino methane, 0.4 g SDS, 100 ml of dH_2O, pH 8.8.

Stacking Gel Buffer (SGB): 6.06 g Tris-(Hydroxymethyl) amino methane, 0.4 g SDS, 100 ml of dH_2O, pH 6.8.

10 ×SDS running buffer: 7.6g Tris-HCl, 36g glycine, 2.5g SDS, 250 ml of dH_2O, pH 8.3

2 × protein gel sample loading solution:2g SDS, 6 mg EDTA, 20 mg Bromophenol Blue, 5 ml of RGB, 50 ml glycerol, 100 ml of dH_2O.

Coomassie blue stain: methanol, dH_2O, acetic acid (10:9:1 v/v/v), Brilliant Blue R-250 (0.25%, w/v).

De-staining solution: methanol, dH_2O, acetic acid (10:9:1, v/v/v).

10 ×PBS: 80 g of NaCl, 2g of KCl, 14.4g of Na_2HPO_4, 2.4g of KH_2PO_4,1 l of dH_2O, pH 7.4.

2.1.4 Primers

	Primers Sequence (5`→ 3`)	DNA construct	5`-Phosphorylation
1	Fw: CCCTGTTCCTGCATCAATAACTTC Rv: TTTTGAGTAGGGTTTAAAAAATTATC	pHT315-Cry2Aa-L144A	**Yes**
3	ATACCCCATTCATCTGC	Cry2Aa N-terminus Sequencing	**No**
4	Fw: catcatcaccatcatcacAATAATGTATTGAATAGTGG Rv: CATATAAAATTCCTCCTTAAATATC	pHT315-HisCry2Aa-L144A	**Yes**
	Fw:AATAATCATAGTTTATATGTAGCTCC Rv: TTTTTTCCACTCCATCCATTCTTTTTGG	pHT315-HisCry2Aa-L144A/KNN	**Yes**
5	Fw: TCATAGTGCAGCAGTAGCTC Rv: TCTGTTCTTTTCCACTCC	pHT315-Cry2Aa-L48A/Y49A	**Yes**
6	Fw: CATAGTTTATATGTAGCTCCTGTAG RV: CATCTAGAATTCCTCCTTAAATA	pHT315-Cry2Aa-Deletion of 45 N-terminal (Δ45).	**Yes**
7	Fw:AATAATCATAGTTTATATGTAGCTCC Rv: TTTTTTCCACTCCATCCATTCTTTTTGG	pHT315-Cry2Aa-KNN (43,44,45)	**Yes**
	Fw: CGTACCGATCATAGTTTATACCTAGATCCT Rv: TTTCCACTCCGTCCATTCCTT	pHT315-Cry2Ab-RTD	**Yes**
10	Fw: CAACATAAATCATTAGATACCATCC Rv: AAAACTAAATGGATCATGGG	pHT315-Cry2Aa-E27Q	**Yes**
12	Fw: CATCATCACCATCACCACTAAGGTTTGAGTGAATGTACA Rv: ATTAGTTGGCACAAACATAAT	pHT315-Cry2Aa-C-terminus His-Tag	**Yes**
13	Fw: TTTTGCTAGCGAAAGTGGGGAGTCTTATTGGAAAAAGG Rv: AACTAGACACAGYCTCGACTACAGG	pHT315-Cry2Aa-T56A	**Yes**
14	Fw: TTTTGCTAGCGAAAGTGGGGAGTCTTATTGGAAAAAGG Rv: AACTAGACACAGYCTCGACTACAGG	pHT315-Cry2Aa-T56A/L63A	**Yes**

2.1.5 Reagents and enzymes

Reagents from Sigma-Aldrich: SDS, Tris-HCl, ammonium persulfate, Bromophenol Blue, β-mercaptoethanol, TEMED, acrylamide/bis-acrylamide 30%, sodium carbonate, Coomassie Brilliant Blue R-250, BSA, and IPTG, and Chymotrypsin.

Reagents from AnalR BDH: glucose, NaOH, EDTA, $CaCl_2$, methanol, 1-butanol, and sodium acetate.

Reagents from Thermo Fisher Scientific: Sucrose, glycine, KCl, NaCl, HCl, glycerol, mono-potassium phosphate, di-potassium phosphate.

Reagents from New England Biolab: Pre-stained Protein Ladder, 1kb DNA ladder, DpnI, T4 DNA ligase, and *HaeIII*.

Reagents from Biotium: Gel red.

Reagents from Melford: Tris-base, ampicillin, and agarose.

Reagents from Roche: Protease inhibitor cocktail.

Antibodies: HRP 6x- His tag Monoclonal Antibody, invetrogen.

2.2 Methods

2.2.1 SDS-PAGE gels

For protein analysis and separation, different percentages of SDS-PAGE (Soduim Dodecyl Sulphate-Polyacrylamide Gel Electrophoresis) gel were used. Two glasses plates were cleaned and wiped by ethanol. The glasses were sealed by 200 µl of 1% of SDS agarose (0.1g in 10 ml of 1x SDS

buffer). The glasses were heated before sealing to facilitate the movement of the agarose to the bottom of the plates.

Resolving gel was prepared freshly as following:

Component	**Volume (µl) 7.5%**	**Volume (µl) 12%**
Water	2000	1400
Resolving gel buffer (RGB)	1000	1000
30% Acrylamide (v/v)	1000	1600
Ammonium per sulphate (APS)	8	8
TEMED	4	4

After applying the gel component into the glasses, 200 µl of water-saturated butanol was added at the top of resolving gel. The gel was left 20-30 minute to polymerize before washing the butanol with distilled water. That was followed by adding the stacking gel.

The component of stacking gel as follow:

Component	Volume (µl)
Water	1170
Stacking gel buffer (SGB)	500
30% Acrylamide (v/v)	333
Ammonium per sulphate (APS)	4
TEMED	2

The comb was applied immediately after adding the stacking gel. The gel was left 20-30 minutes to set up followed by installing it into electrophoresis apparatus as indicated by manufacturer.

5 µl of 2x denaturing sample buffer were added to 5 µl of sample. The mixture was heated for 4 minutes at 95C^{O}.

2.2.2 Native-PAGE gels

For protein analysis and separation, different percentage of native-PAGE gel systems were used. In this system, proteins are running in their natural form instead of denaturing them. Two glasses plates were cleaned and wiped by ethanol. The glasses were sealed by 200 µl of 1% agarose (0.1g in 10 ml of 1x Native running buffer). The glasses were heated before sealing to facilitate the movement of the agarose to the bottom of the plates.

Resolving gel was prepared freshly as following:

Component	**Volume (µl) 7.5%**	**Volume (µl) 12%**
Water	2000	1400
Resolving gel buffer (RGB)	1000	1000
30% Acrylamide (v/v)	1000	1600
Ammonium per sulphate (APS)	8	8
TEMED	4	4

After applying the gel component into the glasses, 200 µl of water-saturated butanol was added at the top of resolving gel. The gel was left 20-30 minute to polymerize before washing the butanol with distilled water. That was followed by adding the stacking gel.

The component of stacking gel as follow:

Component	**Volume (µl)**
Water	1170
Stacking gel buffer (SGB)	500
30% Acrylamide (v/v)	333
Ammonium per sulphate (APS)	4
TEMED	2

The comb was applied immediately after adding the stacking gel. The gel was left 20-30 minutes to set up followed by installing it into electrophoresis apparatus as indicated by manufacturer.

5 µl of 2x naive sample buffer (2.5 ml 1 M Tris-HCl pH 6.8, 0.5 ml H_2O, 0.8 ml 1% bromophenol blue, 4 ml glycerol) were added to 5 µl of sample with no samples heating.

After loading samples, the electrophoresis apparatus was plugged to power supply with inverting the electrode to invert the movement of the current, and set up to 160V and run for 50 minutes. Following the running, the gel was taken from the glass plates and stained with commassie blue stain for 20 minutes with shaking. After visualization of bands, the stain was washed by water until the background became clear.

2.2.3 Transformation

2.2.3.1 Electroporation method for Bt transformation

Bt strain frozen in glycerol at -80C^O was streaked on non-antibiotic LB agar plate and left to grow overnight at 37C^O. Grown culture was scraped and transferred into 100ml of non- antibiotic liquid LB media and let to grow by shaking at 37C^O. The OD_{600} was monitored frequently until it reached 0.4-0.6. After that, the cells was harvested from the media by centrifugation at 15,000 rpm for 10 minutes. Cells were washed and resuspended in sterilized cold water and centrifuged again at 15,000 rpm

for 10 minutes. After that, cells were resuspended and concentrated in 1 ml of cold distilled water and centrifuged for 1 minutes at 14,000 rpm. Cells were resuspended in 200 µl of distilled water. For each transformation reaction, 1 µl of DNA was added to 50 µl of competent cells, followed by transferring the whole mixture into electroporation cuvette. Electrical pulse of 1.8 kv was applied to pass through the mixture followed by transferring the mixture into glass bottle containing non-antibiotic LB media. Sample was let to grow on a shaker for 1 hour at 37C^{O}. Finally, sample was poured on agar plate containing proper antibiotic and left to grow overnight at 37C^{O}.

2.2.3.2 Heat Shock method for *E.coli* transformation

This protocol was provided by the manufacture, New England Biolabs.

A tube containing 50µl of *E.coli* competent cell was thawed on ice for 10 minutes. 1 µl of DNA was added to the competent cells followed by flicking the tube gently. The mixture was placed on ice for 30 minute. The reaction was heat shocked for 30 second at 42^{O}C followed by placing the reaction back to ice for 5 minutes. 950 µl of room temperature SOC media was added to recover the cells and placed on 37^{O}C shaker for 1 hour. 500 µl of the reaction was poured into warm and dry plate containing appropriate antibiotic. Finally, the plate was left in 37C^{O} incubator overnight to let cells grow.

2.2.4 Restriction enzyme digestion

HaeIII restriction enzyme was used to digest DNA plasmid that was extracted to confirm the correct DNA. 2 µl of Plasmid DNA was incubated with 0.5µl of *HaeIII* restriction enzyme with appropriate buffer enzyme buffer. Distilled water was added to make up the volume up to 10 µl. The reaction was placed in 37C^{O} water bath for 60 minutes, followed by running the digestion product on agarose electrophoresis to compare the product with predicted digestion generated by NEBcutter website.

2.2.5 Protein expression and harvesting from *Bt*

After transformation a single colony from a plate was picked and streaked onto a new agar plate containing appropriate antibiotic. After that, plates were left to grow at 30^{O}C for around 3 days. After 3 days, cells were checked under the microscope to confirm lysis of bacterial cells and the presence of crystals. After confirming the presence of crystals, the whole culture of *Bt* was scraped and resuspended in 30ml of distilled water. After that resuspended cell were sonicated for 1 minute for 4 times with 1 minute interval. After sonication, cells were centrifuged at 10,000 rpm for 30 minutes and the supernatant was discarded. Pellets were resuspended in 30ml of distilled water followed by another sonication procedure for 1 minute 4 times with 1 minute interval. After the second sonication, cells were centrifuged again at 10,000 rpm for 20 minutes. Finally, pellets were resuspended in 1 ml of water and the crude sample was kept at -20^{O}C.

2.2.6 Protein expression and harvesting from *E.coli (BL21-D3 pLysS)*

Bacterial growth containing the gene of interest was grown in 500 ml of 2X LB media at 37^{O}C containing appropriate antibiotic until the OD_{600} reached 0.4-0.6 followed by adding IPTG inducer to a final concentration of 1mM. It was then let to grow for 16 hours at 25^{O}C, followed by centrifugation the media to harvest the cells from the media. Pellets were then resuspended in 30ml of distilled water. After that resuspended cells were sonicated for 1 minutes for 4 times with 1 minute interval. After sonication, cells were centrifuged at 10,000 rpm for 30 minutes and the supernatant was discarded. Pellets were resuspended in 30ml of distilled water followed by another sonication procedure for 1 minute 4 times with 1 minute interval. After the second sonication, cells were centrifuged again at 10,000 rpm for 20 minutes. Finally, pellets were resuspended in 1 ml of water and the crude sample was kept at -20^{O}C.

2.2.7 PCR reaction

PCR was undertaken to generate single site-direct mutation from the template, wild-type gene of Cry2Aa. After running PCR, DpnI enzyme was added to destroy the methylated template DNA.

Primers were designed based on the location of the mutagenesis with the gene. Primers were ordered from MWG-Eurofins. As indicated from the manufacture, each primer concentration was adjusted to a concentration of 100 pmol/µl (100µM) followed by a 1:10 dilution.

The protocol for the amplification as follow:

Component	Amount per reaction (µl)	source
Master mix	25	PfuUltra hot start master mix, Agilent.
Forward primer	1	
Reverse primer	1	
DNA template	1	
Distilled water	22	
Total volume	50	

The PCR procedure was set up as follow:

Step	Temperature	Time (seconds)
Heat led	105^{O}C	120
Denaturation	92^{O}C	40
Annealing	51^{O}C	480
Elongation	68^{O}C	330
30 cycles		
Final elongation	68^{O}C	330
Final hold	100^{O}C	

2.2.8 Agarose gel electrophoresis

1% of agarose gel was prepared. That was made by dissolving 0.3 g of agarose in 30 ml of 1X TBE solution (Tris-Borate-EDTA) in glass bottle.

This mixture was put in microwave to dissolve the agarose until the solution became clear. After that, the solution was left to cool down in room temperature followed by adding 0.5 µl of GelRed dye. The gel was then poured into electrophoresis gel tray and placed in the right orientation for running. 5 µl of sample was mixed with 1 µl of loading dye and the whole 6 µl was loaded into wells alongside a DNA marker. The gel containing samples were let to run at 120 V in 1X TBE buffer inside electrophoresis chamber. Samples were detected by exposing the gel to ultraviolet light.

2.2.9 DNA purification form agarose gel

The DNA agarose gel containing PCR samples was placed on the surface on UV trans illuminator at low emission power. Using a clean scalpel, DNA band was excised. The purification was performed using a Qiaprep gel purification kit. 600 µl of QG buffer was added to 1.5 ml Eppendorf tube containing excised band. That was followed by incubating the mixture at 50^{O}C for 10 minutes with regular vortexing to facilitate gel dissolution. The mixture was then transferred to a spin column and centrifuged at 14,000 rpm for 1 minutes. The flow though was discarded and the column was washed by adding 500 µl of QG buffer then centrifuged at 14,000 rpm; followed by adding 750 µl of PE buffer followed by centrifuged at 14,000 rpm for 1 minutes. Spin column was further centrifuged to dry it from any remaining residues of PE buffer. Spin column was then transferred to clean

1.5 ml Eppendorf tube. 30 µl of elution buffer EB (10Mm Tris-HCl pH8.5) was added to spin column and left for 1 minute to ensure complete resuspension of the DNA. Finally, spin column was centrifuged at 14,000 rpm for 1 minute.

2.2.10 Ligation reaction of PCR product

After checking having the correct PCR product and purified the product from the agarose gel, the two phosphorylated ends of the PCR product had to be ligated. 8.5 µl of DNA was mixed with 1 µl of ligation buffer and 0.5 µl of ligase. The reaction was incubated at 16^{O}C overnight (16 hours). Following this ligation reaction, the DNA was ready for bacterial transformation.

2.2.11 Plasmid miniprep and restriction enzyme digestion

After introducing DNA into DH5α bacteria, plasmid extraction kit (miniprep) procedure was done as manufacture indicated:

1- Around 1 cm^2 of bacterial growth was scraped and resuspended in 250 µl of lysis buffer (P1 buffer) in 1.5 ml Eppendorf tube.

2- 250 µl of P2 buffer was added to the mixture and mixed by inverting the tube 4-6 times until the mixture become clear.

3- 350 µl of neutralization buffer (N3 buffer) was added to the mixture and mixed by inverting the tube 4-6 times.

4- The mixture was the centrifuged at 14,000 rpm for 10 min.

5- The clear solution was then transferred into spin column.

6- The spin column was centrifuged at 14,000 rpm for 1 minutes.

7- The spin column was washed by 500 µl of PB buffer

8- The column was washed with 750 µl of PE buffer.

9- Spin column was centrifuged again to remove any remaining residues of PE buffer.

10- Column was transferred into new tube, and 50 µl of elution buffer (EB) was added and left to stand 1 minute to ensure complete resuspension of DNA.

11- Column was centrifuged at 14,000 rpm for 1 minute.

The above procedure was applied on *E.coli* bacteria. However, when plasmid DNA from Bt was required to be extracted, an extra step was to dissolve lysozyme in P1 buffer (10mg/ml) and 30 minutes incubation at $37^{O}C$.

2.2.12 Confirmation of generated mutation

DNA plasmid was required for major confirmation of successful generation of mutations. That was done by sequencing the DNA through MWG Eurofins genomic company. Specific Reverse complement sequencing primer was designed and ordered.

2.2.13 Determination of protein concentration

Crude samples of proteins diluted in known dilution factor were run alongside with known three different concentrations of bovine serum albumin (BSA) on a SDS-PAGE gel. Images of gels were obtained, and analysed using Image J software to quantify protein concentration.

2.2.14 Protein solubilisation and activation by proteases

A known volume of crude samples containing crystals and spores was thawed on ice and vortexed to ensure homogenization. Samples were centrifuged for 5 minutes at 14,000 rpm and pellets containing proteins were resuspended in solubilisation buffer (50mM NaOH pH. 11). The reaction was incubated at 37^{O}C for 1 hour. After that, the reaction was centrifuged for 5 minutes to pellet spores and the supernatant was transferred to a new 1.5 ml Eppendorf tubes. To activate the toxins 1mg/ml of chymotrypsin, at a 2:1 (v/v) protease to toxins ratio was applied. However, to activate toxins by AMJ, 1/5 dilution of AMJ was used in 5:1 (v/v) enzyme to toxin ratio.

2.2.15 Mosquito rearing

A. aegypti eggs were supplied from University of Cardiff in a filter paper, the eggs were cultured in our Sussex University facility.

2.2.15.1 Feeding mosquitoes

Male and female adults were fed on 20% sucrose solution. After preparation, long piece of cotton was soaked in sucrose solution followed by dipping the cotton wool from the bottom of the sucrose bottle in thread

like way to enable the insect to directly drink the sucrose through the cotton wool. Female mosquitoes fed daily with fresh heparinised horse blood. That was done by pouring fresh blood into metal bottle cap followed by sealing the cap by stretched parafilm. The sealed cap containing fresh blood was placed in a hole made on the side of the cage wall where the parafilm side faces inside the cage. After that, 37^{O}C heating block was carefully placed against the outer side of the cap to warm the fresh blood. Blood was changed daily when there was high demand of eggs, or every other day when there was no high demand of eggs. Larvae were fed with grounded fish food.

2.2.15.2 Hatching the eggs

Filter paper containing eggs was submerged in a beaker containing clean water. The beaker was then placed into an incubator at 23^{O}C. Eggs usually hatched within 24 hours, and once they had hatched, little amount of crushed fish food was supplied.

2.2.15.3 Transferring pupae

Larvae usually developed to pupae phase within a period of a week. Once they became pupae, they were transferred by pasteur pipettes from 27^{O}C incubator into adult mosquito cage and remain submerged in water until they finally developed to adult mosquitoes.

2.2.16 Bioassays

Ten third instar *A. aegypti* larvae were placed in a beaker containing 40 ml of sterilized water (4 ml of water per 1 larvae). Each beaker contained one

concentration of toxin: (0 ng/ml, 125 ng/ml, 250 ng/ml, 500 ng/ml, 1000 ng/ml, and 2000 ng/ml); and control beaker contained either just water or solubilisation buffer. That was followed by incubating them at 23^{O}C for 72 hours; dead larvae were recorded and the mortality percentage was calculated after repeating each assay 3 times. The LC50s were calculated using SPSS software.

2.2.17 *A. aegypti* midgut juice preparation

To prepare *A. aegypti* midgut protease, 50 late 3rd larvae (L3) were transferred into ice cold water. Cold water completely restricts larvae movement. Once they are unconscious, one larvae was transferred onto a plain surface with few drops of water, and then were dissected by cutting the head using thin forceps. This is followed by pulling out the end of larvae body where the midgut tissue comes out. The dissected midgets' were then placed in 100µl of 1X PBS, and was crushed using a glass homogenizer. The mixture was then centrifuged for 10 minutes at 9,000 rpm at 4^{O}C. Supernatant containing midgut juice (AMJ) was transferred into new 1.5 ml Eppendorf tubes and pellets were discarded. The protease were stored at -80^{O}C.

2.2.18 BBMV preparation

A. aegypti gut was extracted and placed in 500 µl cold MET buffer (250mM mannitol, 5mM EGTA, 17mM Tris-HCL) pH7.5. Extracted guts were homogenized by a glass homogenizer. 500 µl ice cold 24mM $MgCl_2$+

250mM sucrose was added and the whole mixture was incubated on ice for 30 minutes. After that, the mixture was centrifuged at 14,000 rpm for 15 minutes at $4^{O}C$. The supernatant was collected and centrifuged at 14,000 rpm for 30 minutes at $4^{O}C$. The pellets were then resuspended in half volume of MET buffer followed by adding 1 volume of 24mM $MgCl_2$+ 250mM sucrose, and incubated for 30 minutes. After that, the mixture was centrifuged at 14,000 rpm for 15 minutes at $4^{O}C$. The supernatant was collected and centrifuged at 14,000 rpm for 30 minutes at $4^{O}C$. Finally, the pellets were resuspended in 100µl of 1XPBS and stored at $-80^{O}C$.

2.2.19 Dot blotting

5 µl of samples were dried on nitrocellulose membrane for 5-10 minutes. The membrane was blocked for 1 hour by 10ml of blocking buffer (1.5 g of dried milk dissolved in 30 ml of 1X PBS solution containing Tween-20). The membrane was then washed for 5 minute for five times by washing buffer (TBPS). The membrane was then incubated with antibody (20µl of anti-His-tag added to 10 ml of blocking buffer) for 1 hour. That was followed by 5 minutes washes five times by washing buffer. The membrane was then incubated with ECL buffer (10 ml of 200mM Tris-HCl, 3 ml H_2O_2, 50 µl luminol, 25 µl of coumaric acid) for 1 minutes with rocking. The membrane was then developed to visualize signals.

2.2.20 Affinity column purification

400 µl of slurry Ni-NTA beads (containing 200 µl of pure beads) was pipetted into clean spin tubes and centrifuged for 1 minute at 14,000 rpm to eliminate ethanol. Column was washed 5 times by equilibration buffer (50mM NaOH, 1X PBS pH 9). 100 µl of protein sample was then applied to the equilibrated column and incubated for 1 hour with frequent vortexing at 4^{O}C. The column was then centrifuged for 1 minutes at 3,000 rpm and the flow through was saved and placed on ice for further analysis. Column was then washed 5 times by 200 µl of washing buffer (50mM NaOH, 1X PBS, 2mM imidazole pH. 9) followed by centrifugation at 3,000 rpm for 1 minutes. Wash fractions were placed on ice for further analysis. 50 µl of elution buffer (50mM NaOH, 1X PBS, 150mM imidazole pH. 9) was applied into the column and left for 5 minutes. 5 elution fractions were collected. Flow through, washes, and elution fractions were analysed on SDS-PAGE to detect proteins band.

2.2.21 Binding assay

Binding protocol was adopted from (Wang et al., 2018) with some modifications. 20 µg of *A. aegypti* BBMV was incubated with different forms of Cry2Aa toxin in total volume of 100 µl in binding buffer (1XPBS, 0.1% Tween 20, 0.1%BSA pH7.4) for 2 hours at room temperature. That was followed by centrifuging the mixture for 10 minutes at 14,000 rpm to pull down bound proteins. The unbound proteins were washed out by washing the pellets twice with 100µl of cold binding buffer. Final pellets

were resuspended in 10µl of 2X SDS sample buffer and boiled at 95^{O}C for 5 minutes. It was then analysed on 7% SDS-PAGE. Three biological repeats were included in this experiment.

2.2.22 Western blot

Protein samples were analysed on 7% SDS-PAGE followed by incubating the gel and nitrocellulose membrane simultaneously in semi-dry blotting buffer (Tris-base 48mM, Glycine 39mM, Methanol 20%, SDS 0.04%) for 5 minutes. Transfer sandwich was made by applying one pre-soaked, in semi-dry buffer, filter paper, pre-incubated nitrocellulose membrane; pre-incubated acrylamide gel, and another pre-soaked filter paper. Transferring was set to run for 1hour and 15 minutes at 100mA (or 45 minutes for smaller fragments). After that, nitrocellulose was stained by reversible PonceauS stain (0.1g PonceauS, 5 ml acetic acid, in 100 ml H_2O) to check the successful transferring of the protein; distaining of the PonceauS was done by washing the membrane with 1XPBS. The nitrocellulose membrane then was incubated with blocking buffer (10 ml of 5% dry milk dissolved 1XPBS+Tween20) for 1 hour. For detecting Cry2A protein containing His-tag, 20µl of HRP conjugated His-tag antibody was added to 10 ml 5% dry milk dissolved in 1XPBS+Tween20 (1:500 dilution) and was incubated with the membrane for 1 hour with rocking. That was followed by washing the membrane with 1XPBS+Tween20 three time, 5 minutes for each wash. The membrane was incubated with 10 ml of ECL buffer (5 ml 250mM

Luminol, 90mM Pcoumaic acid, 1 M, 3 µl H_2O_2 Tris-HCl pH 8.5), for 1 minute followed by developing the membrane using UVP ChemStudio image detector. The membrane was then developed using UVP ChemStudio image detector. For detecting Cry2A protein using Cry2A antibody, it was required to add 3µl of secondary anti-body following the third wash after primary anti-body, followed by 1 hour incubation.

2.2.23 Oligomerization assay

Oligomerization assay was similar to the binding assay; however, the final pellets were resuspended in 2X SDS sample buffer and were divided into three samples heated at 30^{O}C, 60^{O}C and 95^{O}C. It was then analysed on 7% SDS-PAGE before performing western blot using Cry2A antibody.

2.2.24 N-terminal sequencing.

Protein samples were analysed on 7% SDS-PAGE followed by incubating the gel in semi-dry blotting buffer (Tris-base 48mM, Glycine 39mM, Methanol 20%, SDS 0.04%). Transfer sandwich was made by applying pre-soaked, in semi-dry transferring buffer, filter paper, pre-incubated PVDF membrane; pre-incubated acrylamide gel, and pre-soaked filter paper. Transferring was set to run for 1 hour and 15 minutes at 100mA. After that, PVDF membrane was stained by reversible PonceauS stain (0.1g Ponceau, 5 ml acetic acid, in 100 ml H_2O) to check the successful transferring of protein; distaining of the Ponceau was done by washing the

membrane with 1XPBS. The PVDF membrane containing protein band was sent to ALTAbioscience Company to perform amino acid sequencing.

3. Investigating the attachment of the cleaved Cry2Aa N-terminus to the rest of the protein.

3.1 Introduction

In this chapter, we aimed to test the validity of the "**intact N-terminal model**", which previously hypothesized that the Cry2Aa N-terminus is cleaved by *Aedes* midgut protease but remains attached to the whole protein; consequently, it can bind to BBMV receptors and the toxin shows activity to *A .aegypti* (Joseph, 2019).

3.2 Results

3.2.1 *pHT315*-Cry2Aa expression system

The gene encoding Cry2Aa was previously cloned into pSVB40 Bt expression plasmid. It is important to note that Cry2Aa gene is located within an operon that has three genes; ORF1, ORF2, and Cry2Aa gene in which sporulation dependent promoter is located upstream of this operon. It has also been shown that the expression of ORF2 gene is crucial for Cry2Aa crystallization (Crickmore and Ellar, 1992). In addition, it was previously shown that another expression plasmid, pHT315, enhanced the expression of Cry toxins (Arantes and Lereclus, 1991). In this project, we

expressed all Cry toxins using pHT315 plasmid. The expression systems of pHT315 is illustrated in figure 3.2.1.1.

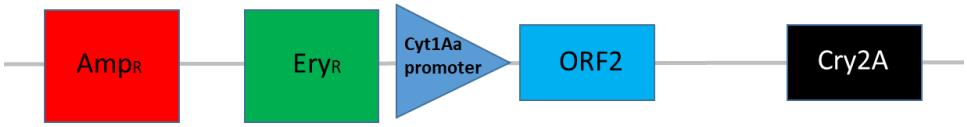

Figure 3.2.1.1: Construction of pHT315 plasmid containing Cry2A toxin. AmpR: ampicillin resistance gene; EryR: Erythromycin resistance gene; ORF2: open reading frame 2; Cry2A: Cry2A toxin

3.2.2 Cry2Aa treatment by *Aedes* midgut juice (AMJ) produces a 58 kDa protein fragment.

The treatment of Cry2Aa by different insect midgut proteases produces different digestion products; for instance, processing of Cry2Aa by AMJ produces a 58 kDa fragment (figure 3.2.1.2), while treating Cry2Aa by chymotrypsin and some lepidopteran species midgut proteases produces a partial digestion of 58 kDa fragment before a final product of 50 kDa. The activities of these digestion products are also different toward different insect species; for instance, Cry2Aa treated by AMJ (58 kDa) showed activity to *Aedes* while chymotrypsin treatment (50 kDa) did not (Joseph, 2019).

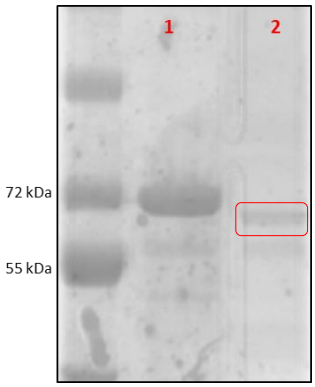

Figure 3.2.1.2: Processing of Cry2Aa by AMJ. **Lane1:** solubilized Cry2Aa; **lane2:** AMJ treated Cry2Aa *(58 kDa fragment is indicated by red box).*

3.2.3 Use of native gel system to compare AMJ treated and untreated Cry2Aa.

In this study, we aimed to compare AMJ activated Cry2Aa and solubilized Cry2Aa by analysing them on native gel electrophoresis in order to determine if the N-terminus remains attached or not. In native gel analysis, there is no protein denaturation and proteins migrate in the gel in their native form. Native gel electrophoresis analysis mainly depends on the difference between protein *pI* and the pH of the gel system. If the N-terminus remains attached after activation, then the AMJ activated protein would be expected to migrate similarly to the solubilized protein.

A previous study in our lab was not able to obtain conclusive data using a Tris-CAPS native gel system. We used different native gel system, gamma aminobutyric acid (GABA) which has a different pH to Tris-CAPS (with *pI* of 4.8). However, we were only able to detect the migration of AMJ treated Cry2Aa; whereas we failed to detect the migration of solubilized Cry2Aa or chymotrypsin treated Cry2Aa as shown in figure 3.2.3.1.

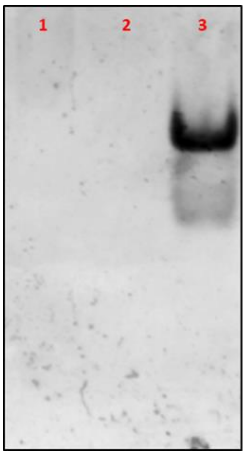

Figure 3.2.3.1: Native-PAGE analysis of solubilized and activated Cry2Aa. **Lane1:** solubilized Cry2Aa; **lane2**: chymotrypsin activated Cry2Aa; **lane3:** AMJ activated Cry2Aa.

Many experiment optimizations, changes, and repeats were applied to this gel system; however, we were unable to achieve protein migration for all samples using native-PAGE gel analysis. Therefore, we moved to an alternative approach.

3.2.4 Creating His-tagged Cry2Aa recombinant protein

This approach aimed to test the interaction of cleaved N-terminus of Cry2Aa to the rest of the protein. 6xHis Tag protein was suggested to be fused with Cry2Aa at the N-terminus. This recombinant protein should enable us to investigate the attachment of cleaved N-terminus to the whole Cry2Aa protein.

DNA template used to create His-tagged protein was Cry2Aa wildtype. Specific primers were designed to anneal at the beginning of the gene with overhanging nucleotides in the forward primer coding for 6xHis-tag. The reverse primer has the complementary sequence of the other strand and it binds at the first base of the opposite direction of the forward primer. The amplification reaction involved amplifying the whole plasmid (10.1 kb). Both primers were phosphorylated at 5`end for ligation as shown in Figure 3.2.4.1

Primers were designed as follow:

Fw: P- catcatcaccatcatcacAATAATGTATTGAATAGTGG
Rv: P- CATATAAAATTCCTCCTTAAATATC

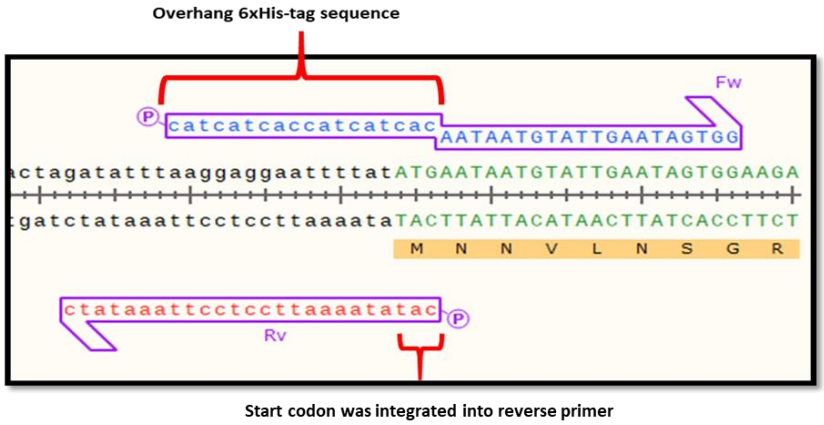

Figure 3.2.4.1: Alignment of DNA sequence of *Cry2Aa*-wildtype with designed primers containing overhang sequence to fuse His-tag.

PCR reaction was performed to create this construct and was analysed on agarose gel to confirm successful amplification as shown in figure 3.2.4.2.

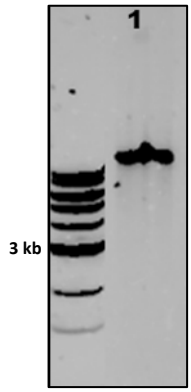

Figure 3.2.4.2: PCR product for creating His-tagged *Cry2Aa*. **Lane1:** PCR product.

After that, the DNA was purified from the agarose gel followed by ligation to form an intact plasmid (figure 3.2.4.3).

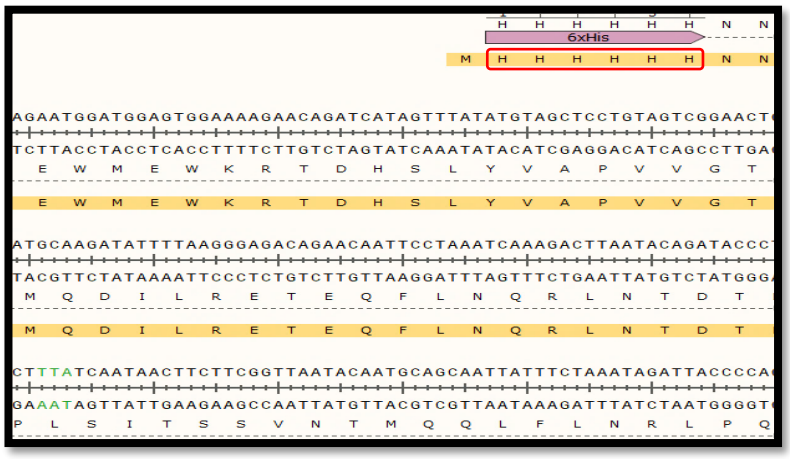

Figure 3.2.4.3: DNA sequence of His-tagged Cry2Aa toxin. Addition of His tag at the 5` end of Cry2Aa gene *(in red box).*

The ligated plasmid was then introduced into *E. coli* (DH5α) competent cells. Colonies were picked and streaked on a new agar plate and incubated overnight followed by extracting plasmids. Obtaining the correct Plasmid was confirmed by *HaeIII* restriction enzyme which then was analysed on agarose gel and compared to the expected DNA digestion generated by NEBcutter software as shown in figure 3.2.4.4.

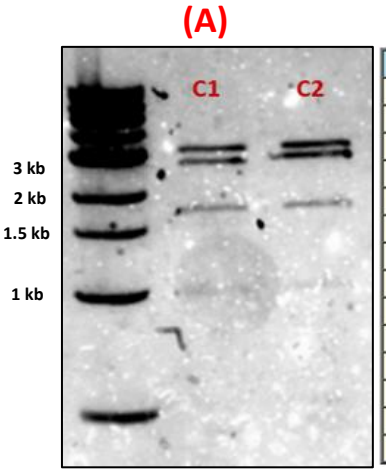

(B)

#	Ends	Coordinates	Length (bp)
1	HaeIII-HaeIII	5324-8182	2859
2	HaeIII-HaeIII	10168-2452	2457
3	HaeIII-HaeIII	8183-9767	1585
4	HaeIII-HaeIII	2958-3881	924
5	HaeIII-HaeIII	2453-2957	505
6	HaeIII-HaeIII	4519-4976	458
7	HaeIII-HaeIII	4085-4518	434
8	HaeIII-HaeIII	9768-10065	298
9	HaeIII-HaeIII	5057-5323	267
10	HaeIII-HaeIII	3882-4055	174
11	HaeIII-HaeIII	10066-10167	102
12	HaeIII-HaeIII	4977-5056	80
13	HaeIII-HaeIII	4067-4084	18
14	HaeIII-HaeIII	4056-4066	11

Figure 3.2.4.4: DNA fragments generated after *HaeIII* digestion. *A) HaeIII* digested DNA plasmid of His-Cry2Aa from two bacterial colonies; *B)* NEBcutter generated DNA fragments of His-Cry2Aa.

Based on the obtained DNA fragments, both colonies from His-Cry2Aa wildtype contained the correct plasmid; this was further confirmed by DNA sequencing.

After this confirmation, plasmid containing His-tagged Cry2Aa gene was introduced into Bt strain (78/11) as described in materials and methods. Transformed cells were incubated at 30^{O}C for 3 days, and that was followed by harvesting the protein. Dot blot analysis was performed to confirm the expression of His-tagged protein. This was applied by blotting crude, solubilized, and chymotrypsin treated Cry2Aa toxins with HRP His-tag antibody. As shown in figure 3.2.4.6, a high signal was detected with both crude and solubilized protein due the presence of the non-cleaved N-terminus containing His-tag. Chymotrypsin treated His-Cry2Aa significantly had a decreased signal due to removal of cleaved N-terminus containing His-tag.

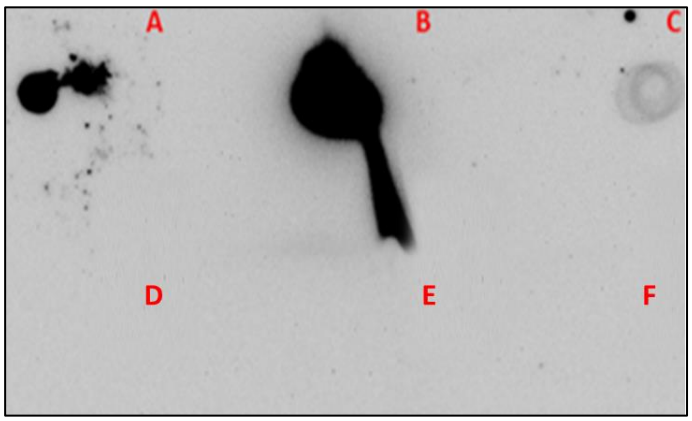

Figure 3.2.4.6: Dot blot analysis of His-Cry2Aa toxins. ***A)*** Crude His-Cry2Aa; ***B)*** solubilized His-Cry2Aa; ***C)*** Chymotrypsin treated His-Cry2Aa; ***D)*** Crude Cry2Aa; ***E)*** Solubilized Cry2Aa; ***F)*** Chymotrypsin treated Cry2Aa.

Figure 3.2.4.7 shows the design of the Cry2Aa tagged protein.

Figure 3.2.4.7: Diagram Illustration of His-tagged *Cry2Aa*.

After that, His-tagged Cry2Aa was treated with AMJ to confirm obtaining a similar product to the wildtype toxin (figure 3.2.4.8).

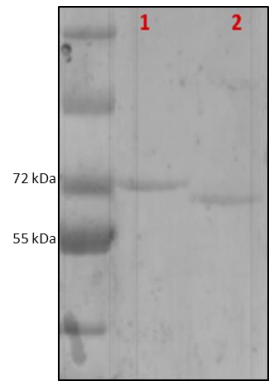

Figure 3.2.4.8: SDS-PAGE of His-Cry2Aa activation by AMJ. **Lane 1:** solubilized His-Cry2Aa; **lane2:** AMJ treated His-Cry2Aa.

3.2.5 Identifying the attachment of His-tagged cleaved N-terminus to the rest of the protein.

N-terminus of Cry2Aa protein containing His-tag is suggested to bind Ni beads as poly Histidine residues have high affinity to Ni beads. Cry2Aa protein was treated with AMJ followed by applying the sample to a column containing Ni beads. After that, the mixture was incubated, washed and eluted from the column. All fractions were analysed on SDS-PAGE and based on the presence of the main toxin fragment (58 kDa) we were able to show if there was attachment or not.

This process should result in two possibilities; first, if the two protein fragments (cleaved His-tagged N-terminus and the rest of the protein)

remained attached, then both fragments should have been detected in the elution fractions. Second, if the two protein fragments do not remain attached, then the His-tagged N-terminus should have been present in the elution fractions while the rest of the protein (58 kDa fragment) should have been detected in the flowthrough or wash fractions. The Ni beads affinity purification strategy is illustrated in Figure 3.2.5.1.

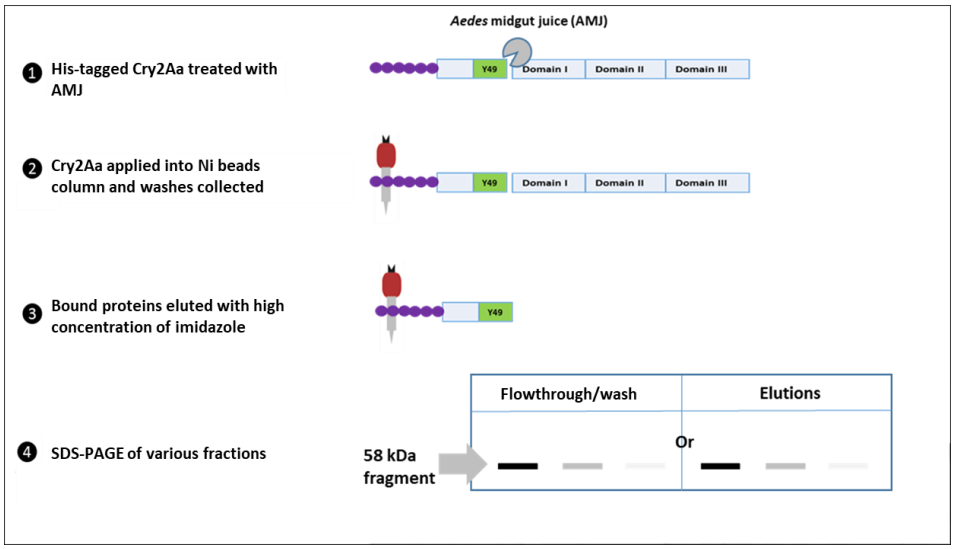

Figure 3.2.5.1: The strategy of investigating the attachment of the Cry2Aa N-terminus after AMJ treatment.

Before testing our hypothesis, we had to confirm that this procedure performs properly. That was confirmed by testing the binding efficiency between the non-cleaved His-tagged Cry2Aa and Ni beads. Ni beads were placed in spin column followed by incubating the mixture for 1 hour at $4C^{O}$ with frequent shaking. After that, the column was centrifuged, and the flow through containing unbound proteins was collected and kept for further analysis. The bound protein was eluted by adding high concentration of

imidazole; followed by analysing all fractions on SDS-PAGE (figure 3.2.5.2).

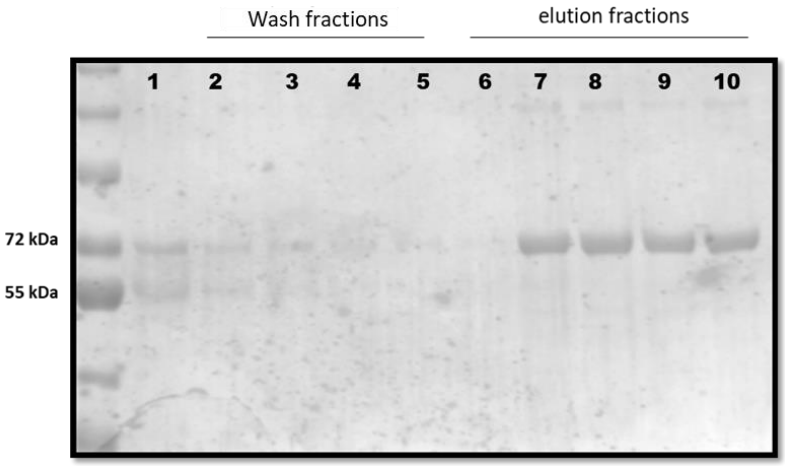

Figure 3.2.5.2: SDS-PAGE of Ni bead affinity binding of solubilized His-Cry2Aa using spin columns. **Lane1:** flow through; **lanes 2-5:** wash fractions; **lanes 6-10:** elution fractions.

From figure 3.2.5.2, the presence of His-tagged Cry2Aa (70 kDa fragment) in the elution fractions indicates successful binding of His-tagged Cry2Aa to the Ni beads. To test our hypothesis, we first confirmed successful cleavage of His-tagged Cry2Aa by AMJ as shown in figure 3.2.5.3. After that, we applied this protein to a spin column containing Ni beads as previously described (figure 3.2.5.4).

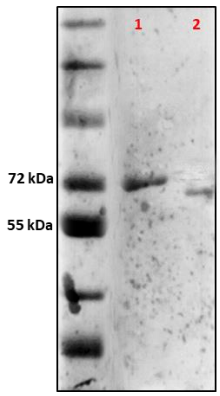

Figure 3.2.5.3: SDS-PAGE confirmation of AMJ activation of His-Cry2Aa. **Lane1**: Solubilized Cry2Aa. **Lane2:** AMJ treated Cry2Aa.

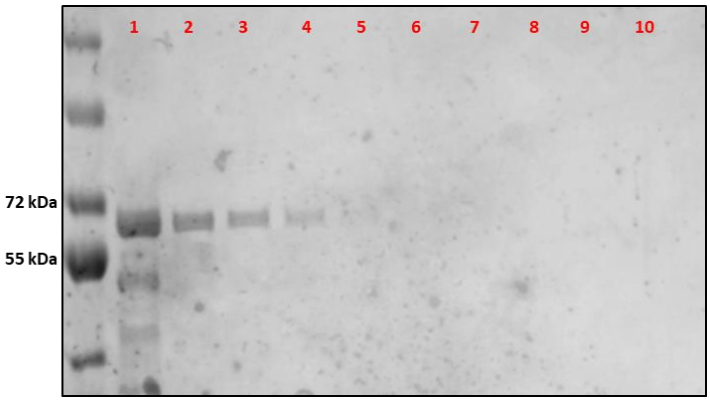

Figure 3.2.5.4: SDS-PAGE of Ni beads affinity binding of AMJ activated His-Cry2Aa protein using spin columns. **Lane1:** flow through; **lanes 2-6**: wash fractions; **lanes 7-10:** elution fractions.

Figure 3.2.5.4, clearly shows that 58 kDa fragment produced from AMJ digestion is present in the flow through (lane 1) and wash fractions (lanes 2-4). This indicates there is no attachment of the cleaved N-terminal region to the rest of the protein.

However, it remained a possibility that the interaction was weak and could be disrupted by the centrifugation and washing steps. Therefore, we aimed to confirm the lack of attachment using a gravity flow column.

To perform gravity flow affinity column, we tested the cleavage of His-tagged Cry2Aa by AMJ, and obtained successful cleavage as shown in figure 3.2.5.5.

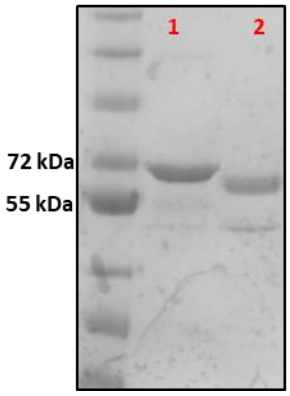

Figure 3.2.5.5: SDS-PAGE confirmation of AMJ digestion of His-Cry2Aa. **Lane1**: Solubilized Cry2Aa. **Lane2:** AMJ activated Cry2Aa.

Ni beads were then equilibrated in gravity flow column followed by incubating protein sample at 4°C for 1 hour with frequent shaking. Flow through, washing, and elution fractions were collected by draining due to gravity force. All fractions were then analysed on SDS-PAGE as shown in figure 3.2.5.6.

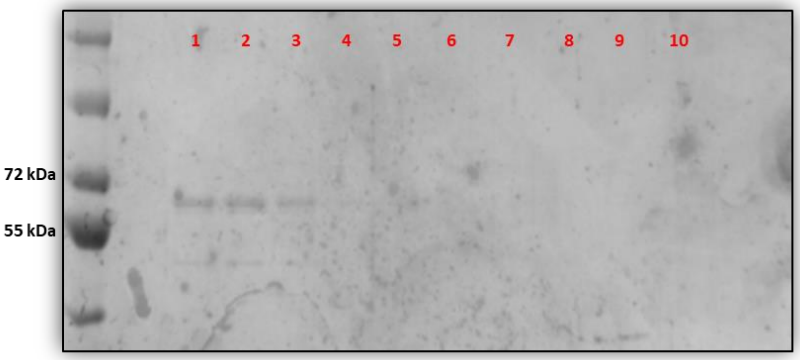

Figure 3.2.5.6: SDS-PAGE of Ni bead affinity column of AMJ activated His-Cry2Aa. **Lane 1-5:** wash fractions; **Lanes 6-10**: elution fractions.

Figure 3.2.5.6 shows that the 58 kDa fragment appeared in the wash fractions (lanes 1-4). This was consistent with our previous experiment performed using Ni beads in a spin column; and confirmed that there is no

attachment of AMJ cleaved N-terminus of Cry2Aa to the rest of the protein.

However, the next step was to confirm that AMJ does not cleave or digest the 6xHis-tag non-specifically. That was achieved by using a mutated toxin (Cry2Aa-KNN) which cleavage by AMJ was blocked. This mutant is described in detail in chapter 4. After that, western blot analysis was applied and the presence of His-tag was detected by His-tag antibody.

From figure 3.2.5.7, it can be seen that neither AMJ nor chymotrypsin digested the His-tag.

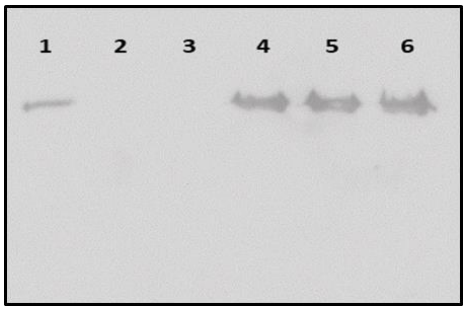

Figure 3.2.5.7: Western blot using 6xHis tag antibody. **Lane1:** Solubilized His-Cry2Aa-wildtype; **lane2:** His-Cry2Aa-wildtype treated by 1mg/ml of chymotrypsin; **lane3:** His-Cry2Aa-wildtype treated by AMJ; **lane4:** Solubilized His-Cry2Aa-KNN; **lane5**: His-Cry2Aa-KNN/L144A treated by 1mg/ml of chymotrypsin; **Lane6:** His-Cry2Aa-KNN treated by AMJ.

We then aimed to observe the 15 kDa N-terminal cleaved fragment containing His-tag. Different gel systems (16%tricine SDS-PAGE and 4-20% SDS-PAGE) were used but we could not observe the 15 kDa fragment. We performed western blot analysis following the Ni bead affinity chromatography using His-tag antibody (figure 3.2.5.8).

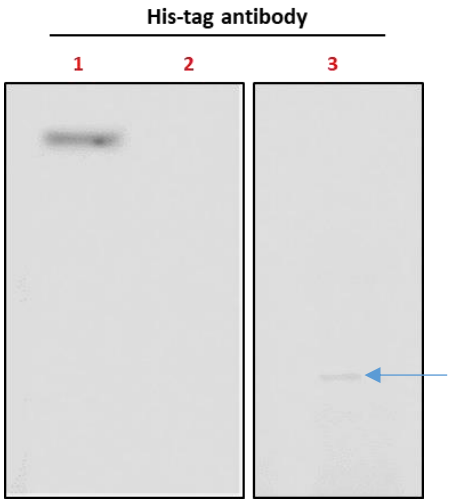

Figure 3.2.5.8: Western blot analysis of Ni bead affinity of AMJ cleaved His-Cry2Aa using His-tag antibody. **Lane1:** Solubilized His-Cry2Aa; **lane2:** Wash fraction; **lane3:** Elution fraction.

From figure 3.2.5.8, there was no signal in the wash fraction as the His-tag was cleaved from the N-terminal (lane 2). However, there was a signal from His-tag antibody in the elution fraction for a smaller size fragment around 15 kDa (lane 3- with a blue arrow).

3.3 Discussion

In this chapter, we were aiming to understand the previously proposed hypothesis "**Intact N-terminal model**" which suggested an attachment of the Cry2Aa N-terminus to the rest of the toxin after AMJ activation. Previous work found that the Cry2Aa N-terminus is important for toxin specificity toward *A. aegypti* (Joseph, 2019). As previously found, Cry2A hybrid proteins containing Cry2Aa N-terminal amino acids and the three domains of Cry2Ab showed activity towards *A. aegypti*. Also, Cry2Ab 49 N-terminal amino acids with the three domains of Cry2Aa lost the activity

to *A. aegypti*. Chymotrypsin cuts Cry2Aa to initially produce a 58 kDa due to cleavage at Y49, then finally a 50 kDa one due to cleavage at L144. Bioassay results revealed that chymotrypsin activated Cry2Aa (50 kDa) showed no activity to *A. aegypti* (Goje et al., 2020, Audtho et al., 1999). It was not clear why the activity of Cry2Aa is lost with further removal of the N-terminus region (50 kDa form).

The intact N-terminal model suggested that Cry2Aa N-terminus remains attached after activation by AMJ, and that attachment contributes to toxin-receptor binding. We initially attempted to test the attachment by using native gel electrophorese system. In this gel system, proteins migrate in their native form without denaturation. We aimed to compare solubilized Cry2Aa with AMJ activated. If there was attachment, we were expecting to see a similar migration pattern between solubilized Cry2Aa and AMJ activated Cry2Aa as the attachment between N-terminus and the whole protein is not disrupted in the native gel system. However, we were unable to compare migration pattern as the solubilized and AMJ activated toxins did not migrate well in the gel. We attempted to optimize the migration conditions, but were not able to obtain conclusive results. Therefore, we moved to use a protein affinity purification approach to test our hypothesis. The N-terminus of Cry2Aa was tagged with His-tag allowing it to bind to Ni beads. After that, we investigated whether the rest of the protein (58

kDa fragment) and the N-terminus remained attached or not. Our initial results showed that the 58 kDa appeared in the wash fractions suggesting no attachment; we repeated the technique using gravity flow column where there is less disrupting force.

4. Differential proteolytic processing of Cry2A proteins is associated with differential activity to *A. aegypti*.

4.1 Introduction

In the previous chapter we showed that the Cry2Aa N-terminus does not remain attached and the ERTD residues was lost after proteolytic processing. In our attempt to understand the role of Cry2Aa`s N-terminus in *Aedes* activity, we proposed that Cry2Aa activity might be related to differential proteolytic cleavage at its N-terminus region. Published evidence showed an association between Cry toxins cleavage and activity; for instance, differential proteolysis of a parasporin-3, Cry41Aa, showed different activities on liver cancer cells (HepG2). The activity of Cry41Aa was different towards HepG2 cells after proteolytic cleavage of its N-terminus by Proteinase K, forming an active toxin, and trypsin, forming non-active toxin (Souissi, 2018).

In Cry2A protein, previous studies showed an association between Cy2A cleavage and its activity toward different insects. In Cry2Ab, for instance, activity toward *Plutella xylostella* was associated with toxin cleavage at amino acids R139 and L144 producing a protein fragment of 50 kDa. Substitution of either R139 or L144 with alanine did not abolish this activity; but when both amino acids were substituted by alanine, the activity was lost and the production of the 50 kDa was blocked (Xu et al., 2016).

In Cry2Aa, there are some contradictions on the toxicity of processed forms of Cry2Aa. A study found that the midgut juice of *Lymantria dispar* cleaves Cry2Aa forming 58 kDa and 49 kDa fragments. It was found that there was no significant difference in the LC50 between the protoxin and the 58 kDa fragment; while the 49 kDa had no toxicity to *L. dispar*. That study also involved blocking the production of the 49 kDa fragment by creating a mutation at leucine 144 by substituting leucine to alanine, aspartate, glycine, valine, and histidine. All mutations blocked the production of the 49 kDa except L144H which had some production of the 49 kDa. The LC50 of all mutants showed no significant increase or decrease in activity to *L. dispar* compared to Cry2Aa-wildtype. Additionally, N-terminal sequencing showed that *L. dispar* midgut juice cleaves Cry2Aa between Y49 and V50 producing a 58 kDa band, and then between L144 and S145 producing the 49 kDa fragment (Audtho et al., 1999). Another study showed that Cry2Aa cleaved by chymotrypsin produced 58 kDa and 50 kDa fragments, but it showed toxicity to *Lymantria dispar* (figure 4.1.1) (Ohsawa et al., 2012).

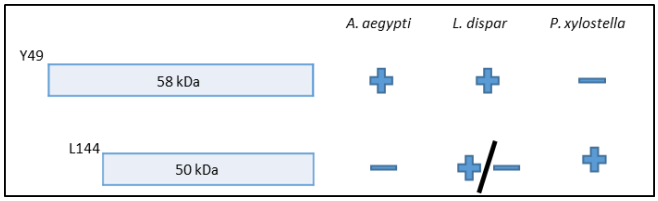

Figure 4.1.1: Illustration of differential activity of different cleavage products of Cry2A toxins towards different insects.

Cry2Aa is the only Cry2A member with its structure resolved; and based on that, Morse et al hypothesized that removal of the N-terminus of Cry2Aa (during proteolysis process) is required for its activity to dipteran and lepidopteran species (Morse et al., 2001). In the previous chapter, we showed that Cry2Aa is processed by AMJ, producing a 58 kDa fragment. However, the closely related toxin Cry2Ab, non-active to *Aedes*, was not processed by AMJ and did not produce a 58 kDa fragment (figure 4.1.2- lane 3) and showed no activity to *Aedes* (figure 4.1.3). To assess whether this differential activity resulted from the differential proteolytic cleavage, we aimed in this chapter to investigate Cry2A proteolytic cleavage and its association with activity toward *A. aegypti*.

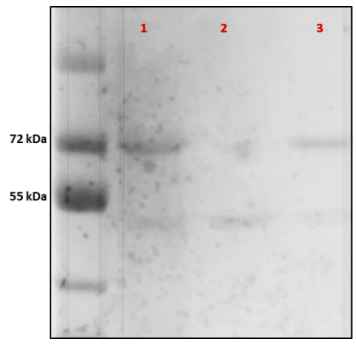

Figure 4.1.2: AMJ treatment of Cry2Ab-wildtype. **Lane 1:** solubilized Cry2Ab; **lane 2:** Cry2Ab treated by 1mg/ml of chymotrypsin; **lane 3:** Cry2Ab treated by AMJ.

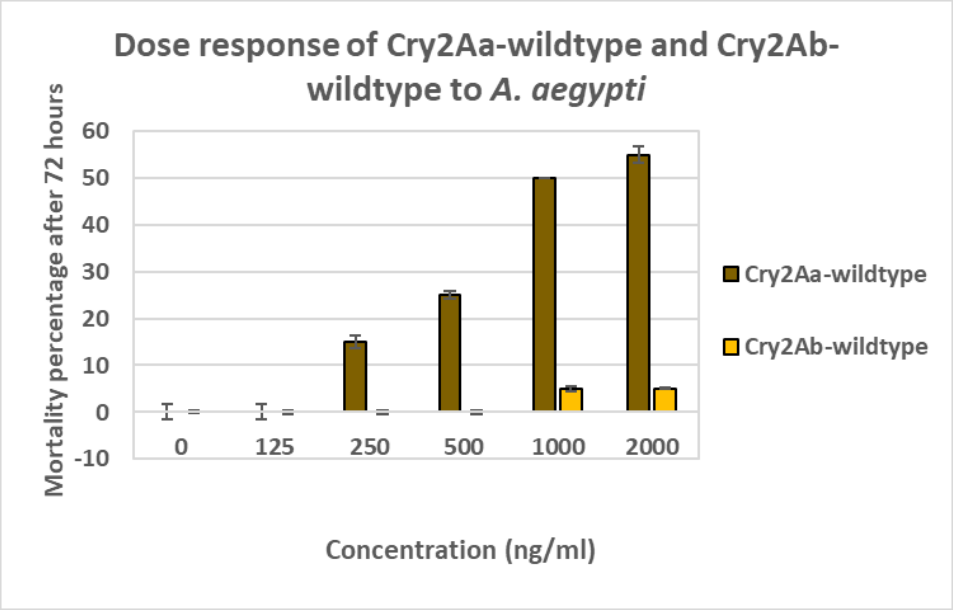

Figure 4.1.3: Dose response bioassay of different concentrations of Cry2Aa-wildtype and Cry2Ab-wildtype to *A. aegypti* after 72 hours.

4.2 Results

4.2.1 Identifying *Aedes* midgut juice cleavage site and testing if blocking its cleavage affects Cry2Aa activity towards *A. aegypti*.

4.2.1.1 Identifying the AMJ cleavage site in Cry2Aa

Initially, we attempted to identify the cleavage site of AMJ in Cry2Aa; that was achieved by performing proteolytic cleavage of Cry2Aa by AMJ followed by transferring the protein into a PVDF membrane and staining the membrane with a reversible staining (PonceuS stain). The membrane was distained and was sent for N-terminal sequencing (figure 4.2.1.1.1).

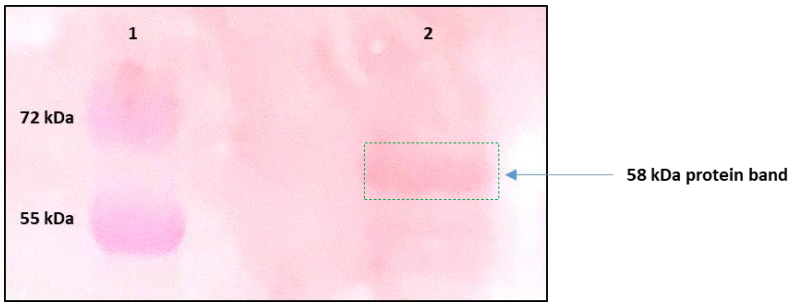

Figure 4.2.1.1.1: PonceuS stained PVDF membrane containing the 58 kDa fragment. **Lane1:** protein standard marker; **lane2:** AMJ processed Cry2Aa-wildtype

The N-terminal sequencing gave the following result: V- A - G? -N/G? - V? (figure 4.2.1.1.2 -*[A]*); although the results was weak, it was consistent with a cleavage after Y49 as seen with gut enzymes from other insects (figure 4.2.1.1.2 *[B]*).

(A)

Residue		
1	V	
2	A	
3	G ?	
4	N ?	G ?
5	V ?	

(B)

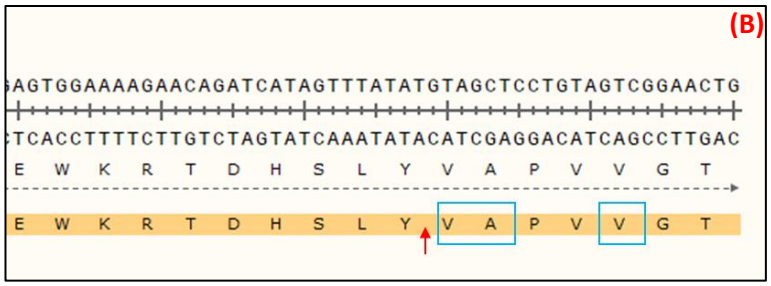

Figure 4.2.1.1.2: N-terminal sequencing results showing AMJ cleavage site in Cry2Aa. ***(A):*** Results indicating the first detected amino acids. ***(B):*** diagram shows the cleavage site of AMJ in Cry2Aa; *(red arrow denotes to where AMJ cleaves, while the blue boxes denotes to the alignment of the most likely amino acids following cleavage.*

The next step was to try and block this cleavage site, and test its cleavage by AMJ and its activity to *Aedes.*

4.2.1.2 Creating Cry2Aa-L48A/Y49A

We initially attempted to test the effect of blocking AMJ cleavage in Cry2Aa on its activity towards *A. aegypti*. As mentioned previously, a previous study suggested that some lepidopteran midgut proteases cleave Cry2Aa after Y49, producing a 58 kDa protein fragment (Audtho et al., 1999). The amino acid at position 48 contains leucine, which is also known to be a potential cleavage site for serine proteases (Xu et al., 2016); therefore, we aimed to substitute both L48 and Y49 to alanine (figure 4.2.1.1).

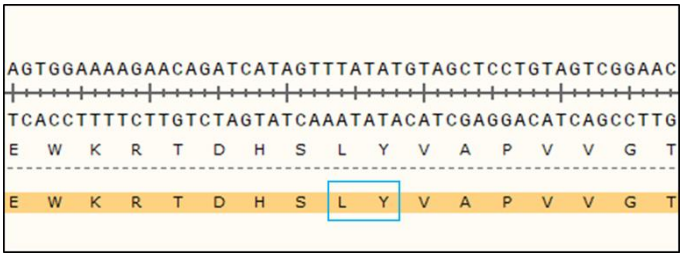

Figure 4.2.1.1.2: Illustration of Cry2Aa L48 and Y49 at the N-terminus *(indicated in blue box).*

Cry2Aa-L48A/Y49A construct was made in a similar way to that described in chapter 3 (section 3.2.4). After that, Cry2Aa-L48A/Y49A was introduced into Bt (78/11 strain) to express crystals. Crystals were solubilized and treated by AMJ to check whether the AMJ cleavage site was blocked or not.

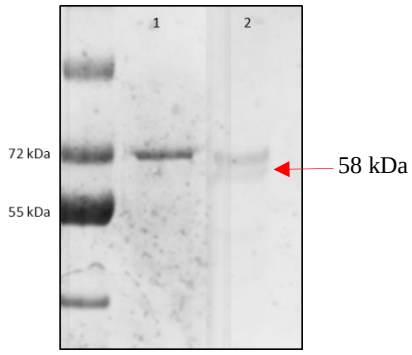

Figure 4.2.1.1.3: SDS-PAGE showing the cleavage pattern of Cry2Aa-L48A/Y49A by AMJ. Lane1: solubilized Cry2Aa-L48A/Y49A; Lane 2: Cry2Aa-L48A/Y49A treated with AMJ.

Figure 4.2.1.2 shows the production of the 58 kDa fragment (lane 2 shown by an arrow) indicating that AMJ stills cleaves Cry2Aa. The activity of Cry2Aa-L48A/Y49A was determined and showed similar activity to *Aedes* compared to Cry2Aa-wildtype (figure 4.2.1) (table 4.2.1.1.1).

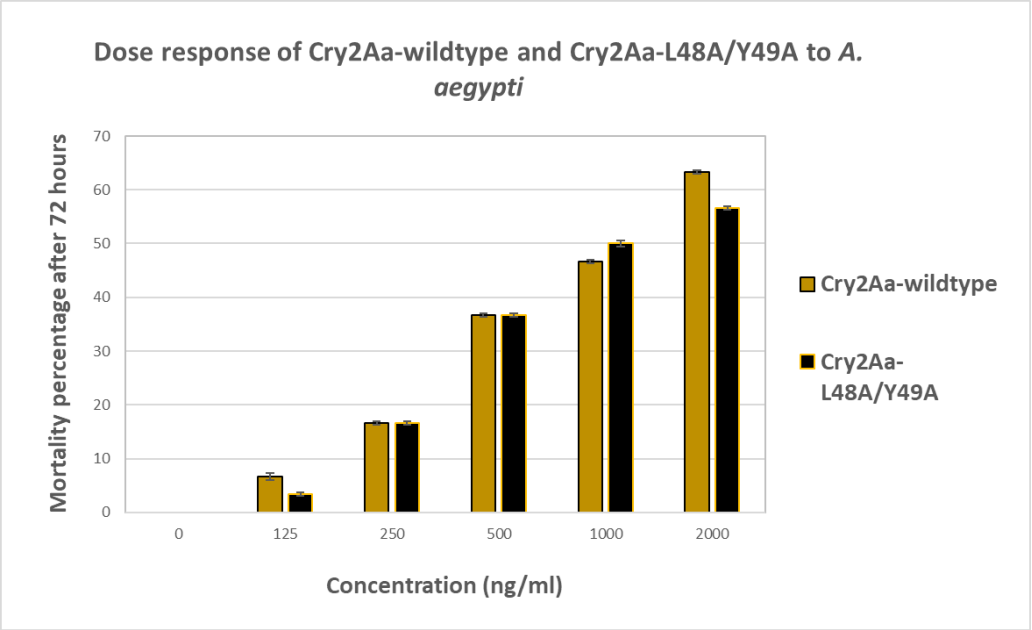

Figure 4.2.1.1.4: Dose response bioassay of different concentrations of Cry2Aa-wildtype and Cry2Aa-L48A/Y49A to *A. aegypti* after 72 hours.

Table 4.2.1.1.1: Lethal concentration (LC_{50}) of Cry2Aa-wildtype and Cry2Aa-L48A/Y49A to *A. aegypti*.

Toxin	LC50 (µg/ml)	95% CL (µg/ml)
Cry2Aa-wildtype	1.565	1.01-3.86
Cry2Aa-L48A/Y49A	1.167	0.70- 3.33

It is important to note that Cry2Ab also contains the same residues (L48 and Y49) in that region (figure 4.2.1.1.5- blue box). It was previously shown that there are differences in the conserved sequences between *Aedes* active and non-active Cry2A toxins as the active ones contain RTD at positions 43-45 while the non-active toxins contain KNN in equivalent positions (Joseph, 2019) (figure 4.2.1.1.5 red box).

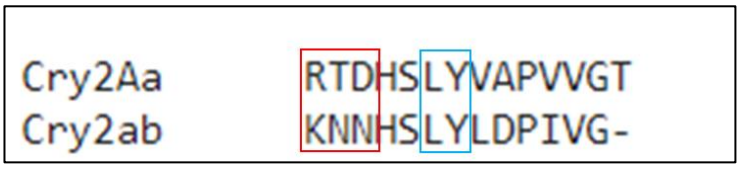

Figure 4.2.1.1.5: alignment of amino acids between Cry2Aa and Cry2Ab showing conserved and non-conserved regions.

Therefore, we proposed that the RTD/KNN residues may contribute in changing the structure of the protein, and hypothesized that the structure around this region may affect proteolytic cleavage.

To test this, we aimed to investigate the cleavage and activity of Cry2Aa containing KNN residues, and see if there was an association between these residues and toxin proteolysis.

4.2.2 The RTD residues within Cry2Aa N-terminus are crucial for toxin activation by AMJ.

4.2.2.1 Creating Cry2Aa-KNN

Cry2Aa-KNN was created in a similar way to that described in chapter 3 (section 3.2.4). After that, Cry2Aa-KNN was introduced into Bt (78/11 strain) to express crystals followed by protein harvesting. After that, crystals was solubilized and activated by AMJ to check whether AMJ cleavage site was blocked or not (figure 4.2.2.1.1).

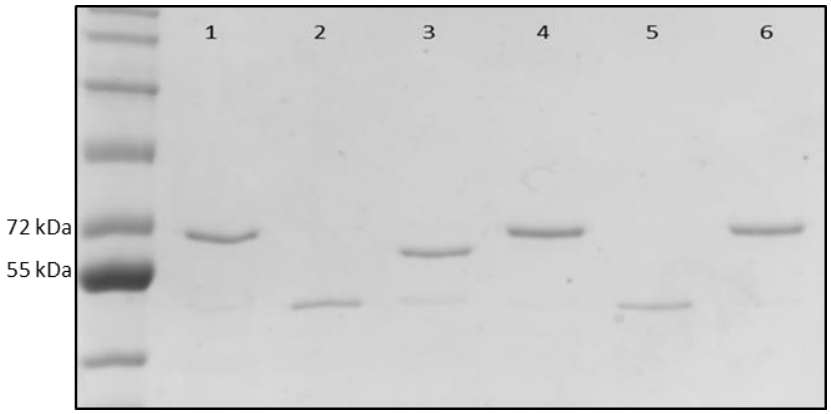

Figure 4.2.2.1.1: SDS-PAGE comparison of Cry2Aa-KNN and Cry2Aa-wildtype activation by AMJ and chymotrypsin. **Lane 1:** solubilized Cry2Aa-wildtype; **lane 2**: Cry2Aa-wildtype activated by 1mg/ml of chymotrypsin; **lane 3:** Cry2Aa-wildtype activated by AMJ; **lane 4:** Solubilized Cry2Aa-KNN; **lane 5:** Cry2Aa-KNN activated by 1mg/ml of chymotrypsin; **lane 6:** Cry2Aa-KNN activated by AMJ.

Figure 4.2.2.1.1 shows that the proteolytic pattern between Cry2Aa-wildtype and Cry2Aa-KNN are different. It is obvious from lane 3 that Cry2Aa treatment by AMJ produced the 58 kDa fragment. On the other hand, lane 6 shows a protein band corresponding to 72 kDa similar to the non-activated (solubilized) form of Cry2Aa (lanes 1 and 4); it shows that

Cry2Aa-KNN was not processed and did not produce the 58 kDa fragment; thereby, we proposed that the KNN residues heavily contributed to blocking the cleavage of AMJ in Cry2Aa. The activity of Cry2Aa-KNN was determined, and it was found that Cry2Aa-KNN had lost activity to *Aedes* (figure 4.2.2.1.2). As a result, we hypothesized that Cry2Aa cleavage is crucial for its activity to *A. aegypti*.

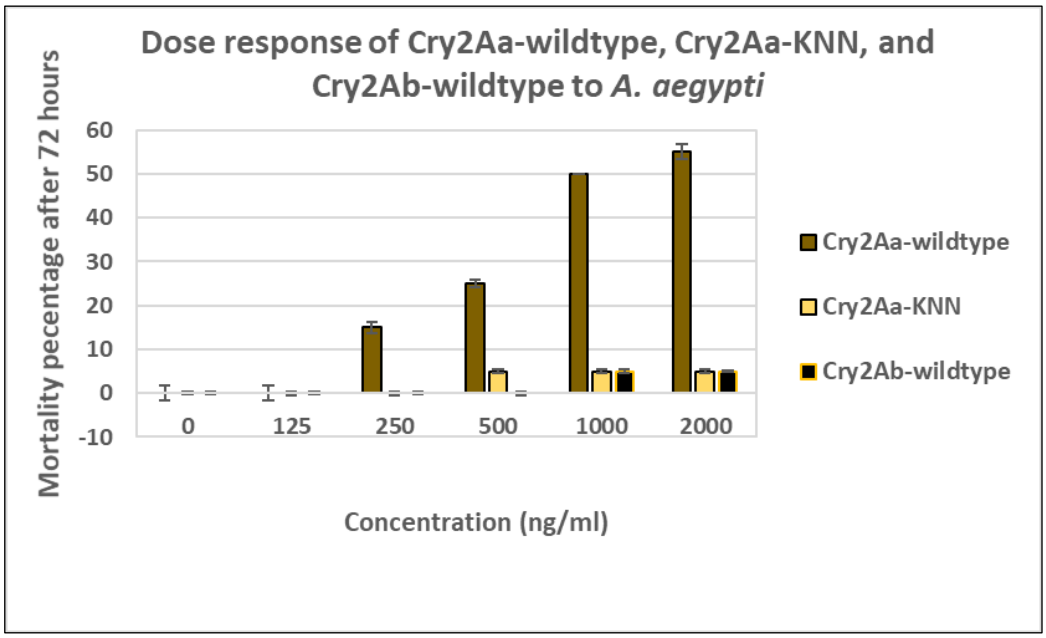

Figure 4.2.2.1.2: Dose response bioassay of different concentrations of Cry2Aa-wildtype, Cry2Aa-KNN, and Cry2Ab-wildtype to *A. aegypti* after 72 hours.

4.2.3 The non-active Cry2Ab toxin gained *A. aegypti* activity after RTD substitution.

Previous work showed that substituting QKNN to ERTD conferred *Aedes* activity to Cry2Ab (Joseph, 2019). However, in this section, we aimed to substitute only KNN residues to RTD and then test its proteolytic cleavage and activity to *A. aegypti* in order to confirm the importance of these RTD residues.

4.2.3.1 Creating Cry2Ab-RTD

Cry2Ab-RTD construct was created in a similar way to that described in chapter 3 (section 3.2.4). After that, Cry2Ab-RTD was introduced into Bt (78/11 strain) to express crystals followed by protein harvesting as mentioned in the materials and methods. After that, crystals were solubilized and activated by AMJ to check whether AMJ cleavage site was blocked or not (figure 4.2.3.1.1).

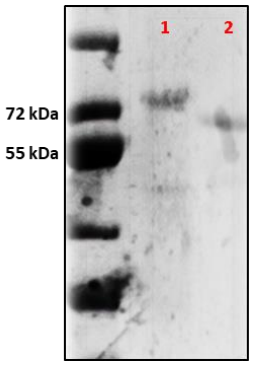

Figure 4.2.3.1.1: SDS-PAGE of mutant Cry2Ab-RTD treated with AMJ; **lane1:** Solubilized Cry2Ab-RTD; **lane2**: AMJ treated Cry2Ab-RTD.

Figure 4.2.3.1.1 shows the activation pattern of Cry2Ab-RTD by AMJ. Lane 1 shows solubilized Cry2Ab-RTD. Lane 2 shows a production of the active 58 kDa fragment from Cry2Ab-RTD, suggesting that the AMJ was able to cleave Cry2Ab-RTD and produce a 58 kDa fragment similar to Cry2Aa-wildtype. It is important to note we previously showed that AMJ could not cleave Cry2Ab-wildtype (figure 4.2.3.1.2 - lane 3).

For further testing of our hypothesis, we conducted a bioassay to test the activity of Cry2Ab-RTD to *A. aegypti*; and compared its toxicity with Cry2Aa-wildtype. We previously showed that Cry2Ab-wildtype had no

activity to *Aedes* (figure 4.1.3). The activity of Cry2Ab-RTD was determined (figure 4.2.3.1.2) and the LC50 was calculated (table 4.2.3.1.1).

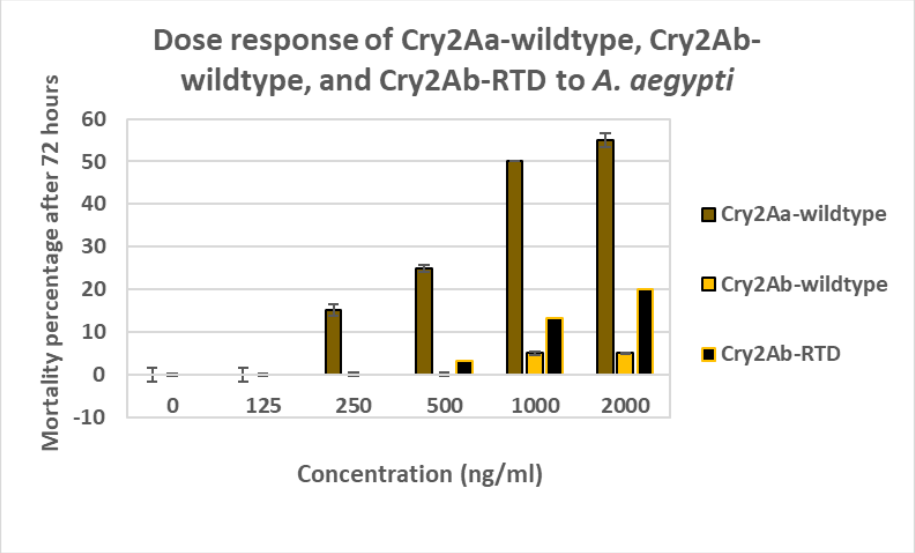

Figure 4.2.3.1.2: Dose response bioassay of different concentrations of Cry2Aa-wildtype and Cry2Ab-RTD to *A. aegypti* after 72 hours.

Table 4.2.3.1.1: Lethal concentration (LC50) of Cry2Aa-wildtype and Cry2Ab-QRTD to *A. aegypti*.

Toxin	LC50 (µg/ml)	95% CL (µg/ml)
Cry2Aa-wildtype	1.565	1.01-3.86
Cry2Ab-RTD	2.837	2.01- 7.79

Bioassay results from figure 4.2.3.1.3 and lethal concentration, which kills 50% of tested *Aedes* population (LC50) in table 4.2.3.1.1 showed that both proteins are active. These finding shows consistency with the previous hypothesis showing the ability of ERTD in conferring *Aedes* activity to non-active Cry2A toxin (Joseph, 2019). However, here we showed that the RTD residues were sufficient to enable the non-active Cry2A to undergo proteolysis and produce the 58 kDa fragment following AMJ cleavage; we,

as a result, hypothesized that *A. aegypti* activity is associated with the ability of the toxin to produce the 58 kDa through proteolytic cleavage at this point.

4.2.4 Further confirmation of the 58 kDa fragment`s association with *A. aegypti* activity in Cry2A protein.

In the previous sections, we showed an association between the presence of RTD, cleavage by AMJ, and activity towards *A. aegypti*. To confirm this association, we aimed to treat Cry2Aa by chymotrypsin. Previous study showed that chymotrypsin and some lepidopteran midgut juices cleaves Cry2Aa to produce a partial digestion product of an active 58 kDa fragment due to cleavage at amino acid Y49, and a final digestion product of 50 kDa fragment, which showed no activity to *A. aegypti* (Goje et al., 2020) *L. dispar* (Audtho et al., 1999) following cleavage at amino acid at L144.

In this section, we aimed to produce only the 58 kDa protein fragment from chymotrypsin, and test the activity of this fragment on *A. aegypti* to seek further confirmation of the association between *Aedes* activity and the production of the 58 kDa fragment.

4.2.4.1 Creation of Cry2Aa-L144A

We aimed to create a single amino acid substitution at position L144 in Cry2Aa. The aim of creating this mutation was to block the final cleavage site of chymotrypsin in Cry2Aa; therefore, preventing the formation of 50 kDa fragment. It was intended that this blockage will only produce 58 kDa

fragment, hence mimicking the production of the 58 kDa fragment produced by *A. aegypti* midgut protease.

Cry2Aa-L144A construct was made in a similar way to that described in chapter 3 (section 3.2.4). After that, Cry2Aa-L144A was introduced into Bt (78/11 strain) to express crystals followed by protein harvesting as mentioned in the materials and methods. After that, crystals were solubilized and activated by AMJ to check whether AMJ cleavage site was blocked or not (Figure 4.2.4.1.1.)

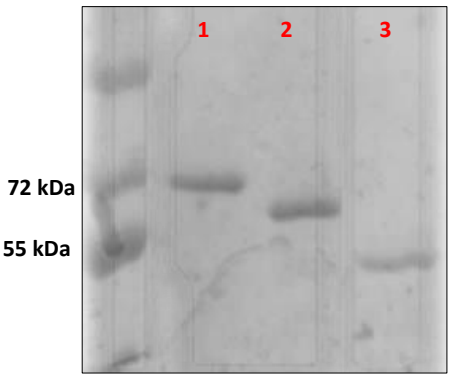

Figure 4.2.4.1.1: SDS-PAGE of Cry2Aa-L144 treated with chymotrypsin. **Lane 1:** solubilized Cry2Aa-L144; **lane 2:** Cry2Aa-L144A activated by 1mg/ml of chymotrypsin; **lane 3:** Cry2Aa-wildtype activated by 1mg/ml of chymotrypsin.

From figure 4.2.4.1.1, it is obvious that chymotrypsin cleaved Cry2Aa-L144A and produced only a 58 kDa fragment (lane 2) similar to the AMJ pattern as shown previously (figure 4.2.2.1.1 – lane 3); while chymotrypsin activated Cry2Aa-wildtype produced only 50 kDa fragment (lane 3). The next step was to test the activity of Cry2Aa-L144 on *A. aegypti* (figure 4.2.4.1.2).

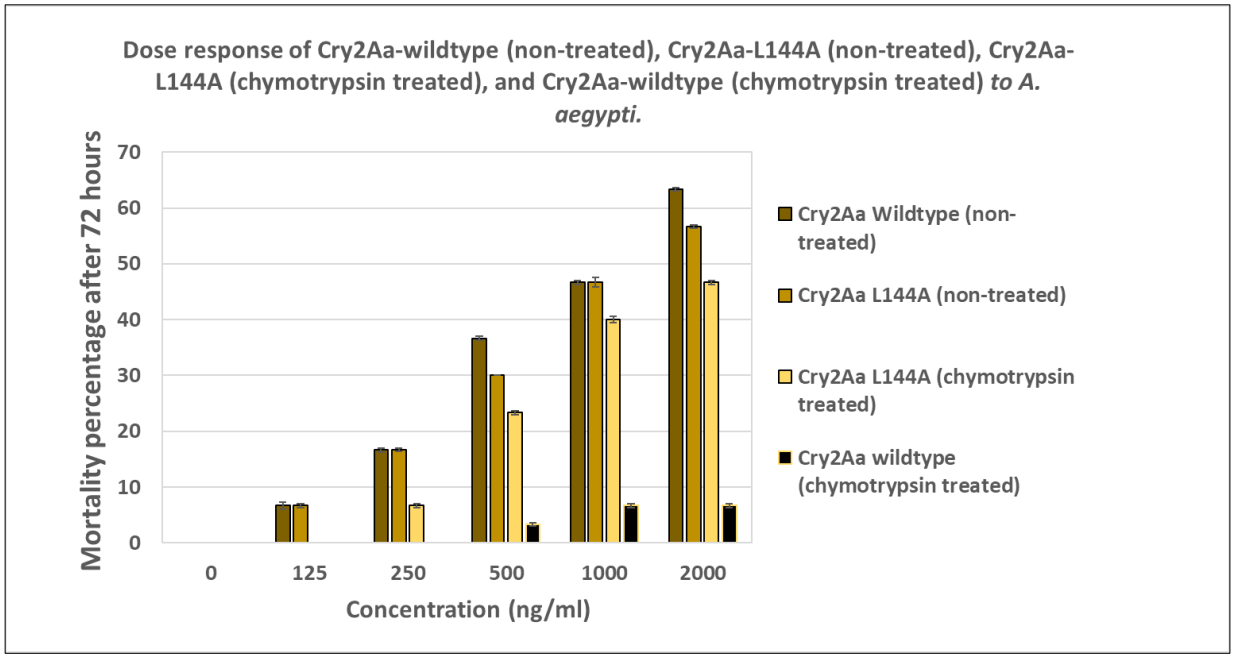

Figure 4.2.4.1.2: Dose response bioassay of different concentrations of activated and non-activated Cry2Aa-wildtype and Cry2Aa-L144A to *A. aegypti* after 72 hours.

Bioassay results in figure 4.2.4.1.2 shows that Cry2Aa-wildtype is active as expected. Chymotrypsin activated Cry2Aa-L144A showed high activity. In contrast, the 50 kDa fragment produced from cleaving Cry2Aa-wildtype by chymotrypsin showed a major reduction of activity. The LC50s of all toxins were also calculated (table 4.2.4.1.1).

Table 4.2.4.1.1: Lethal concentration (LC_{50}) of Cry2Aa-wildtype and Cry2Aa-L144A to *A. aegypti*.

Toxin	LC50 (µg/ml)	95% CL (µg/ml)
Cry2Aa-wildtype	1.087	0.88- 1.40
Cry2Aa-L144A (untreated)	1.311	1.03- 1.79
Cry2Aa-L144A (chymotrypsin treated)	1.742	1.02- 7.32
Cry2Aa-wildtype (chymotrypsin treated)	9.259	4.59- 5.43

These data clearly support our hypothesis, which suggests an association between producing the 58 kDa protein fragment in Cry2A protein and *Aedes* activity; while the 50 kDa fragment loses the ability to kill *A. aegypti*.

4.2.4.2 Testing whether deleting Cry2Aa N-terminus affects activity to *A. aegypti*.

The next step was to produce a 58 kDa fragment from Cry2Aa by deleting the N-terminus instead of cleaving it by proteases; then test if it follows our hypothesis or not. This construct involved deleting the first 45 amino acids, proposing the production of a protein around 58 kDa.

Cry2Aa-Δ45 construct was created in a similar way described in chapter 3 (section 3.2.4).

After that, Cry2Aa-Δ45 was introduced into Bt (78/11 strain) to express crystals followed by protein harvesting as mentioned in the materials and methods. Crystals were solubilized and activated by AMJ to check whether AMJ cleavage site was blocked or not (Figure 4.2.4.2.1).

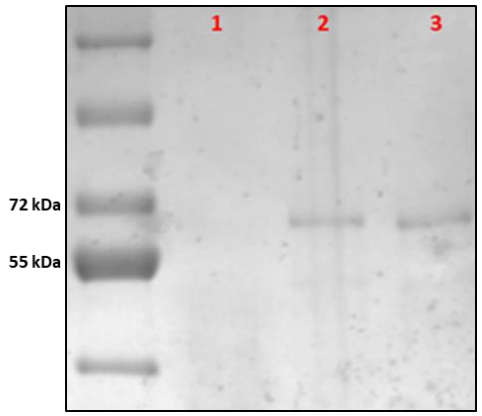

Figure 4.2.4.2.1: SDS-PAGE showing the cleavage pattern of Cry2Aa-Δ45 by AMJ and chymotrypsin. Lane1: Cry2Aa-Δ45treated by AMJ; Lane 2: Cry2Aa-Δ45 treated by 1mg/ml of chymotrypsin; Lane3: solubilized Cry2Aa-Δ45.

Figure 4.2.4.2.1 shows the cleavage pattern of Cry2Aa-Δ45 protein. Cry2Aa-Δ45 was solubilized (lane 3), but when exposed to AMJ, the whole toxin was degraded (lane 1); moreover, we repeated AMJ activation using different dilutions of AMJ to ensure that this degradation was a characteristic pattern of the mutant toxin (Cry2Aa-Δ45) and not due to a general susceptibility of Cry2Aa to concentrated AMJ. We obtained the same degradation even at lower concentrations; therefore, we hypothesized that this degradation is due to a major structural changes in Cry2Aa caused by the deletion of the 45 N-terminal amino acids.

To support our hypothesis, Cry2Aa-Δ45 was also treated with chymotrypsin (figure 4.2.4.2.1 - lane 2); it was found that there was no production of the 50 kDa fragment. We believe that chymotrypsin cleavage site is far from the deleted N-terminal, at L144; therefore, we concluded that the structural changes caused the cleavage site of chymotrypsin to be hidden and prevented its activation.

Cry2Aa-Δ45 was tested on *A. aegypti*; bioassay showed that Cry2Aa-Δ45 has lost the activity to *Aedes* (figure 4.2.4.2.2); which supported our hypothesis on the significant change of toxin`s structure.

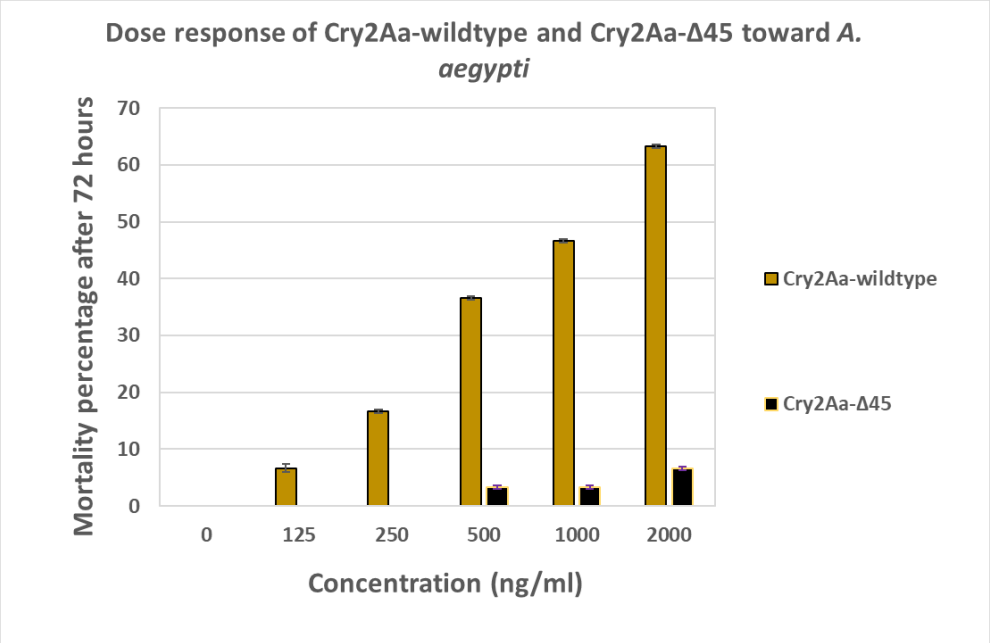

Figure 4.2.4.2.2: Dose response bioassay of different concentrations of Cry2Aa-wildtype and Cry2Aa-Δ45 to *A. aegypti* after 72 hours.

4.2.5 Investigating whether the 58 kDa fragment is important for *A. aegypti* activity in other Cry2A protein.

We aimed in this section to test the activation pattern of other Cry2A proteins including active and non-active toxins, and see if they follow our hypothesis on the association of Cry2A activation and the production of the 58 kDa fragment with activity to *A. aegypti*. It was previously shown that ERTD residues are conserved in most *Aedes* active Cry2A toxins, while most of the *Aedes* non-active Cry2A proteins contained conserved QKNN residues (Joseph, 2019).

4.2.5.1 Proteolytic cleavage of other Cry2A proteins by AMJ

In this section, we included other Cry2A toxins; Cry2Ab, Cry2Ah, and Cry2Aa17 (non-active to *A. aegypti*); Cry2Ac and Cry2Am (active to *A. aegypti*). All these proteins were previously cloned into BL21 *E.coli*

expression system (Joseph, 2019); therefore, we induced the expression of these proteins, solubilized them, and treated them by AMJ (figure 4.2.5.1.1) as described in materials and method chapter.

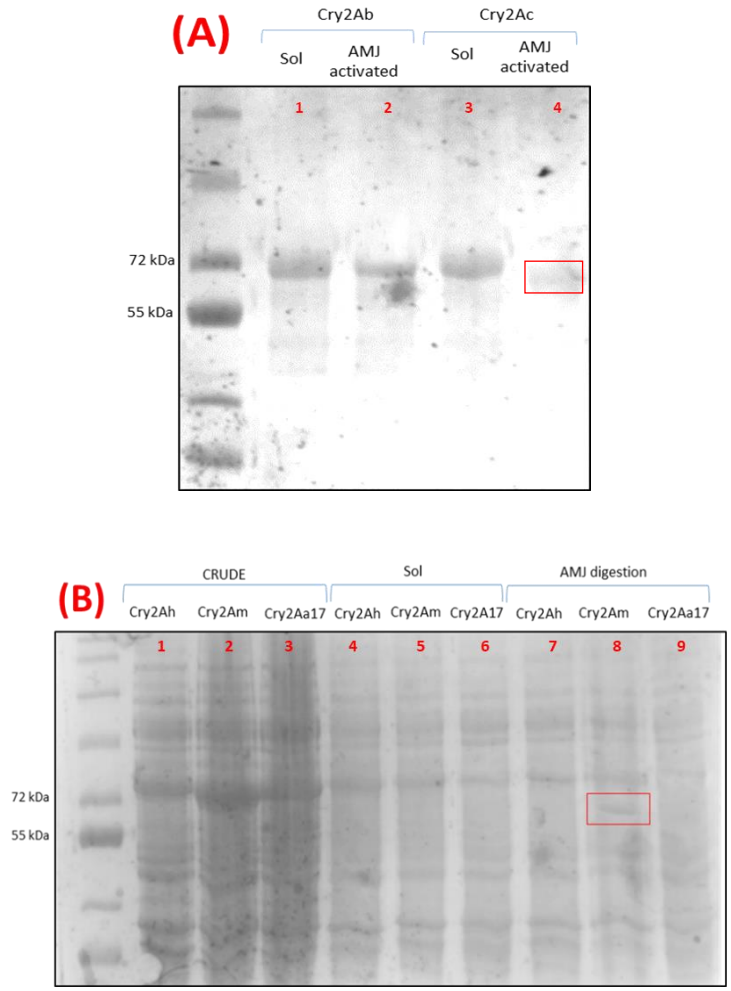

Figure 4.2.5.1.1: SDS-PAGE of different Cry2A treated by AMJ. ***(A)*** Solubilisation and AMJ treatment of Cry2Ab and Cry2Ac. **Lane1:** solubilized Cry2Ab; **lane2:** AMJ treated Cry2Ab; **lane3:** solubilized Cry2Ac, **lane4:** AMJ treated Cry2Ac. ***(B)*** Solubilisation and AMJ treatment of Cry2Ah, Cry2Am, and Cry2Aa17. **Lane1:** crude Cry2Ah, **lane2:** crude Cry2Am, **lane3:** crude Cry2Aa17; **lane4:** solubilized Cry2Ah, **lane5:** solubilized Cry2Am; **lane6:** solubilized Cry2Aa17, **lane7:** AMJ treated Cry2Ah; **lane8:** AMJ treated Cry2Am; **lane9:** AMJ treated Cry2Aa17.

Figure 4.2.5.1.1 shows the cleavage pattern of different Cry2A toxins. It shows that Cry2Ac, which is active against *A. aegypti*, produced a 58 kDa fragment as with Cry2Aa (lane A-4); while Cry2Ab, non-active to *A. aegypti*, did not produce the 58 kDa fragment (lane A-2). Additionally,

only Cry2Am, active to *A. aegypti*, produced the 58 kDa fragment, indicated in red box (lane B-8) while Cry2Ah and Cry2Aa17 did not (lane B-7 and B-9). However, due to the huge amount of contaminating proteins from *E.coli* expression, we aimed to confirm that the obtained bands corresponding to Cry2A molecular weight are actually Cry2A proteins; we, therefore, performed western blot analysis using Cry2A antibody (Figure 4.2.5.1.2).

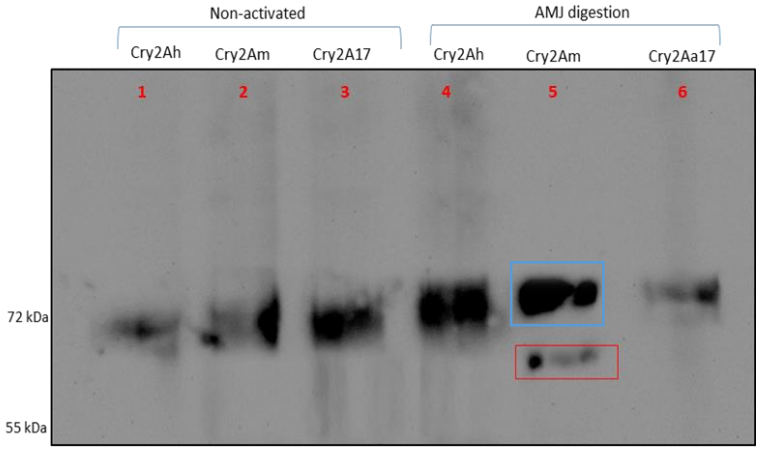

Figure 4.2.5.1.2: Western blot analysis of different solubilized and AMJ treatment of Cry2A toxins. **Lane1:** Solubilized Cry2Ah; **Lane2:** Solubilized Cry2Am **Lane3:** Solubilized Cry2Aa17; **Lane4:** AMJ treated Cry2Ah; **lane5:** AMJ treated Cry2Ah, **lane6:** AMJ treated Cry2Aa17.

Figure 4.2.5.1.2 confirmed that the protein bands identified in the previous gel are Cry2A toxins; additionally, it confirms that treating Cry2Am with AMJ does produce a 58 kDa fragment (lane 5- highlighted by red box), while some of the non-digested fragment at 72 kDa size (lane 5- highlighted with blue box). This supports our hypothesis on Cry2A cleavage association with activity to *A. aegypti*.

4.2.6 Amino acid 27 in Cry2A toxins has no contribution to *A. aegypti* activity.

Previous work showed that ERTD residues conferred *A. aegypti* activity to the non-active Cry2A toxin. It was also shown that all the four residues must be included in order to cause activity (Joseph, 2019). E27 was, in particular, proposed to form a docking-cavity which is important for receptor binding, and substituting E27 to Q27 caused loss of activity to *Aedes*. In our work, when E27 was not changed, while changing RTD residues, there was no effect on Cry2Aa activation (see section 4.2.2.1); therefore, we hypothesized that E27 is not required for Cry2A activity to *A. aegypti*. To confirm our hypothesis, we aimed to test the activation and the activity after substitution of E27 with Q27.

4.2.6.1 Creating Cry2Aa-E27Q

Cry2Aa-E27Q construct was made in a similar was described in chapter 3 (section 3.2.4).

After that, Cry2Aa-E27Q was introduced into Bt (78/11 strain) to express crystals followed by protein harvesting as mentioned in the materials and methods. After that, crystals were solubilized and activated by AMJ to check whether AMJ cleavage site was blocked or not (Figure 4.2.6.1).

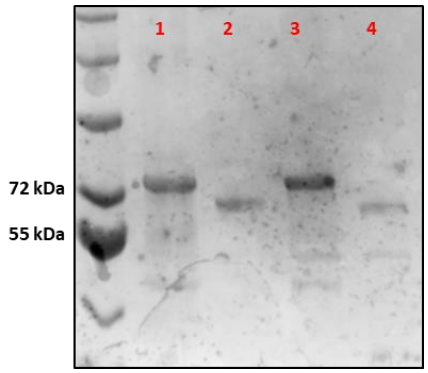

Figure 4.2.6.1: SDS-PAGE of Cry2Aa-wildtype and Cry2Aa-E27Q treated with AMJ. **Lane1:** Solubilized Cry2Aa; **Lane2:** AMJ treated Cry2Aa; **Lane3:** Solubilized Cry2Aa-E27Q; **Lane4:** AMJ treated Cry2Aa-E27Q.

Figure 4.2.6.1 shows comparison of Cry2Aa-wildtype and Cry2Aa-E27Q cleavage by AMJ. It is clear that AMJ still cleaves Cry2Aa containing Q at position 27 and produces 58 kDa fragment in a similar pattern to Cry2Aa-wildtype.

The next step was to test the activity of Cry2Aa-E27Q on *A. aegypti* (figure 4.2.6.1.2).

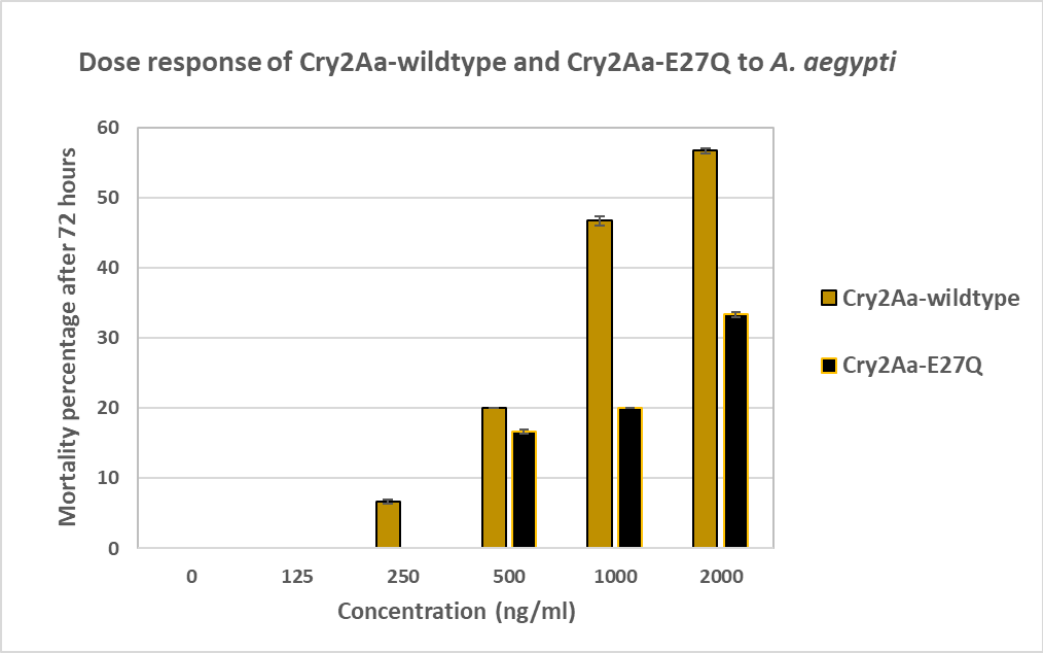

Figure 4.2.6.1: Dose response bioassay of different concentrations of Cry2Aa-wildtype and Cry2Aa-E27Q to *A. aegypti* after 72 hours.

Bioassay results in figure 4.2.6.2 shows that both Cry2Aa-and Cry2Aa-E27Q were active to *A. aegypti*. The LC50 was also calculated in table 4.2.5.1.1.

Table 4.2.5.1.1: Lethal concentration (LC_{50}) of Cry2Aa-wildtype and Cry2Aa-E27Q to *A. aegypti*.

Toxin	LC50 (µg/ml)	95% CL (µg/ml)
Cry2Aa-wildtype	1.565	1.01-3.86
Cry2Aa-E27Q	2.327	1.49- 2.47

We, as a result, hypothesized that E27 in Cry2Aa N-terminus does not have any significant contribution to *A. aegypti* activity.

4.3 Discussion

Many studies showed the importance of toxin activation in order to cause toxicity to different insects; for instance, differential in proteolytic cleavage of an anti-cancer toxin, Cry41Aa, showed differential activity towards HepG2 cells (Souissi, 2018). Additionally, Audtho et al showed that *L. dispar* midgut juice cleaved Cry2Aa, producing two protein fragments; an active 58 kDa and a non-active 50 kDa. They also suggested that the production of the 58 kDa fragment is due to cleavage at Y49 while the production of the 50 kDa fragment is due to cleavage at L144. They also were able to produce only the 58 kDa by blocking the cleavage site at L144 responsible of forming the 50 kDa fragment (Audtho et al., 1999). Another

study showed the activation importance in Cry2Ab to *P. xylostella.* It showed that *P. xylostella* midgut juice cleaves Cry2Ab at R139 and L144. It also revealed that blocking the activation site in either R139 or L144 did not abolish the activity to *P. xylostella.* However, when both residues were substituted to alanine, toxicity was lost. (Xu et al., 2016).

In this chapter, we aimed to give explanations on why the differential activation of Cry2A proteins results in differential activity toward *A. aegypti*. First, we aimed to test the effect of blocking the proposed activation site of AMJ (Y49). This followed the identification of AMJ cleavage site in Cry2Aa through N-terminal sequencing, revealing that AMJ cleaves Cry2Aa after Y49. We then aimed to test whether substituting Y49 to A49 would block AMJ cleavage, leading to causing loss of activity to *Aedes* or not. However, leucine at position 48 might have had a potential cleavage site for AMJ; and therefore, we substituted both L48 and Y49 to alanine attempting to block AMJ activation site. Our results, however, showed a production of the 58 kDa fragment, suggesting that AMJ cleaves Cry2Aa at other sites upstream of Y49. Amino acid comparison between Cry2Aa and Cry2Ab showed that both toxins contain L48 and Y49 residues; however, Cry2Ab showed no proteolytic cleavage when treated with AMJ while Cry2Aa did. Four residues were previously identified within *A. aegypti* active toxins; ERTD corresponding to positions

27, 43, 44, and 45 while the non-active toxins contained QKNN in the equivalent positions, showing ability to confer *Aedes* activity to non-active toxins. It was also found that all four residues must be included in the N-terminus to show activity, and changing one of them caused loss of activity to *A. aegypti*. Therefore, we proposed that these four residues structurally affect Cry2A cleavage. Structural comparison between two forms of Cry2Aa containing RTD and KNN residues, using *Phyre2* software, revealed likely structural differences. Therefore, it was hypothesized that these differences affect cleavage of the 49 N-terminal amino acids by the midgut proteases, leading to activity to *Aedes*.

After that, we started reassessing the role of the RTD residues by testing their role in toxin activation. When RTD residues in Cry2Aa were replaced by KNN from the non-active Cry2A proteins, it caused loss of activity and prevented the AMJ from activating Cry2Aa and producing the active 58 kDa fragment. On the other hand, RTD residues were able to confer *A. aegypti* activity to the non-active Cry2Ab after substituting KNN residues, and were able to show cleavage of Cry2Ab by AMJ, producing the active 58 kDa fragment.

Further investigations on the association of the 58 kDa fragment, through proteolytic cleavage, with *Aedes* activity involved testing the production of the 58 kDa fragment by chymotrypsin. It is important to note that partial

cleavage of Cry2Aa by chymotrypsin produces a mixture of 58 kDa and 50 kDa fragments. However, we successfully blocked the cleavage site that produces the 50 kDa fragment in Cry2Aa through substituting L144 to A144. The bioassay of the chymotrypsin activated Cry2Aa-L144A showed activity to *A. aegypti*; while the 50 kDa fragment, produced after chymotrypsin cleavage of Cry2Aa-wildtype, showed no activity. This finding confirmed our hypothesis on the association of cleavage and activity to *Aedes*, but more importantly has revealed a preliminary hypothesis proposing a potential binding motif in the 58 kDa fragment, resulted from cleavage at Y49; which is lost in the 50 kDa fragment produced by cleavage at L144 (figure 4.3.1).

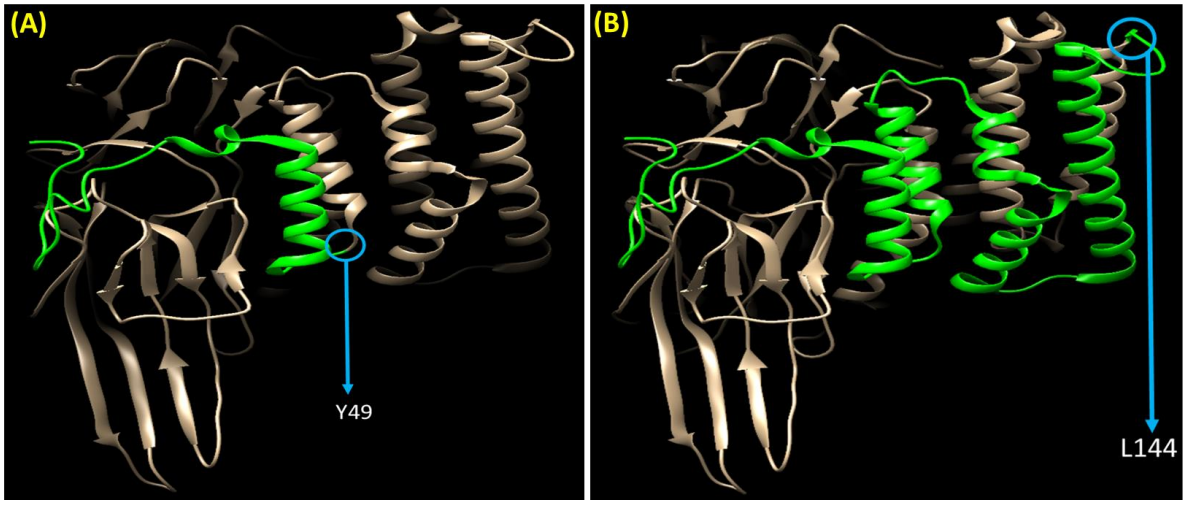

Figure 4.3.1: 3D structure of Cry2Aa showing the N-terminal region. ***(A):*** 49 N-terminal amino acids of Cry2Aa; the green highlighted region denotes the cleaved region upon AMJ cleavage at Y49. ***(B):*** 144 N-terminal amino acids of Cry2Aa; the green highlighted region denotes the extended removed region upon chymotrypsin cleavage at L144.

The production of the 58 kDa fragment involves the removal of only helices α-0 of domain I. However, chymotrypsin proteolysis, and some lepidopteran species midgut juice, are shown to occur at L144 and is involved in also removing of helices α1-α4 (figure 4.3.2), which subsequently caused loss of activity to *Aedes*. Therefore, we hypothesized that helices α1-α4, located between amino acid 50-144, contain this potential activity motif to *Aedes*, and further N-terminal cleavage at L144 are involved in removing more helices; thereby, causes loss of activity to *A. aegypti*, but not to lepidopteran species.

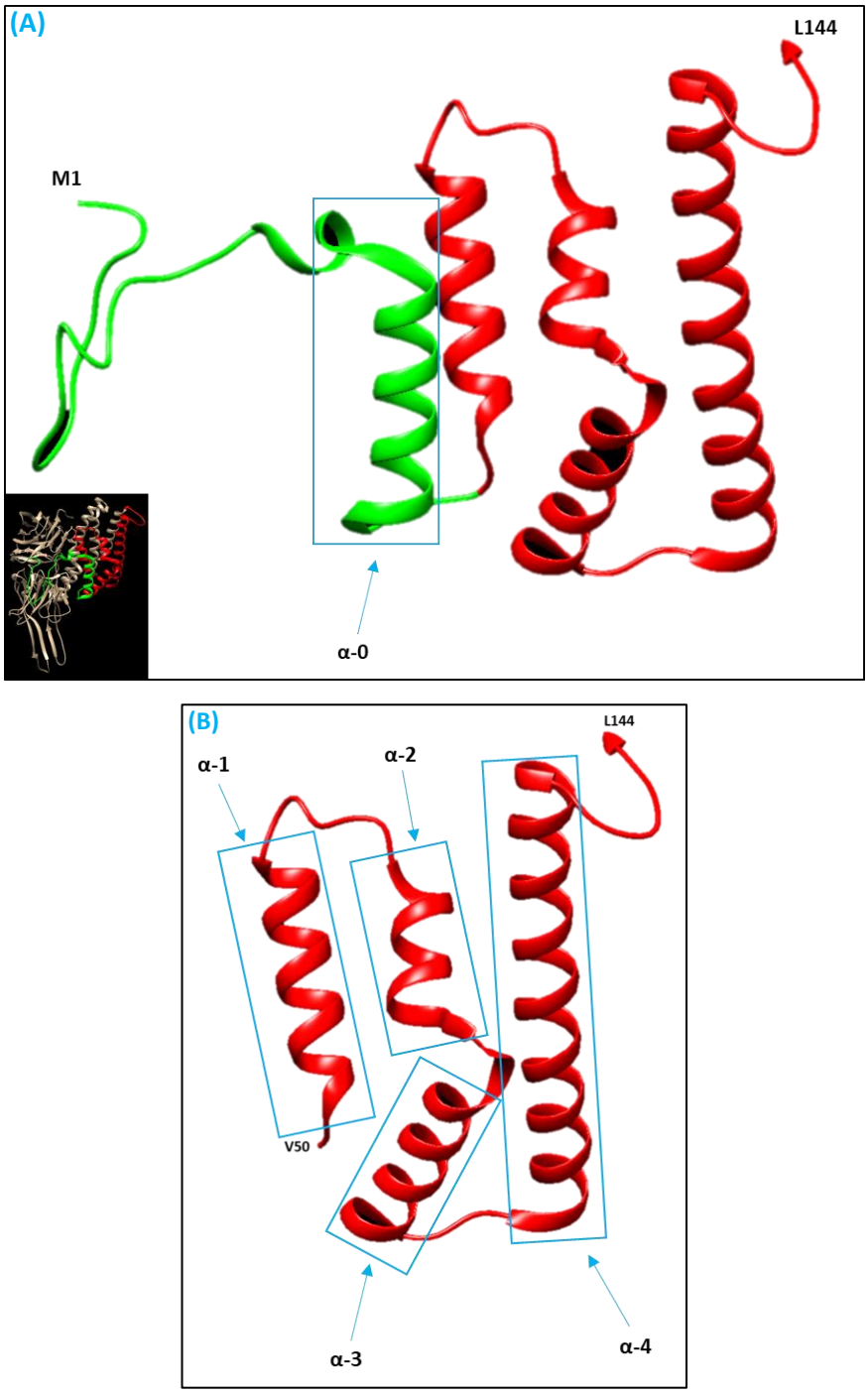

Figure 4.3.2: 3D structure of Cry2Aa`s N-terminal region. ***(A):*** 3D structure of the 144 N-terminal amino acids of Cry2Aa showing five α–helices within that region; the green highlighted region denotes the cleaved 49 amino acids by AMJ which includes removing α-0 helix (highlighted in blue box); while the red highlighted region denotes the region between amino acid 50-144. *The minimized image on the left bottom corner shows the full three-domain Cry2Aa for referencing.* ***(B):*** 3D structure showing helices α1-α4 within the proposed activity motif located between amino acids 50-144.

Another attempt to investigate the importance of the 58 kDa fragment in activity was to test the effects of deleting the N-terminal region (Cry2Aa-Δ45), which hypothetically should result in mimicking the production of the AMJ activated toxin, 58 kDa fragment. We found though that the Cry2Aa-Δ45 showed no activity to *A. aegypti*, and it was degraded when exposed to AMJ *in vitro*. In addition, Cry2Aa-Δ45 was not activated by chymotrypsin, suggesting that there was a major change in toxin`s structure that masked the cleavage sites. We hypothesized that Cry2Aa N-terminus are important for proper protein folding, and losing the N-terminal affected Cry2Aa`s activity to *Aedes*.

Moreover, we further confirmed our hypothesis of the association between the production of the 58 kDa fragment and activity by testing the production of the 58 kDa fragment from other Cry2A proteins. We found the 58 kDa fragment was produced in Cry2Ac and Cry2Am, which previously showed activity to *A. aegypti* (Joseph, 2019); while (Cry2Ab, Cry2Aa17, and Cry2Ah) showed neither a production of the 58 kDa fragment nor activity to *Aedes* (Joseph, 2019).

E27 amino acid in Cry2Aa N-terminus was previously hypothesized to participate in receptor binding (Joseph, 2019). Cry2Aa-E27Q showed successful cleavage by AMJ and its bioassay showed toxicity to *Aedes*, which suggested that E27 has no effect on Cry2A activity to *A. aegypti*.

We then concluded that there is a strong association between Cry2A proteins activation, and subsequently production of the 58 kDa fragment, with activity toward *A. aegypti*. We also concluded that that 58 kDa fragment exhibits activity motif, particularly the helices α1-α4 (between amino acid 50-144) (figure 4.3.2). However, the function of this motif was unknown.

5. Understanding the mode of action mechanism of Cry2A insecticidal proteins in *A. aegypti.*

5.1 Introduction

In the previous chapter, we showed that differential activation of Cry2A toxins shows differential activity to *A. aegypti* and the necessity of Cry2A activation, through the production of the 58 kDa fragment, for *A. aegypti* activity. Also, we found that further activation at the N-terminal of Cry2Aa, producing the 50 kDa fragment by chymotrypsin activation, caused loss of the activity to *A. aegypti* but not to other insects. In this chapter, we aimed to understand the mode of action of Cry2Aa in *A. aegypti* by understanding why the activation is important, and why different activation products of Cry2Aa are associated with different activities to *A. aegypti*.

The sequential binding model, based on the mode of action of Cry1Ab in *M. sexta*, toxin activation (first cleavage in insect`s midgut) followed by binding to initial receptor; such as cadherin, which then induces a second cleavage. The second cleavage triggers the formation of toxins oligomers complex followed by a second receptor binding, such as APN. That, as a result, initiates pore-formation process on the cell membrane.

In the previous chapter, we hypothesized that the N-terminus of Cry2A toxins must be removed to expose a region that has potential binding motif to *A. aegypti*. Therefore, in this chapter we focused on testing the mechanistic process based on this hypothesis; that includes testing the ability of toxin-binding to *Aedes* brush border microvilli membrane vesicles (BBMV), and its post binding event (toxin oligomerization) of both active and non-active Cry2Aa forms. We then aimed to investigate any association between this mechanistic process, in particular toxin-binding and oligomerization, with activity to *Aedes*.

5.2 Results

5.2.1 Testing the binding of Cy2Aa toxins to *A. aegypti* BBMV.

In this section, we tested the binding of different forms of Cry2Aa toxin to *A. aegypti* BBMV. Cry2Aa-wildtype was activated by AMJ (producing an active 58 kDa fragment) and chymotrypsin (producing a non-active 50 kDa fragment); additionally, *A. aegypti* BBMV was prepared from late third instar larvae as described in material and methods (chapter 2). It is important to note that a fundamental hypothesis states the necessity of removing Cry2A N-terminus as a key step in Cry2Aa activity to *Aedes*; therefore, we also included testing the non-activated Cry2Aa (72 kDa solubilized toxin) in this binding assay.

After performing the binding assay, we analysed it on SDS-PAGE followed by performing western blot analysis using Cry2A antibody, which confirmed that the observed bands are from Cry2Aa toxin (figure 5.2.1.1).

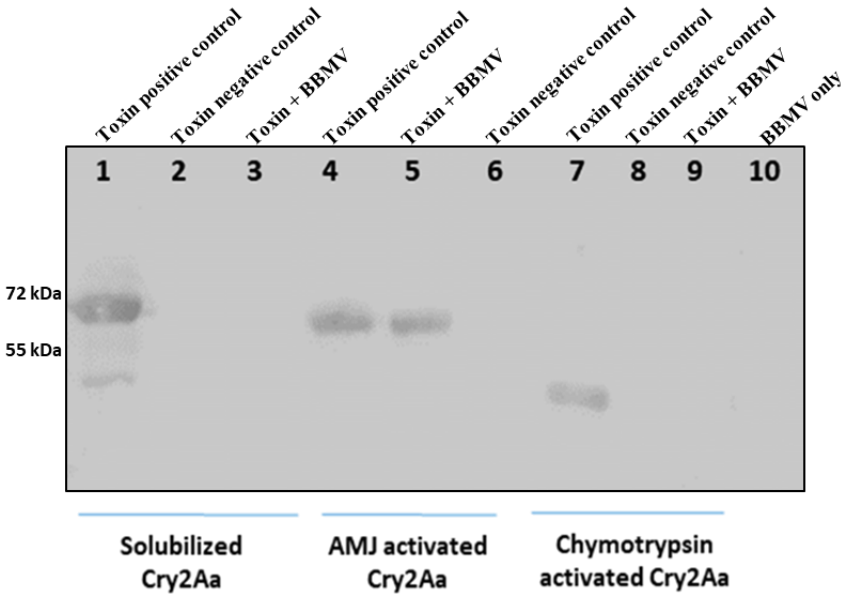

Figure 5.2.1.1: western blot analysis of Cry2Aa binding assay to *Aedes* BBMV using Cry2A antibody. **Lane1**: Positive control of only solubilized Cry2Aa; **lane2**: solubilized Cry2Aa incubated with *Aedes* BBMV; **lane3**: Negative control of solubilized Cry2Aa treated similarly to the incubated toxin with BBMV. **Lane 4:** Positive control of only AMJ activated Cry2Aa; **lane 5:** AMJ activated Cry2Aa incubated with *Aedes* BBMV; **lane 6**: Negative control of AMJ activated Cry2Aa treated similarly to the incubated toxin with BBMV. **Lane 7:** Positive control of only chymotrypsin activated Cry2Aa; **lane 8**: Negative control of; **lane 9:** chymotrypsin activated Cry2Aa treated similarly to the incubated toxin with BBMV. **Lane 10:** *Aedes* BBMV only.

Figure 5.2.1.1, shows the binding assay of different forms of Cry2Aa. For each toxin form, we included two controls; the positive control aimed to confirm the correct form of the toxin after solubilisation or activation, while the negative controls aimed to confirm that the toxin had not precipitated under the same conditions as the experimental condition, but without BBMV.

Our binding assay clearly showed that there was no binding between the solubilized Cry2Aa with the BBMV while the AMJ activated Cry2Aa was

able to bind and was pulled down with the BBMV. The chymotrypsin activated Cry2Aa, however, was not able to bind the BBMV. The binding assay was repeated three times to confirm this result.

As a result, we hypothesized that the 58 kDa fragment is active due to its ability to bind *A. aegypti* BBMV; that also revealed further explanations on the previous suggested model that states the 58 kDa fragment possess a potential binding motif for *A. aegypti* by showing that this region is crucial for receptor binding in *A. aegypti* BBMV. Moreover, we hypothesized that the 50 kDa is not active to *Aedes* due to lacking of this motif, thereby, it lost the ability to bind *A. aegypti* BBMV. We also confirmed that the non-activated Cry2Aa did not bind the BBMV due to the presence of the N-terminus, which is suggested to partially mask the binding motif; therefore, preventing it from binding.

The next step is to test another factor in the mode of action of Cry toxins; toxin oligomerization.

5.2.2 Testing whether toxin oligomerization is important for activity.

Many studies showed the importance of Cry toxin oligomerization in showing activity whether in the absence (Guereca and Bravo, 1999) or in the presence of insect BBMV (Ocelotl et al., 2017).

In Cry2A toxins, Xu et al showed that after Cry2Ab activation, helices α4 and α5 were important for toxin oligomerization (Xu et al., 2018). That was

confirmed in Pan et al study that identified the key residues important for Cry2Ab oligomerization including; N151, T152, F157, L183, L185, and I188 (Pan et al., 2021).

Therefore, in this section we aimed to test if Cry2Aa oligomerization requires *A. aegypti* BBMV or not. In addition, we aimed to test if there is any association between Cry2Aa oligomerization and activity to *A. aegypi*.

5.2.3 Investigating Cry2Aa oligomerization and its association with activity to *A. aegypti*.

We performed the oligomerization assay in similar method to the binding assay. We only included the AMJ activated Cry2Aa (58 kDa) as the oligomerization process is a post binding event (as shown in section 5.2.1.1). However, after adding the SDS sample buffer, we divided our sample into three group; the first was heated at 30^{O}C for 10 minutes, the second was at 60^{O}C for 10 minutes. The third was boiled at 100^{O}C. All samples were analysed on SDS-PAGE followed by performing western bolt analysis to confirm that all protein bands are from Cry2A toxins (Figure 5.2.3.1).

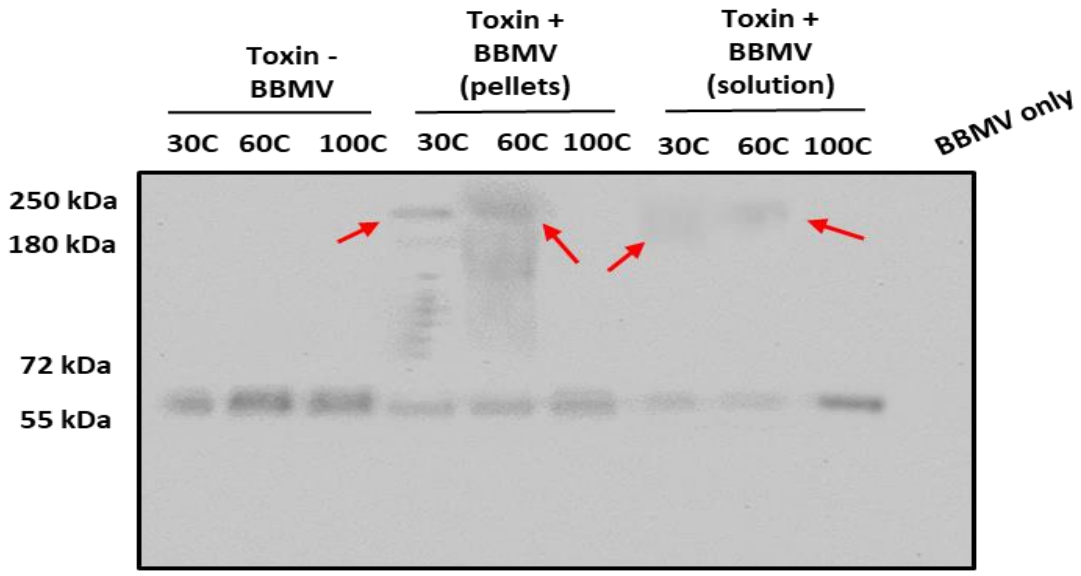

Figure 5.2.3.1: Western blot analysis of AMJ activated Cry2Aa (58 kDa) oligomerization assay in the absence and presence of *A. aegypti* BBMV. **Lanes 1-3**: only AMJ activated Cry2Aa in absence of BBMV; **lanes 4-6:** AMJ activated Cry2Aa incubated with *Aedes* BBMV present in pellets; **lanes 7-9:** AMJ activated Cry2Aa incubated with *Aedes* BBMV present in solution; **lane 10:** negative control of *Aedes* BBMV only.

Figure 5.2.3.1 shows the oligomerization assay of the 58 kDa fragment of Cry2Aa. First, it shows that 58 kDa fragment does not form oligomers in the absence of *A. aegypti* BBMV (lanes 1-3). However, in the presence of the BBMV, the 58 kDa fragment oligomerized and formed a high molecular weight band around 250 kDa at 30^{O}C and 60^{O}C (lanes 4-9).

(Lanes 4-6) show that the oligomers were present in the pelleted sample. That indicates that the 58 kDa oligomers were bound to the BBMV. On the other hand, the presence of some 58 kDa oligomers in the solution is believed due to the potential disruption of the oligomers during the centrifugation and washing steps; suggesting that the interaction between the oligomers and the BBMV is not very strong.

The next step aimed to determine the key residues that may affect the binding of the 58 kDa fragment, and subsequently, affecting *Aedes* activity.

5.2.4 Determining the key residues involved in Cry2Aa binding and oligomerization.

We previously hypothesized that a binding motif to *Aedes* is present in the 58 kDa fragment but not the 50 kDa fragment. In this section, we compared the sequence alignment of the proposed active motif region in groups of *Aedes* active and the non-active Cry2A toxins. This comparison was established on three criteria:

- The region must be masked by the N-terminus.
- The region must be conserved in both groups, as cleaving the non-active toxins showed activity.
- The R-group is exposed and available for binding.

We then aligned the amino acids sequence of the region present in 58 kDa but not the 50 kDa in both toxin groups; we found two amino acids that satisfied the three criteria; T56 and K63 (figure 5.3.1).

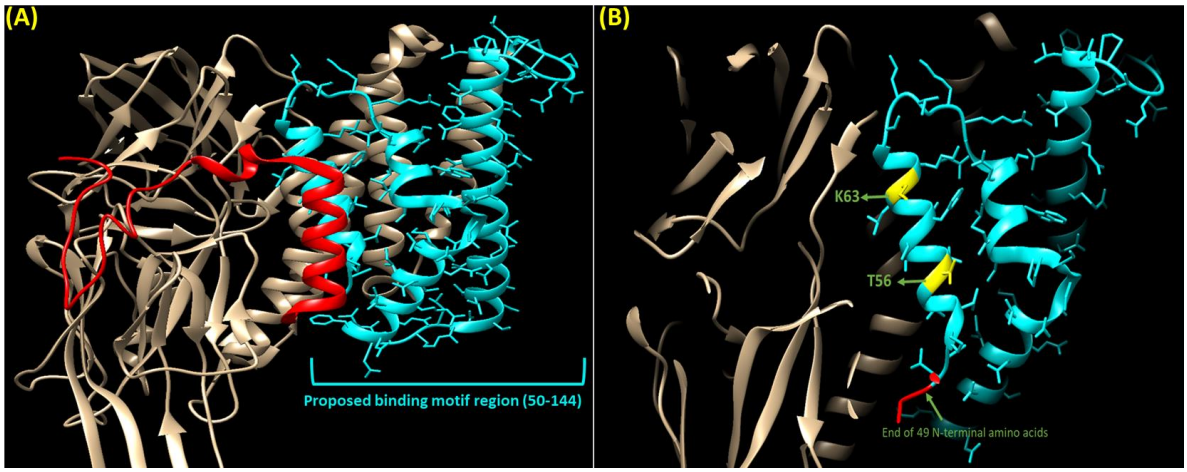

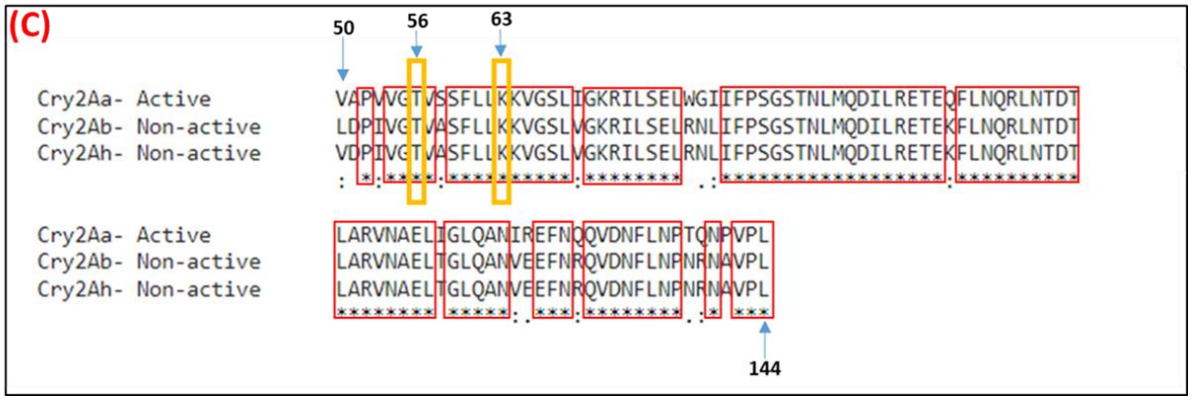

Figure 5.2.4.1: 3D structure of the proposed binding motif (highlighted in cyan) within Cry2Aa N-terminal. ***A):*** Structure of non-activated Cry2Aa showing the N-terminus (highlighted in red) masking key residues within the proposed binding motif. ***B):*** Structure of activated Cry2Aa showing removal of the N-terminal and the exposure of the key residues (highlighted in yellow) within the proposed binding motif. ***C):*** Amino acids alignment of the proposed binding motif in active and non-active toxins showing the key residues; *red boxes indicates the conserved sequences while yellow boxes indicate residues satisfying the three criteria.*

5.2.5 Creating Cry2Aa-T56A/K63A and testing their activity to *A. aegypti.*

Cry2Aa-T56A and Cry2Aa-T56A/K63A constructs were made in similar method shown in chapter 3 (section 3.2.4). The designed forward primer contained "Y" which allowed us to get 50% chance of PCR product containing ACT (threonine) and 50% chance of getting GCT (alanine); while the reverse primer contained GCG which only encodes alanine. After that, both constructs were introduced into Bt (78/11 strain) to express crystals followed by protein harvesting as mentioned in the materials and methods. The activity of both toxins was tested on *Aedes* larvae (figure 5.3.1.1).

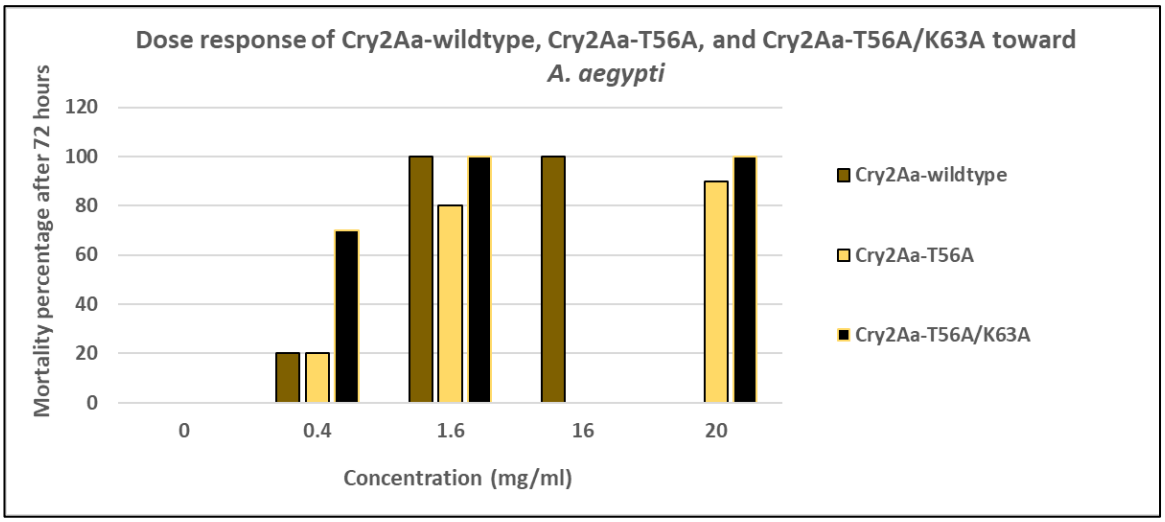

Figure 5.2.5.1: Dose response assay of different concentrations of Cry2Aa-wildtype, Cry2Aa-T56A, and Cry2Aa-T56A/K63A to *A. aegypti* after 72 hours.

Figure 5.2.5.1 shows no effects of the mutated residues on *Aedes* activity compared to the wildtype even at high concentrations. Therefore, it was concluded that mutating T56 and K63 was not enough to abolish the activity of the 58 kDa fragment to *Aedes*, and therefore they are not crucial residues.

5.2.6 Identifying the binding receptor for Cry2Aa in *A. aegypti* BBMV.

After observing a binding between the activated Cry2Aa and *Aedes* BBMV, we aimed in this section to identify the receptor for the 58 kDa fragment using Co-immunoprecipitation (Co-IP) approach. That was initially intended by fusing Cry2Aa with a tag protein. In chapter 3, we created a recombinant protein of 6xHis tag protein at the N-terminus of Cry2Aa to test the N-terminal attachment upon activation. However, in this section, we aimed to create a C-terminal 6xHis-tagged Cry2Aa. The reason of this fusion at the C-terminus is that proteolytic cleavage takes place at

the N-terminus of Cry2A toxins; and therefore, it is not possible to the N-terminal for pull down.

5.2.7 Creating C-terminal Cry2Aa-His-tagged protein.

Initially, we had to confirm that there was no cleavage at the Cry2Aa C-terminus. There is no evidence of an implication of Cry2Aa C-terminus cleavage during toxin activation. Nevertheless, the very C-terminus end of Cry2Aa contains residues that might have a potential cleavage site for serine proteases (figure 5.2.7.1- highlighted in blue boxes); therefore, we deleted these residues before fusing the 6xHis tag protein to the C-terminus of Cry2Aa.

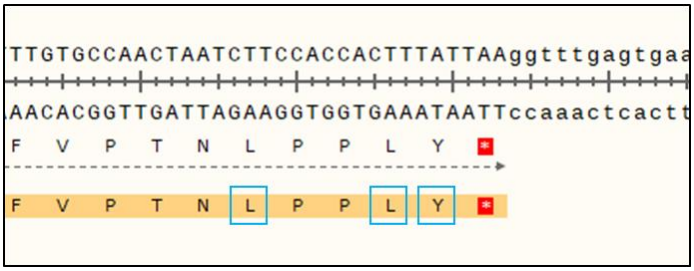

Figure 5.2.7.1: Illustration of the Cry2Aa C-terminus residues, which are believed to have high potential as cleavage sites of AMJ.

Cry2Aa-His-tag construct was made in similar method shown in chapter 3 (section 3.2.4).

After that, Cry2Aa-His-tagged was introduced into Bt (78/11 strain) to express crystals followed by protein harvesting as mentioned in the materials and methods. After that, crystals were solubilized and activated by AMJ to check whether AMJ cleavage site was blocked or not (Figure 5.2.7.2).

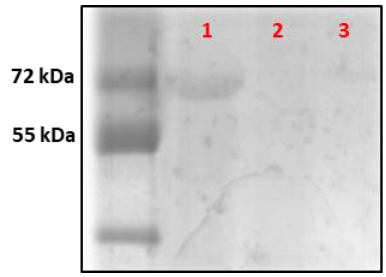

Figure 5.2.7.2: SDS-PAGE analysis of crude and solubilized of Cry2Aa-His-tagged. **Lane1:** Crude Cry2Aa-His; **lane2:** solubilized Cry2Aa-His in 50mM NaOH; **lane3:** solubilized Cry2Aa-His-tagged in 50mM Na_2CO_3.

Figure 5.2.7.2 showed comparison of crude and solubilized Cry2Aa-His-tagged. It is obvious that there was protein in the crude sample (lane 1) but solubilisation did not produce soluble toxins; even with different solubilisation buffers; 50mM NaOH, pH 11 (lane 2) or 50mM Na_2CO_3, pH 10.5 (lane 3).

We also tried to solubilized crystals in different buffers; 20mM Tris-HCl pH 8.6, 6M guanidine hydrochloride, 2mM EDTA and 300mM dithiothreitol; however, we could not solubilize the crystals properly (figure 5.2.7.3).

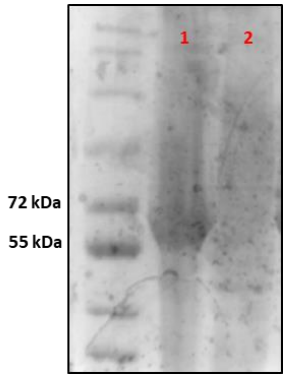

Figure 5.2.7.3: SDS-PAGE analysis crude and solubilized of Cry2Aa-His-tagged protein. **Lane1:** Crude Cry2Aa-His-tagged; **lane2:** solubilized Cry2Aa-His-tagged in 20mM Tris-HCl pH 8.6, 6M guanidine hydrochloride, 2mM EDTA and 300mM dithiothreitol.

Due to time limitation for this research project, we could do further optimization to solubilize the C-terminal His-tagged protein, therefore, we did not identify the receptor for the 58 kDa fragment.

5.3 Discussion

We showed previously that the 58 kDa fragment produced upon cleavage possess a proposed binding motif to *Aedes* whereas the 50 kDa does not; thereby, we aimed to understand the reason why the 58 kDa, but not the 50 kDa, is active by initially performing a binding assay between active and non-active cleaved products of Cry2Aa with *Aedes* BBMV.

We performed the binding assay of three forms of Cry2Aa: non-treated, AMJ treated, and chymotrypsin treated. Our data showed that neither the non- treated (70 kDa fragment) nor the chymotrypsin treated (50 kDa fragment) bound to the BBMV; while the AMJ treated bound to *Aedes* BBMV. We hypothesized that the 58 kDa is active to *A. aegypti* due to possessing a binding motif that is lost in the 50 kDa fragment, which enables the toxin to bind is receptor in *Aedes* BBMV. Moreover, the failure of the non-activated form to bind the BBMV confirms our previous hypothesis on the importance of toxin activation through removing the 49 N-terminal amino acids, which partially masks the active motif. Post binding events, in addition, showed to have specificity, one of which is toxin oligomerization. Previous studies showed the importance of toxin oligomerization in showing activity after binding. We aimed to test if the

activated toxin is able to oligomerize in the presence or absence of *A. aegypti* BBMV. Our oligomerization assay showed that the 58 kDa fragment oligomerized in the presence of *Aedes* BBMV.

After that, we aimed to identify the key residues within the 50-144 region that could be involved in binding. T56 and K63 were identified as a candidate amino acids but mutations did not affect the activity of Cry2Aa to *Aedes*.

6. General discussion

In this research project, we aimed to investigate the role of Cry2Aa`s N-terminus in *Aedes* activity. Cry2Aa, a three domain insecticidal protein possesses dual activity toward lepidopteran and dipteran species, has been extensively studied. Previous studies hypothesized that the specificity of *Aedes* activity is associated with a region in domain II (between amino acids 302-382)c (Liang and Dean, 1994) (Widner and Whiteley, 1990).

Morse et al hypothesized that the N-terminus of Cry2Aa masks a binding region located in domain II, and that it is crucial to cleave the N-terminus to reveal this binding site and get toxicity (Morse et al., 2001). On the other hand, recent work established that the specificity of Cry2A toxins to *Aedes* is influenced by domain I. That was established by testing a naturally existing hybrid (Cry2Aa17) which has domain I from Cry2Ab, non-active

to *Aedes*, while domain II and III are from Cry2Aa (Shu et al., 2017). Additionally, further investigations showed that this effect was due to the 49 N-terminal amino acids of domain I. That was established after exchanging the 49 N-terminal amino acids between Cry2Aa and Cry2Ab (non-active to *Aedes*), which conferred *Aedes* activity to Cry2Ab (Joseph, 2019). Moreover, comparison of the amino acids sequence between *Aedes* active and non-active Cry2A toxins showed that the active toxins contained conserved residues in this region; structural analysis indicated that all four of the residues were surface exposed and could be involved in receptor binding. It was also found that all the ERTD residues must be included in Cry2A N-terminus in order to confer *Aedes* activity, and losing just one of them caused loss of activity (Joseph, 2019).

However, published evidence indicates that the 49 N-terminal amino acids are cleaved off during toxin activation step in *Aedes* gut, and so would not be available for receptor binding. This led to an "**intact N-terminal model**" which hypothesized that Cry2Aa`s N-terminus remains attached after activation by *Aedes* midgut enzymes allowing the ERTD residues to still participate in binding (Joseph, 2019).

In this research project, we first aimed to investigate the validity of the "intact N-terminal model"; we, however, showed that Cry2Aa`s N-

terminus does not remain attached following the proteolytic cleavage by midgut enzymes.

The next aim was to determine whether blocking the cleavage of Cry2Aa`s N-terminus affects *Aedes* activity or not. This aim was established by previous evidence that showed an association between Cry2A proteolysis and activity; for instance, Cry2Ab cleavage by *P. xylostella* midgut proteases was blocked by mutating R139 and L144, which subsequently led to loss of activity to *P. xylostella* (Xu et al., 2016). Additionally, Audtho et al found that differential cleavage of Cry2Aa showed differential activity to *L. dispar*. They showed that Cry2Aa cleavaed by *L. dispar* midgut protease produced an active 58 kDa fragment and then a final non-active 50 kDa fragment. Therefore, we initially identified the cleavage site of AMJ in Cry2Aa by N-terminally sequencing the AMJ processed Cry2Aa. It revealed that AMJ cleaves Cry2Aa after amino acid Y49; we then aimed to substitute this amino acid to block AMJ cleavage site. Since amino acid at L48 also showed a potential cleavage site, we substituted both amino acids L48 and Y49 to alanine (Cry2Aa-L48A/Y49A). That was followed by treating Cry2Aa-L48A/Y49A by AMJ; but it showed a cleavage and production of the 58 kDa fragment in a similar way to Cry2Aa-wildtype. Combining this finding with our finding that the N-terminus containing RTD residues is removed following the activation, we aimed to test if the

RTD residues contribute to toxin cleavage or not. That was established after testing the proteolytic cleavage of Cry2Ab, non-active to *Aedes*, which like Cry2Aa also contains L48 and Y49 while it contains KNN in contrast to RTD in Cry2Aa. We found that there was no proteolytic cleavage of Cry2Ab by AMJ, and therefore, we hypothesized that there are higher structural effects within this region caused by RTD/KNN residues that affected cleavage.

We hypothesized that RTD residues allow cleavage of Cry2A by AMJ. To test this hypothesis, we created Cry2Aa-KNN by substituting the RTD residues in Cry2Aa to KNN residues from *Aedes* non-active Cry2Ab; followed by treating Cry2Aa-KNN with AMJ. We found that Cry2Aa-KNN was not cleaved and did not produce a protein fragment around 58 kDa which is produced when Cry2Aa-wildtype is treated by AMJ. The activity assay of Cry2Aa-KNN showed loss of activity to *Aedes*; therefore, we concluded that KNN residues prevented Cry2Aa cleavage by AMJ.

We further investigated the importance of RTD residues in cleavage by substituting KNN residues in Cry2Ab to RTD from Cry2Aa (creating Cry2Ab-RTD), followed by treating Cry2Ab-RTD with AMJ. We found that Cry2Ab-RTD was cleaved by AMJ and produced a 58 kDa protein fragment in a similar way to Cry2Aa-wildtype. The activity assay of Cry2Ab-RTD showed activity to *Aedes*. That led to the hypothesis

suggesting an association between Cry2A toxin proteolysis, through producing the 58 kDa fragment, and activity to *A. aegypti*.

This hypothesis was further investigated by producing the 58 kDa fragment from other sources. First, we aimed to produce 58 kDa from chymotrypsin treatment; however, it was previously shown that Cry2Aa chymotrypsin treatment produces partial digestion of 58 kDa before a final digestion product of 50 kDa; the 58 kDa fragment was found toxic to *A. aegypti* and *L. dispar*; while the 50 kDa showed no activity to either insect (Joseph, 2019, Audtho et al., 1999). However, Audtho et al showed that only 58 kDa can be produced by substituting chymotrypsin cleavage site, L144, to alanine. We created Cry2Aa-L144A and treated it with chymotrypsin, which only produced a 58 kDa fragment. We tested that activity of Cry2Aa-L144A and it showed activity to *Aedes*. More importantly, the 50 kDa fragment produced from Cry2Aa-wildtype treated by chymotrypsin showed loss of activity to *A. aegypti*. These finding confirmed our hypothesis on the association of toxin activation through producing the 58 kDa fragment, with *Aedes* activity.

The second attempt in investigating the role of Cry2Aa`s N-terminus was to mimick producing the 58 kDa in *Aedes* gut through deleting the 45 N-terminal amino acids of Cry2Aa (creating Cry2A-Δ45). The activity assay showed loss of activity of Cry2Aa-Δ45; the activation pattern of Cry2A-

D45 showed a complete degradation of this toxin when treated by AMJ, even at low concentrations of AMJ. Moreover, we treated Cry2Aa-Δ45with chymotrypsin and found that there was no cleavage or production of the 50 kDa, despite the fact that chymotrypsin cleavage site at L144 is far from the deleted N-terminal. We, as a result, suggested that there was a major structural changes caused by deleting 45 amino acids; subsequently, caused the toxin not to fold properly. That led to hypothesizing that although Cry2Aa`s N-terminal proteolytic cleavage is crucial for *A. aegypti* activity, the N-terminus also has an important role in the toxin`s structure and proper folding.

For consistency, we tested the association between toxin cleavage and activity to *Aedes* by testing the proteolytic cleavage of other members of Cry2A toxin family including: Cry2Ac and Cry2Am (active to *Aedes*); Cry2Ah, Cry2Ab, and Cry2Aa17 (non-active to *Aedes*). We found that both Cry2Ac and Cry2Am produced the 58 kDa while Cry2Ah, Cry2Ab, and Cry2Aa17 did not. This was consistent with our hypothesis.

We concluded that the Cry2A N-terminus is important during the early stages of its folding and solubilisation. However, the N-terminus must be cleaved by the insect`s proteases and produce the 58 kDa fragment that is active to *A. aegypti*. This proposed pathway of Cry2A toxin does not explain why the 58 kDa is active to *Aedes* while the 50 kDa is not. Initially,

we hypothesized that there is a binding motif located between AMJ cleavage site (Y49) and chymotrypsin cleavage site (L144). We further investigated this concern in the next aim.

The third aim in this project was to understand why the region between amino acids 49-144 within the the 58 kDa fragment is important for *Aedes* activity. That was initially achieved by testing the ability of the 58 kDa fragment to bind to *Aedes* brush border membrane vesicles (BBMV). We performed a binding assay between different forms of Cry2Aa and *Aedes* BBMV. That involved non-treated (72 kDa), AMJ treated (58 kDa), and chymotrypsin treated (50 kDa) Cry2Aa. We found that neither the non-treated nor the chymotrypsin treated forms of Cry2Aa bound to *Aedes* BBMV, while the AMJ treated form did bind. This supports our proposal concerning having a binding motif in the 58 kDa, which would to be important for receptor binding in *Aedes* BBMV. This motif is believed to be lost in the 50 kDa fragment due to further cleavage at L144, while it is believed that this motif is masked behind the non-cleaved 49 N-terminal amino acids.

Additionally, we investigated another factor that is believed to be important for toxicity. That was testing the ability of the 58 kDa fragment to form toxin oligomers as an oligomerization step is believed to be an important step in Cry toxin mode of action (Pan et al., 2021, Xu et al., 2018). There

was no prior indication as whether Cry2Aa was able to oligomerize in the absence or in the presence of insect BBMV, therefore, we tested its oligomerization in both situations. It is important to note that most Cry toxin oligomerization is triggered after the being activated by midgut protease followed by a secondary cleavage following binding to an initial receptor, such as cadherin (Bravo et al., 2004). We only tested the oligomerization of the 58 kDa as we previously showed that it is active and bound to *Aedes* BBMV. Our oligomerization assay revealed that the 58 kDa only oligomerized in the presence of *Aedes* BBMV.

The final step aimed to identify key residues that are important for this putative binding motif within the 58 kDa fragment, but not with the 50 kDa fragment. There were three criteria for determining them:

- The investigated residues must be hidden by the 49 N-terminal amino acids before the proteolytic cleavage.
- The R-group of the investigated residues must be structurally exposed and available for receptor binding.
- The investigated residues must be conserved in both *Aedes* active and non-active Cry2A toxins.

Structural analysis identified two amino acids that met the three criteria; T56 and L63. The next step was substituting these residues to alanine, by creating two mutant constructs; Cry2Aa-T56A and Cry2Aa-T56A/L63A,

followed by testing its activity to *Aedes.* However, the activity assays showed that both mutants were as active to *Aedes* compared as Cry2Aa-wildtype, suggesting that at least these two residues are not enough to abolish the activity of the 58 kDa to *Aedes*; and hypothetically, not preventing the 58 kDa fragment from binding its receptor in *A. aegypti* BBMV.

In this research project we showed that Cry2A activation is crucial for *Aedes* activity. This activation only occurred in the presence of RTD residues, when is treated with AMJ, it produces a 58 kDa fragment, which hypothetically contains a binding motif to *Aedes* BBMV; while cleavage by chymotrypsin and other lepidopteran species midgut enzymess produces a 50 kDa fragment which loses this binding motif. We also showed that blocking AMJ activation prevented the toxin from binding *Aedes* BBMV due to masking this binding motif; and subsequently losing *Aedes* activity.

Finally, we concluded that Cry2A activation is the first and a key step in *Aedes* activity. Although N-terminal sequencing revealed that AMJ cleaves Cry2Aa after L48/Y49, we still observed cleavage when L48/Y49 were mutated to alanine. Having the same residues (L48/Y49) as the non-active Cry2Ab but different residues in another region (RTD/KNN) without

showing cleavage and activity suggested two possibilities for this differential proteolytic cleavage:

- The cleavage after L48/Y49 is facilitated upon a previous cleavage in different region; for instance, RTD (figure 6.1).
- Structural differences between RTD and KNN may allow the RTD residues in Cry2Aa to expose L48/Y49 to proteases more than the KNN residues in Cry2Ab (figure 6.2).

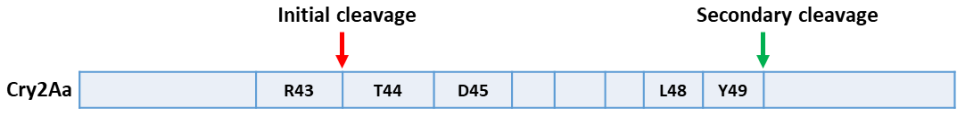

Figure 6.1: Diagram illustration showing one possible proteolytic cleavage pattern of Cry2Aa by AMJ.

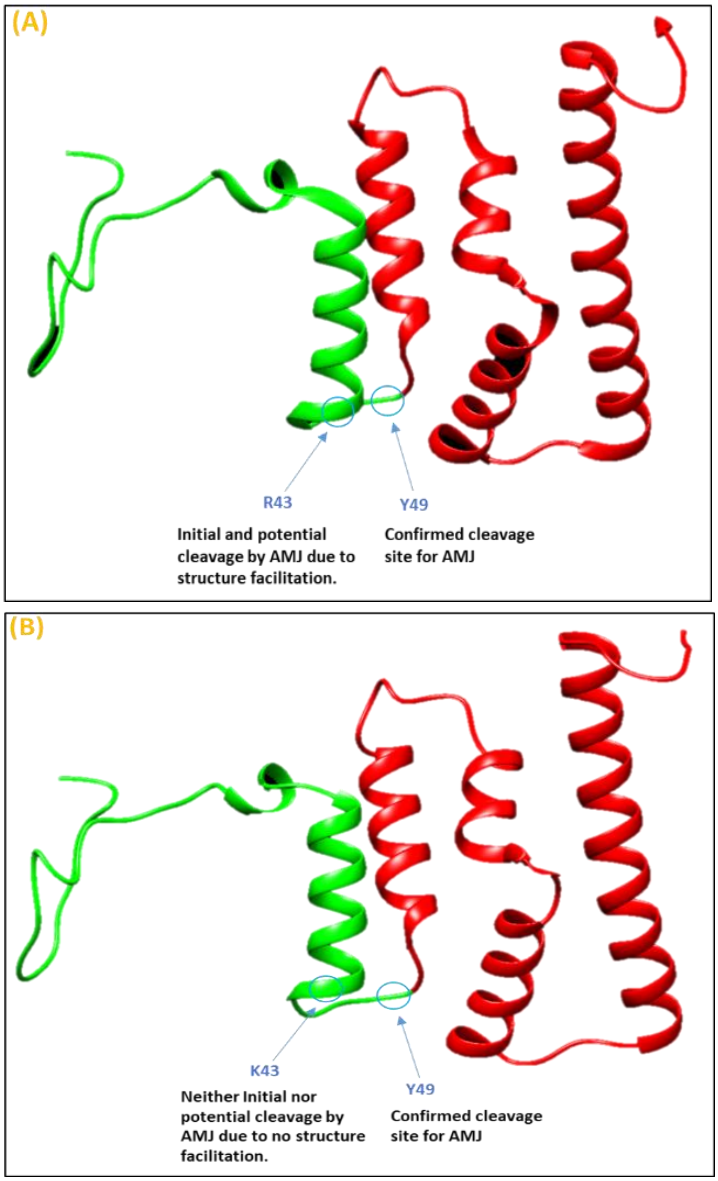

Figure 6.2: 3D structure of Cry2Aa ***(A)*** and Cry2Ab ***(B)*** 144 N-terminal amino acids. The green highlighted region denotes the 49 amino acids. The red highlighted region denotes the region containing a proposed binding motif (within amino acids 50-144).

7. Reference

Alphey, L., Mckemey, A., Nimmo, D., Neira Oviedo, M., Lacroix, R., Matzen, K. & Beech, C. 2013. Genetic control of *Aedes* mosquitoes. *Pathog Glob Health,* 107**,** 170-9.

Angst, B. D., Marcozzi, C. & Magee, A. I. 2001. The cadherin superfamily: diversity in form and function. *J Cell Sci,* 114**,** 629-41.

Angus, T. A. 1954. A bacterial toxin paralysing silkworm larvae. *Nature,* 173**,** 545-6.

Arantes, O. & Lereclus, D. 1991. Construction of cloning vectors for *Bacillus thuringiensis*. *Gene,* 108**,** 115-9.

Asano, S. I., Nukumizu, Y., Bando, H., Iizuka, T. & Yamamoto, T. 1997. Cloning of novel enterotoxin genes from *Bacillus cereus* and Bacillus thuringiensis. *Appl Environ Microbiol,* 63**,** 1054-7.

Audtho, M., Valaitis, A. P., Alzate, O. & Dean, D. H. 1999. Production of chymotrypsin-resistant *Bacillus thuringiensis* Cry2Aa1 delta-endotoxin by protein engineering. *Appl Environ Microbiol,* 65**,** 4601-5.

Bradley, D., Harkey, M. A., Kim, M. K., Biever, K. D. & Bauer, L. S. 1995. The insecticidal CryIB crystal protein of *Bacillus thuringiensis* ssp. *thuringiensis* has dual specificity to coleopteran and lepidopteran larvae. *J Invertebr Pathol,* 65**,** 162-73.

Brandt, C., Adang, M. & Spence, K. 1978. The peritrophic membrane: Ultrastructural analysis and function as a mechanical barrier to microbial infection in *Orgyia pseudotsugata*. *Journal of Invertebrate Pathology - J INVERTEBR PATHOL,* 32**,** 12-24.

Bravo, A., Gomez, I., Conde, J., Munoz-Garay, C., Sanchez, J., Miranda, R., Zhuang, M., Gill, S. S. & Soberon, M. 2004. Oligomerization triggers binding of a *Bacillus thuringiensis* Cry1Ab pore-forming toxin to aminopeptidase N receptor leading to insertion into membrane microdomains. *Biochim Biophys Acta,* 1667**,** 38-46.

Bretschneider, A., Heckel, D. G. & Pauchet, Y. 2016. Three toxins, two receptors, one mechanism: Mode of action of Cry1A toxins from *Bacillus thuringiensis* in *Heliothis virescens*. *Insect Biochem Mol Biol,* 76**,** 109-117.

Burton, S. L., Ellar, D. J., Li, J. & Derbyshire, D. J. 1999. N-acetylgalactosamine on the putative insect receptor aminopeptidase N is recognised by a site on the domain III lectin-like fold of a *Bacillus thuringiensis* insecticidal toxin. *J Mol Biol,* 287**,** 1011-22.

Buzdin, A. A., Revina, L. P., Kostina, L. I., Zalunin, I. A. & Chestukhina, G. G. 2002. Interaction of 65- and 62-kD proteins from the apical membranes of the *Aedes aegypti* larvae midgut epithelium with

Cry4B and Cry11A endotoxins of *Bacillus thuringiensis*. *Biochemistry (Mosc)*, 67**,** 540-6.

Carvalho, D. O., Mckemey, A. R., Garziera, L., Lacroix, R., Donnelly, C. A., Alphey, L., Malavasi, A. & Capurro, M. L. 2015. Suppression of a Field Population of *Aedes aegypti* in Brazil by Sustained Release of Transgenic Male Mosquitoes. *PLoS Negl Trop Dis,* 9**,** e0003864.

Chen, J., Aimanova, K. G., Fernandez, L. E., Bravo, A., Soberon, M. & Gill, S. S. 2009. *Aedes aegypti* cadherin serves as a putative receptor of the Cry11Aa toxin from *Bacillus thuringiensis* subsp. israelensis. *Biochem J,* 424**,** 191-200.

Clements, A., N., 1999. *The Biology of Mosquitoes, volume 2,* Cabi, Wallingford.

Contreras, E., Schoppmeier, M., Real, M. D. & Rausell, C. 2013. Sodium solute symporter and cadherin proteins act as *Bacillus thuringiensis* Cry3Ba toxin functional receptors in *Tribolium castaneum*. *J Biol Chem,* 288**,** 18013-21.

Crickmore, N., Berry, C., Panneerselvam, S., Mishra, R., Connor, T. R. & Bonning, B. C. 2021. A structure-based nomenclature for *Bacillus thuringiensis* and other bacteria-derived pesticidal proteins. *J Invertebr Pathol,* 186**,** 107438.

Crickmore, N. & Ellar, D. J. 1992. Involvement of a possible chaperonin in the efficient expression of a cloned CryIIA delta-endotoxin gene in *Bacillus thuringiensis*. *Mol Microbiol,* 6**,** 1533-7.

Crickmore, N., Zeigler, D. R., Feitelson, J., Schnepf, E., Van Rie, J., Lereclus, D., Baum, J. & Dean, D. H. 1998. Revision of the nomenclature for the *Bacillus thuringiensis* pesticidal crystal proteins. *Microbiol Mol Biol Rev,* 62**,** 807-13.

Dankocsik, C., Donovan, W. P. & Jany, C. S. 1990. Activation of a cryptic crystal protein gene of *Bacillus thuringiensis* subspecies kurstaki by gene fusion and determination of the crystal protein insecticidal specificity. *Mol Microbiol,* 4**,** 2087-94.

De Maagd, R. A., Bravo, A. & Crickmore, N. 2001. How *Bacillus thuringiensis* has evolved specific toxins to colonize the insect world. *Trends in Genetics,* 17**,** 193-199.

Donovan, W. P., Gonzalez, J. M., Jr., Gilbert, M. P. & Dankocsik, C. 1988. Isolation and characterization of EG2158, a new strain of *Bacillus thuringiensis* toxic to coleopteran larvae, and nucleotide sequence of the toxin gene. *Mol Gen Genet,* 214**,** 365-72.

Du, C., Martin, P. A. & Nickerson, K. W. 1994. Comparison of Disulfide Contents and Solubility at Alkaline pH of Insecticidal and Noninsecticidal *Bacillus thuringiensis* Protein Crystals. *Appl Environ Microbiol,* 60**,** 3847-53.

Elleuch, J., Zribi Zghal, R., Lacoix, M. N., Chandre, F., Tounsi, S. & Jaoua, S. 2015. Evidence of two mechanisms involved in *Bacillus thuringiensis* israelensis decreased toxicity against mosquito larvae: Genome dynamic and toxins stability. *Microbiol Res,* 176**,** 48-54.

Fernandez, L. E., Aimanova, K. G., Gill, S. S., Bravo, A. & Soberon, M. 2006. A GPI-anchored alkaline phosphatase is a functional midgut receptor of Cry11Aa toxin in *Aedes aegypti* larvae. *Biochem J,* 394**,** 77-84.

Foster, W., A, Walker, E,D. 2002a. Mosquitoes (Culicidae) Medical and Veterinary Entomology.

Gahan, L. J., Gould, F. & Heckel, D. G. 2001. Identification of a gene associated with Bt resistance in *Heliothis virescens. Science,* 293**,** 857-60.

Goje, L. J., Elmi, E. D., Bracuti, A., Courty, T., Rao, T., Alzahrani, F. A. & Crickmore, N. 2020. Identification of *Aedes aegypti* specificity motifs in the N-terminus of the *Bacillus thuringiensis* Cry2Aa pesticidal protein. *J Invertebr Pathol,* 174**,** 107423.

Gomez-Dantes, H. & Willoquet, J. R. 2009. Dengue in the Americas: challenges for prevention and control. *Cad Saude Publica,* 25 Suppl 1**,** S19-31.

Guereca, L. & Bravo, A. 1999. The oligomeric state of *Bacillus thuringiensis* Cry toxins in solution. *Biochim Biophys Acta,* 1429**,** 342-50.

Gunning, R. V., Dang, H. T., Kemp, F. C., Nicholson, I. C. & Moores, G. D. 2005. New resistance mechanism in *Helicoverpa armigera* threatens transgenic crops expressing *Bacillus thuringiensis* Cry1Ac toxin. *Appl Environ Microbiol,* 71**,** 2558-63.

Guo, Z., Kang, S., Sun, D., Gong, L., Zhou, J., Qin, J., Guo, L., Zhu, L., Bai, Y., Ye, F., Wu, Q., Wang, S., Crickmore, N., Zhou, X. & Zhang, Y. 2020. MAPK-dependent hormonal signaling plasticity contributes to overcoming *Bacillus thuringiensis* toxin action in an insect host. *Nat Commun,* 11**,** 3003.

Hayakawa, T., Shitomi, Y., Miyamoto, K. & Hori, H. 2004. GalNAc pretreatment inhibits trapping of *Bacillus thuringiensis* Cry1Ac on the peritrophic membrane of *Bombyx mori*. *FEBS Lett,* 576**,** 331-5.

Heckel, D. G. 2012. Learning the ABCs of Bt: ABC transporters and insect resistance to *Bacillus thuringiensis* provide clues to a crucial step in toxin mode of action. *Pesticide Biochemistry and Physiology,* 104**,** 103-110.

Hernandez-Martinez, P., Hernandez-Rodriguez, C. S., Krishnan, V., Crickmore, N., Escriche, B. & Ferre, J. 2012. Lack of Cry1Fa binding to the midgut brush border membrane in a resistant colony of

Plutella xylostella moths with a mutation in the ABCC2 locus. *Appl Environ Microbiol,* 78**,** 6759-61.

Hilbert, D. W. & Piggot, P. J. 2004. Compartmentalization of gene expression during *Bacillus* subtilis spore formation. *Microbiology and Molecular Biology Reviews,* 68**,** 234-+.

Hofmann, C., Vanderbruggen, H., Hofte, H., Van Rie, J., Jansens, S. & Van Mellaert, H. 1988. Specificity of *Bacillus thuringiensis* delta-endotoxins is correlated with the presence of high-affinity binding sites in the brush border membrane of target insect midguts. *Proc Natl Acad Sci U S A,* 85**,** 7844-8.

Hua, G., Jurat-Fuentes, J. L. & Adang, M. J. 2004. Fluorescent-based assays establish *Manduca sexta* Bt-R(1a) cadherin as a receptor for multiple *Bacillus thuringiensis* Cry1A toxins in *Drosophila* S2 cells. *Insect Biochem Mol Biol,* 34**,** 193-202.

Hua, G., Zhang, R., Abdullah, M. A. & Adang, M. J. 2008. *Anopheles gambiae* cadherin AgCad1 binds the Cry4Ba toxin of *Bacillus thuringiensis israelensis* and a fragment of AgCad1 synergizes toxicity. *Biochemistry,* 47**,** 5101-10.

Jimenez-Juarez, N., Munoz-Garay, C., Gomez, I., Saab-Rincon, G., Damian-Almazo, J. Y., Gill, S. S., Soberon, M. & Bravo, A. 2007. *Bacillus thuringiensis* Cry1Ab mutants affecting oligomer formation are non-toxic to *Manduca sexta* larvae. *J Biol Chem,* 282**,** 21222-9.

Joseph, L. 2019. Understanding the basis of specificity of *Bacillus thuringiensis* Cry2A toxins towards *Aedes aegypti*. PhD, University of Sussex.

Jurat-Fuentes, J. L., Karumbaiah, L., Jakka, S. R., Ning, C., Liu, C., Wu, K., Jackson, J., Gould, F., Blanco, C., Portilla, M., Perera, O. & Adang, M. 2011. Reduced levels of membrane-bound alkaline phosphatase are common to lepidopteran strains resistant to Cry toxins from *Bacillus thuringiensis*. *PLoS One,* 6**,** e17606.

Khorramnejad, A., Bel, Y., Talaei-Hassanloui, R. & Escriche, B. 2022. Activation of *Bacillus thuringiensis* Cry1I to a 50 kDa stable core impairs its full toxicity to *Ostrinia nubilalis*. *Appl Microbiol Biotechnol,* 106**,** 1745-1758.

Knowles, B. H. & Dow, J. a. T. 1993. The Crystal Delta-Endotoxins of *Bacillus thuringiensis* - Models for Their Mechanism of Action on the Insect Gut. *Bioessays,* 15**,** 469-476.

Knowles, B. H. & Ellar, D. J. 1987. Colloid-osmotic lysis is a general feature of the mechanism of action of *Bacillus thuringiensis* δ-endotoxins with different insect specificity. *Biochimica et Biophysica Acta (BBA) - General Subjects,* 924**,** 509-518.

Li, J. D., Carroll, J. & Ellar, D. J. 1991. Crystal structure of insecticidal delta-endotoxin from *Bacillus thuringiensis* at 2.5 A resolution. *Nature,* 353**,** 815-21.

Liang, Y. & Dean, D. H. 1994. Location of a lepidopteran specificity region in insecticidal crystal protein CryIIA from *Bacillus thuringiensis*. *Mol Microbiol,* 13**,** 569-75.

Luo K, S. S., Masson L, Mazza a, Brousseau R, Adang Mj. 1997 The heliothis virescens 170 kDa aminopeptidase functions as "receptor A" by mediating specific *Bacillus thuringiensis* Cry1A delta-endotoxin binding and pore formation. *Insect Biochem Mol Biol.* , 27(8-9):735-43.

Maduell, P., Armengol, G., Llagostera, M., Orduz, S. & Lindow, S. 2008. *B. thuringiensis* is a poor colonist of leaf surfaces. *Microb Ecol,* 55**,** 212-9.

Masson, L., Lu, Y. J., Mazza, A., Brousseau, R. & Adang, M. J. 1995. The CryIA(c) receptor purified from *Manduca sexta* displays multiple specificities. *J Biol Chem,* 270**,** 20309-15.

Mcnall, R. J. & Adang, M. J. 2003. Identification of novel *Bacillus thuringiensis* Cry1Ac binding proteins in *Manduca sexta* midgut through proteomic analysis. *Insect Biochemistry and Molecular Biology,* 33**,** 999-1010.

Milne, R., Wright, T., Kaplan, H. & Dean, D. 1998. Spruce budworm elastase precipitates *Bacillus thuringiensis* delta-endotoxin by specifically recognizing the C-terminal region. *Insect Biochem Mol Biol,* 28**,** 1013-23.

Milner, R. J. 1994. History of *Bacillus-Thuringiensis*. *Agriculture Ecosystems & Environment,* 49**,** 9-13.

Milutinovic, B., Hofling, C., Futo, M., Scharsack, J. P. & Kurtz, J. 2015. Infection of *Tribolium castaneum* with *Bacillus thuringiensis*: quantification of bacterial replication within cadavers, transmission via cannibalism, and inhibition of spore germination. *Appl Environ Microbiol,* 81**,** 8135-44.

Morse, R. J., Yamamoto, T. & Stroud, R. M. 2001. Structure of Cry2Aa suggests an unexpected receptor binding epitope. *Structure,* 9**,** 409-17.

Nelson, M. J. 1986. *Aedes aegypti*: biology and ecology. *Pan American Health Organization*.

Ocelotl, J., Sanchez, J., Arroyo, R., Garcia-Gomez, B. I., Gomez, I., Unnithan, G. C., Tabashnik, B. E., Bravo, A. & Soberon, M. 2015. Binding and Oligomerization of Modified and Native Bt Toxins in Resistant and Susceptible Pink Bollworm. *PLoS One,* 10**,** e0144086.

Ocelotl, J., Sanchez, J., Gomez, I., Tabashnik, B. E., Bravo, A. & Soberon, M. 2017. ABCC2 is associated with *Bacillus thuringiensis* Cry1Ac

toxin oligomerization and membrane insertion in diamondback moth. *Sci Rep*, 7**,** 2386.

Ohsawa, M., Tanaka, M., Moriyama, K., Shimazu, M., Asano, S., Miyamoto, K., Haginoya, K., Mitsui, T., Kouya, T., Taniguchi, M. & Hori, H. 2012. A 50-Kilodalton Cry2A Peptide Is Lethal to *Bombyx mori* and *Lymantria dispar*. *Applied and Environmental Microbiology,* 78**,** 4755-4757.

Palma, L., Munoz, D., Berry, C., Murillo, J. & Caballero, P. 2014. *Bacillus thuringiensis* toxins: an overview of their biocidal activity. *Toxins (Basel),* 6**,** 3296-325.

Pan, Z. Z., Xu, L., Liu, B., Chen, Q. X. & Zhu, Y. J. 2021. Key residues of *Bacillus thuringiensis* Cry2Ab for oligomerization and pore-formation activity. *AMB Express,* 11**,** 112.

Park, Y., Gonzalez-Martinez, R. M., Navarro-Cerrillo, G., Chakroun, M., Kim, Y., Ziarsolo, P., Blanca, J., Canizares, J., Ferre, J. & Herrero, S. 2014. ABCC transporters mediate insect resistance to multiple Bt toxins revealed by bulk segregant analysis. *BMC Biol*, 12**,** 46.

Pigott, C. R. & Ellar, D. J. 2007. Role of receptors in *Bacillus thuringiensis* crystal toxin activity. *Microbiol Mol Biol Rev,* 71**,** 255-81.

Rasko, D. A., Altherr, M. R., Han, C. S. & Ravel, J. 2005. Genomics of the *Bacillus cereus* group of organisms. *Fems Microbiology Reviews,* 29**,** 303-329.

Rausell, C., Garcia-Robles, I., Sanchez, J., Munoz-Garay, C., Martinez-Ramirez, A. C., Real, M. D. & Bravo, A. 2004. Role of toxin activation on binding and pore formation activity of the *Bacillus thuringiensis* Cry3 toxins in membranes of Leptinotarsa decemlineata (Say). *Biochim Biophys Acta,* 1660**,** 99-105.

Schnepf, E., Crickmore, N., Van Rie, J., Lereclus, D., Baum, J., Feitelson, J., Zeigler, D. R. & Dean, D. H. 1998. *Bacillus thuringiensis* and its pesticidal crystal proteins. *Microbiol Mol Biol Rev,* 62**,** 775-806.

Shu, C., Zhang, F., Chen, G., Joseph, L., Barqawi, A., Evans, J., Song, F., Li, G., Zhang, J. & Crickmore, N. 2017. A natural hybrid of a *Bacillus thuringiensis* Cry2A toxin implicates Domain I in specificity determination. *J Invertebr Pathol,* 150**,** 35-40.

Shu, C., Zhou, J., Crickmore, N., Li, X., Song, F., Liang, G., He, K., Huang, D. & Zhang, J. 2016. In vitro template-change PCR to create single crossover libraries: a case study with *B. thuringiensis* Cry2A toxins. *Sci Rep,* 6**,** 23536.

Simpson Rm, N. R. 2000. Binding of *Bacillus thuringiensis* delta-endotoxins Cry1Ac and Cry1Ba to a 120-kDa aminopeptidase-N of *Epiphyas postvittana* purified from both brush border membrane vesicles and baculovirus-infected Sf9 cells. *Insect Biochem Mol Biol.,* 30(11):1069-78.

Souissi, W. 2018. Cytocidal activity of Cry41Aa, an anticancer toxin from *Bacillus thuringiensis.* PhD, University of Sussex.

Tabachnick, W. J., Munstermann, L. E. & Powell, J. R. 1979. Genetic Distinctness of Sympatric Forms of *Aedes Aegypti* in East Africa. *Evolution,* 33**,** 287-295.

Tay, W. T., Mahon, R. J., Heckel, D. G., Walsh, T. K., Downes, S., James, W. J., Lee, S. F., Reineke, A., Williams, A. K. & Gordon, K. H. 2015. Insect Resistance to *Bacillus thuringiensis* Toxin Cry2Ab Is Conferred by Mutations in an ABC Transporter Subfamily A Protein. *PLoS Genet,* 11**,** e1005534.

Valaitis, A. P. & Podgwaite, J. D. 2013. *Bacillus thuringiensis* Cry1A toxin-binding glycoconjugates present on the brush border membrane and in the peritrophic membrane of the Douglas-fir tussock moth are peritrophins. *J Invertebr Pathol,* 112**,** 1-8.

Walters, F. S., Stacy, C. M., Lee, M. K., Palekar, N. & Chen, J. S. 2008. An engineered chymotrypsin/cathepsin G site in domain I renders *Bacillus thuringiensis* Cry3A active against Western corn rootworm larvae. *Appl Environ Microbiol,* 74**,** 367-74.

Wang, Z., Fang, L., Zhou, Z., Pacheco, S., Gomez, I., Song, F., Soberon, M., Zhang, J. & Bravo, A. 2018. Specific binding between *Bacillus thuringiensis* Cry9Aa and Vip3Aa toxins synergizes their toxicity against Asiatic rice borer (*Chilo suppressalis*). *J Biol Chem,* 293**,** 11447-11458.

Wei, J., Zhang, M., Liang, G., Wu, K., Guo, Y., Ni, X. & Li, X. 2016. APN1 is a functional receptor of Cry1Ac but not Cry2Ab in *Helicoverpa zea*. *Sci Rep,* 6**,** 19179.

Wei, J., Zhang, M., Liang, G. Et Al. 2016. APN1 is a functional receptor of Cry1Ac but not Cry2Ab in *Helicoverpa zea*. Sci Rep 6, 19179.

Widner, W. R. & Whiteley, H. R. 1990. Location of the dipteran specificity region in a lepidopteran-dipteran crystal protein from *Bacillus thuringiensis*. *J Bacteriol,* 172**,** 2826-32.

Wolfersberger, M. G. 1990. The toxicity of two *Bacillus thuringiensis* delta-endotoxins to gypsy moth larvae is inversely related to the affinity of binding sites on midgut brush border membranes for the toxins. *Experientia,* 46**,** 475-7.

Wu, Y. D. 2014. Detection and Mechanisms of Resistance Evolved in Insects to Cry Toxins from *Bacillus thuringiensis*.

Xu, L., Pan, Z. Z., Zhang, J., Liu, B., Zhu, Y. J. & Chen, Q. X. 2016. Proteolytic Activation of *Bacillus thuringiensis* Cry2Ab through a Belt-and-Braces Approach. *Journal of Agricultural and Food Chemistry,* 64**,** 7195-7200.

Xu, L., Pan, Z. Z., Zhang, J., Niu, L. Y., Li, J., Chen, Z., Liu, B., Zhu, Y. J. & Chen, Q. X. 2018. Exposure of helices alpha4 and alpha5 is

required for insecticidal activity of Cry2Ab by promoting assembly of a prepore oligomeric structure. *Cell Microbiol,* 20**,** e12827.

Yamamoto, T. & Mclaughlin, R. E. 1981. Isolation of a protein from the parasporal crystal of *Bacillus thuringiensis* var. Kurstaki toxic to the mosquito larva, *Aedes taeniorhynchus. Biochem Biophys Res Commun,* 103**,** 414-21.

Zhang, R., Hua, G., Andacht, T. M. & Adang, M. J. 2008. A 106-kDa aminopeptidase is a putative receptor for *Bacillus thuringiensis* Cry11Ba toxin in the mosquito *Anopheles gambiae*. *Biochemistry,* 47**,** 11263-72.

Zhang, X., Candas, M., Griko, N. B., Rose-Young, L. & Bulla, L. A., Jr. 2005. Cytotoxicity of *Bacillus thuringiensis* Cry1Ab toxin depends on specific binding of the toxin to the cadherin receptor BT-R1 expressed in insect cells. *Cell Death Differ,* 12**,** 1407-16.